POST-BUCKLING RESPONSE OF STRUCTURES USING THE FINITE ELEMENT METHOD

by

THEODORE EDMUND LANG

A thesis submitted in partial fulfillment
of the requirements for the degree of

DOCTOR OF PHILOSOPHY

UNIVERSITY OF WASHINGTON

1969

Approved by B. J. Hartz

Department Civil Engineering

Date Aug. 22, 1969

UNIVERSITY OF WASHINGTON

Date: August 5, 1969

We have carefully read the dissertation entitled Post-Buckling Response of Structures Using the Finite Element Method

submitted by Theodore E. Lang in partial fulfillment of the requirements of the degree of Doctor of Philosophy and recommend its acceptance. In support of this recommendation we present the following joint statement of evaluation to be filed with the dissertation.

The refined theory of Elastic Stability of Koiter is extended for Finite Element formulation of the immediate post-buckling response of elastic systems. The pre-buckling, critical point, and initial post-buckling equilibrium conditions are mathematically defined using appropriate non-linear geometric terms. The initial post-buckling state is evaluated for conservative static systems by perturbation of the total incremental potential energy from the point of critical load.

The finite element matrix terms corresponding to the additional non-linear terms required for the refined theory are evaluated for beam-column and plate-type elastic systems and the stable initial post-buckling configurations obtained for various finite element sizes for comparison with known behavior in particular cases. Column results were obtained for inextensible and extensible theories and new results on the contribution of axial deformation obtained.

Additional results are obtained for the shallow arch and the sensitivity of the arch to geometric imperfections in the assumed modal shapes is evaluated for small and moderate height-to-span ratio arches.

DISSERTATION READING COMMITTEE: B. J. Hartz

R. J. Clark

K. A. Holsapple

In presenting this thesis in partial fulfillment of the requirements for an advanced degree at the University of Washington I agree that the Library shall make it freely available for inspection. I further agree that permission for extensive copying of this thesis for scholarly purposes may be granted by my major professor, or, in his absence, by the Director of Libraries. It is understood that any copying or publication of this thesis for financial gain shall not be allowed without my written permission.

Signature Theodore E. Lang

Date 9/22/69

TABLE OF CONTENTS

LIST OF FIGURES

ACKNOWLEDGEMENT

The author is indebted to Professor R. G. Hennes (Chairman) and the faculty of the Department of Civil Engineering for monetary assistance during the course of this work.

Helpful discussions and constructive criticism by Professor R. J. Evans and Professor K. A. Holsapple, as members of the thesis reading committee, are gratefully acknowledged.

The deep feeling of appreciation and gratitude held by the author cannot be expressed for the technical and non-technical values gained while in association with Professor B. J. Hartz, graduate advisor.

I. INTRODUCTION

The sufficient condition for stability of a mechanical system is that, given independent generalized coordinates, q_i, and an initial configuration of equilibrium, $q_i=0$, the configuration is stable if it is possible to find positive bounds, β_{1_i} and β_{2_i}, for the moduli of a kinematically admissible initial disturbance such that $|q_i(0)| < \beta_{1_i}$ and $|\dot{q}_i(0)| < \beta_{2_i}$ for all time. This is an abbreviated statement of dynamic stability for which the mathematical theorems were developed by Liapunov (1) in 1892. Time dependent response is the essence of the study of stability and setting up the theory in the framework of dynamics is natural. However, attendant to this general approach is description of motion by nonlinear differential equations. These are difficult to solve even in the simpliest of problems. Liapunov, working with the total energy for discrete systems, showed that by introducing small disturbances, information on system stability can sometimes be determined without having to solve the complete nonlinear differential equations of motion (1,2). This approach has evolved as the theory of small oscillations (modern reference (3)). Alternately, for conservative systems working directly with the total energy under the assumption of quasi-static response, consideration becomes that of stability of equilibrium--and the approach is called the energy method (4). These approximate methods are powerful and are used often with success; however, exceptional cases do arise which

preclude their use due to the approximations made (5,6).

A large class of problems is included in conservative system approximations which can be treated by static techniques. If the total potential energy, constituting strain energy and work done by external forces, is derived in terms of kinematically admissible displacement variables (e.g., generalized coordinates), then the detection of stability or instability for a given point in equilibrium configuration space of the system depends upon whether or not the total potential energy is at a relative minimum. Denoting a displacement variable by q_i and the total potential energy by P, the procedure is to examine how P varies under displacement changes from an initial equilibrium state, say q_{o_i}. The Taylor series expansion is a rigorous technique for expansion from the initial state, so that the change in total potential energy to an adjacent point in configuration space is

$$\Delta P = P - P|_{q_o} = \frac{\partial P}{\partial q_i}\Big|_{q_o} \delta q_i + \frac{1}{2!} \frac{\partial^2 P}{\partial q_i \partial q_j}\Big|_{q_o} \delta q_i \delta q_j +$$

$$+ \frac{1}{3!} \frac{\partial^3 P}{\partial q_i \partial q_j \partial q_k}\Big|_{q_o} \delta q_i \delta q_j \delta q_k + \cdots$$

If $\Delta P > 0$, the system is stable, if $\Delta P < 0$ the system is unstable and if $\Delta P = 0$ the system is neutrally stable. The kinematically admissible displacement variations, δ_{q_i}, representing the disturbance, can be made as small in magnitude as

we wish, so that the terms in ΔP become successively smaller. Thus, unless the first term on the right equals zero, ΔP can always be made negative. This term equals zero if the initial state (q_{o_i}) is in a state of equilibrium, and the term is recognized as representing the principle of virtual displacements. In the second variation the quadratic terms in q, if non-zero, are dominant so that positive-definitness of ΔP insures stability. If the quadratic terms are identically zero the question of stability is resolved by examining higher order terms in q.

Assuming the quadratic terms non-zero, the important relation to bifurcation buckling is ΔP becoming positive semi-definite at particular values of the loading. The eigenvalue problem resulting from this condition characterizes a type of bifurcation mechanism in which a state of neutral equilibrium is attained at the critical load and a different deformation state suddenly develops. The initial slope of the equilibrium path into the initial post-buckled state is zero and it is the curvature of this path at the critical point that defines stability (Figure 1a).

A second type of bifurcation buckling occurs in structural configurations such as arches and thin shells. The point of bifurcation is a singular point determined from non-homogeneous equations. It develops when an additional deformation mode of a defined set becomes admissible under increasing load. Over a wide range of arch and shell geometries transition of deformation into the new mode is unstable and

snap-through occurs. In this case the slope of the initial post-buckling response path is negative (Figure 1b).

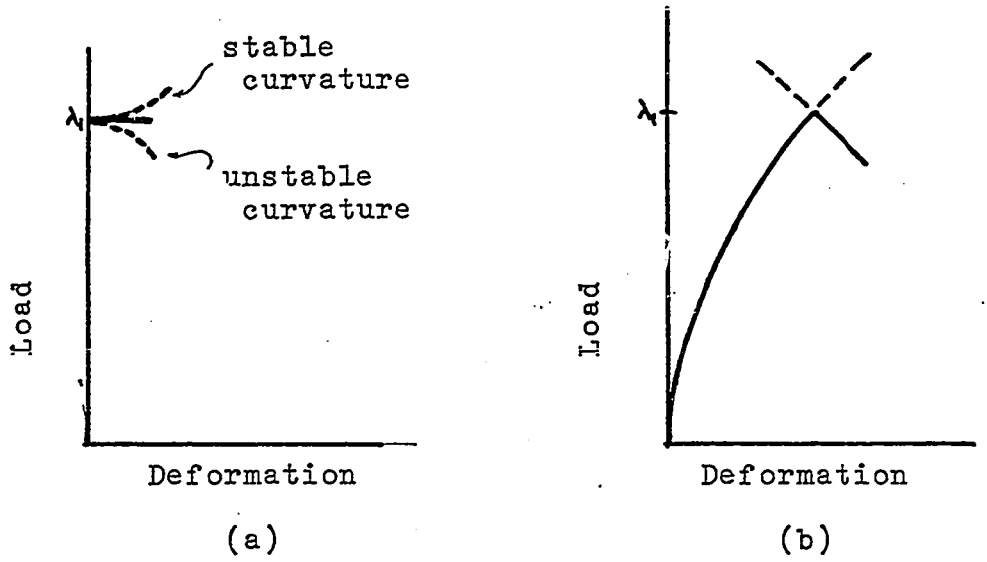

Figure I-1: Bifurcation Buckling Types

These bifurcation types are considered herein as they relate to prediction of initial post-buckling response of structures. The feasibility of use of the finite element method as an approximate method of analysis for predicting post-buckling response is investigated.

The eigenvalue theory for predicting critical loads using finite elements is contained in current texts (8,9,10), one of the original formulations appearing in 1963 by Gallagher and Padlog (11). Application to plate structures is reported by Kapur and Hartz (12). The axial loaded cylindrical shell idealized to an eigenvalue problem as well as extreme idealization of a doubly curved shell are evaluated by Gallagher and Yang (14). The more accurate representation of shell

buckling as a snap-through mechanism is considered by Gallagher et al. (13) and critical load of a spherical shell is estimated by an iteration technique.

Basic to buckling and post-buckling response is representation of geometric nonlinearity. This appears in energy formulations in the form of higher order displacement terms in the total potential energy--a result of refinement in definition of the strain-displacement relations. Geometric nonlinearity in finite element representations is a recent development first considered by Turner et al. (15) in 1960 in determining large deflection of structures. Reported in this work are two algorithms, one an iteration scheme to search out the equilibrium configuration by a usually convergent process applied to the equilibrium equations, and two a stepwise linear approach by use of incremental equilibrium equations. Both schemes are developed using a representation of the total potential energy through the quadratic terms in displacement. Further developments on this subject and a summary of the state-of-the-art are reported by Martin (16).

A more recent development in nonlinear analysis is the energy search method, which was developed by Bogner et al. (17) and Schmit (18). In this method, the total potential energy is derived in terms of displacement functions with unknown generalized components, and minimization carried out with respect to these components appearing in nonlinear equations. Various algorithms have been used to locate the minimum energy state (19,20). In this formulation third and

higher order displacement terms are retained in the total potential energy for accuracy in representation and to improve solution convergence. The requirement to use higher order terms in the potential energy for finite deflection analyses, suggested a possible improvement on the step-wise linear incremental technique. Incremental equations that admit third and fourth order terms were subsequently developed by Marcal (21) with additional applications by Mallett and Marcal (22).

Recent effort in nonlinear mechanics with finite elements is centered on rational representation of higher order and special effects in what is basically an approximate analysis technique. Felippa (23) has developed a systematic procedure for definition of elements and treatment of geometric and physical nonlinearities for two-dimensional continuous structures. More recently Nathan (24) has considered geometric nonlinearities in the context of nonlinear elasticity, and Oden (25) approaches the subject from the standpoint of continuum mechanics. These and other rapid advances in the field stem from the basic utility of the method to solve complex problems by substructure idealization.

In finite deflection analysis of structures, geometrically nonlinear terms enter into the representation in both classical and finite element methods in like manner, the basic difference being the structural representation. The need for higher order terms is essential also in studying post-buckling response of structures. Classically, Koiter has

studied this case extensively (26,27). Koiter, by perturbation of the incremental potential energy in the vicinity of the point of bifurcation, is able to estimate initial post-buckling response. For post-buckling unstable structures the nature of the post-buckling response when influenced by assumed structural imperfections yields information on the sensitivity of the structure to jump from the initial state to an adjacent state at loads below the perfect structure critical load. This phenomona, originally investigated by von Kármán and Tsien (28), was described mathematically by Koiter and reported in 1945 (26). Application of the theory to the axial loaded cylindrical shell shows extreme sensitivity of this structure to small imperfections. This development greatly aided in explaining the wide discrepancy between theoretical and experimental critical loads and the wide scatter in experimental data (29). Varying degrees of lesser sensitivity are exemplified by other structural types subsequently classically analyzed (30).

Other contributions to this theory include work by Budiansky and Hutchinson on dynamic buckling as well as derivation of Koiter's theory starting from the principle of virtual work (31). Several applications of the theory to line-column, plate and shell structures are reported in the literature (32,33,34).

The purpose of the present investigation is to develop the equations for post-buckling response in the context of the finite element method. This extends the application of the

theory to problems not amenable to classical approaches. In addition, conditions that must be met in finite element representations are examined and convergence and accuracy of approximations in the governing equations are explored. Numerical examples are presented to clarify details of the theory.

Chapter II of this text consists of a derivation of the equations for initial state, critical point, and post-buckling response. This follows the development by Koiter with certain modifications based upon characteristics of the finite element method. Wherever practical, notation is used that corresponds to notation in classical derivations of the equations. In Chapter III the line element column is treated and correspondence shown with classical theory. Derivation of the stiffness matrices associated with higher order terms in the total potential energy is presented. Corresponding matrices for the plate element are developed in Chapter IV. The numerical precedure for predicting post-buckling response of plate structures is presented. In Chapter V, the arch and bent line-element configurations are studied and approximate solutions obtained by extended application of the theory. Finally, Chapter VI is a summarization of results and conclusions.

II. GOVERNING EQUATIONS FOR POST-BUCKLING RESPONSE

2.1 The Perfect Structure: Total Potential Energy.

This development of equations to describe the response of a structure having no imperfections or load misalignments is restricted to structural systems conservative both in external loading and internal energy absorption. Change of state from a known equilibrium configuration (State I) to an adjacent configuration (State II) occurs through bifurcation rather than snap-through buckling. The existence of a relative minimum of the total potential energy in State I is a necessary and sufficient condition for stability of this configuration. This implies that for a small but finite increase in the external loading, the increase in strain energy (plus the energy dissipated, if accounted for) exceeds the external work increment. The increment in potential energy in transition from State I to II,

$$\mathcal{P}[\Delta] = \mathcal{P}_{II} - \mathcal{P}_{I} \tag{1}$$

if non-negative, is a sufficient condition for stability of the system in State II.

The total potential energy consists of the energy of deformation and work done by applied external loads. It must be defined with sufficient terms included that nonlinear behavior is represented. In a finite deformation problem, fiber rotations and possible strains become large so that geometry changes under loading must be evaluated. In

contrast, the need for nonlinear terms in considering bifurcation buckling is to detect the change of state at the bifurcation. At this point deflection of the structure is normally small and the change of state is the sudden appearance of a different mechanism of deformation.

Initial consideration is given to development of the post-buckling response equation omitting details on the type or types of finite elements used. The basic restriction imposed by the fact that the structure is represented by an assemblage of finite elements is that the retention of nonlinear terms precludes formation of a compact total structure equation. Thus, defining the total potential energy on a per element basis, its form is

$$\begin{aligned}\Phi[\Delta] = \lambda \sum_{i=1}^{N} \{C\}_i^T \{\Delta\}_i + \sum_{i=1}^{N} \{\Delta\}_i^T [K_0]_i \{\Delta\}_i + \lambda \sum_{i=1}^{N} \{\Delta\}_i^T [K_1]_i \{\Delta\}_i + \\ + \lambda \sum_{i=1}^{N} \{\Delta\}_i^T [L_1]_i \{\Delta\}_i + \sum_{i=1}^{N} \{\Delta\}_i^T [H_1]_i \{\Delta\}_i + \\ + \lambda \sum_{i=1}^{N} \{\Delta\}_i^T [L_2]_i \{\Delta\}_i + \sum_{i=1}^{N} \{\Delta\}_i^T [H_2]_i \{\Delta\}_i + \end{aligned} \qquad (2)$$

The matrices $[K_0]$ and $[K_1]$ are the linear equilibrium and stability coefficient matrices which have constant element values. The higher order matrices $[H_j]$ and $[L_j]$ are expressed in similar format, but they contain the displacement function $\{\Delta\}_i$ to power j in their coefficient definition. The factor λ is the load intensity factor assumed constant for all elements which implies proportionate loading. Finally N is the

number of finite elements that constitute the total structure. In Eq. (2) the subscript i is sufficient to indicate summation so that the summation signs are dropped in the following development.

2.2 Initial State and Critical Point.

The pre-buckling response of the structure is assumed linear so that for a displacement state of the form

$$\{\Delta\}_i = \{\Delta_0\}_i \tag{3}$$

the total potential energy is

$$P_I[\Delta] = \lambda \, [C]_i \{\Delta_0\}_i + [\Delta_0]_i [K_0]_i \{\Delta_0\}_i \tag{4}$$

The variation with respect to $\{\Delta_0\}_i$ is simply a statement of the principle of virtual displacements, from which the relation between load and displacement to satisfy equilibrium in State I is obtained. Thus, for λ specified, $\{\Delta_0\}_i$ is determined.

Stability of the structure in State I up to the point of bifurcation in configuration space can be investigated by considering a displacement perturbation into State II. Assuming the existence of an adjacent state an appropriate displacement function is

$$\{\Delta\}_i = \{\Delta_0\}_i + a\{\bar{\Delta}\}_i \tag{5}$$

where $\{\bar{\Delta}\}_i$ is the modal function (of small amplitude $\underline{a}$) of

displacement into State II. Substituting, the total potential energy in State II is

$$\begin{aligned}\Phi_{II}[\Delta] = {} & \lambda \, L C J_i \{\Delta_0\}_i + \lambda a \, L C J_i \{\bar{\Delta}\}_i + L\Delta_0 J_i [K_0]_i \{\Delta_0\}_i \\ & + a \, L\Delta_0 J_i [K_0]_i \{\bar{\Delta}\}_i + a^2 L\bar{\Delta} J_i [K_0]_i \{\bar{\Delta}\}_i + \lambda a^2 L\bar{\Delta} J_i [K_1]_i \{\bar{\Delta}\}_i \\ & + a^3 L\bar{\Delta} J_i [H_1] \{\bar{\Delta}\}_i + \lambda a^3 L\bar{\Delta} J_i [L_1]_i \{\bar{\Delta}\}_i \\ & + a^4 L\bar{\Delta} J_i [H_2]_i \{\bar{\Delta}\}_i + \lambda a^4 L\bar{\Delta} J_i [L_2]_i \{\bar{\Delta}\}_i + \cdots \end{aligned} \tag{6}$$

Substituting Eq's. (4) and (6) into Eq. (1) the increment in total potential energy is

$$\begin{aligned}\Psi[\Delta] = {} & a \left[\lambda \, L C J_i \{\bar{\Delta}\}_i + L\bar{\Delta} J_i [K_0]_i \{\Delta_0\}_i \right] + \\ & + a^2 \left[L\bar{\Delta} J_i [K_0]_i \{\bar{\Delta}\}_i + \lambda \, L\bar{\Delta} J_i [K_1]_i \{\bar{\Delta}\}_i \right] + \\ & + a^3 \left[L\bar{\Delta} J_i [H_1]_i \{\bar{\Delta}\}_i + \lambda \, L\bar{\Delta} J_i [L_1]_i \{\bar{\Delta}\}_i \right] + \\ & + a^4 \left[L\bar{\Delta} J_i [H_2]_i \{\bar{\Delta}\}_i + \lambda \, L\bar{\Delta} J_i [L_2]_i \{\bar{\Delta}\}_i \right] + O(a^5) \end{aligned} \tag{7}$$

The term of order a is a restatement of the principle of virtual displacements and equals zero. This leaves terms quadratic and higher order in a. If this increment is positive then the system is stable in State I. Should it happen that the quadratic term is zero, that is

$$L\bar{\Delta} J_i [K]_i \{\bar{\Delta}\}_i = L\bar{\Delta} J_i [K_0]_i \{\bar{\Delta}\}_i + \lambda \, L\bar{\Delta} J_i [K_1]_i \{\bar{\Delta}\}_i = 0 \tag{8}$$

then the question of stability rests with the value of the higher order terms. Necessary conditions for equilibrium are

that the third order term in $\underline{a}$ equals zero and the fourth order term have non-negative value. The question of a sufficient condition for equilibrium in State I is more complex. Koiter (1) shows that the key to a sufficiency proof is selection of a homogeneous positive-definite quadratic function $\{\bar{a}\}_i^T [T]_i \{\bar{a}\}_i$ such that if the minimum problem

$$\mu_1 = \min \frac{\{\bar{a}\}_i^T [K]_i \{\bar{a}\}_i}{\{\bar{a}\}_i^T [T]_i \{\bar{a}\}_i} \tag{9}$$

has a solution, then a necessary condition for stability in State I is $\mu_1 \geq 0$ and a sufficient condition is $\mu_1 > 0$. No decision on stability can be made if $\mu_1 = 0$, and the system is unstable if $\mu_1 < 0$. The quadratic function containing $[T]$ is introduced to insure that for small finite displacement from State I that as $a \rightarrow 0$ the quadratic term in $\underline{a}$ is larger than the sum of the remaining higher order terms in $\underline{a}$.

Variation of Eq. (9) with respect to $\{\bar{a}\}_i$, if arbitrary, leads to

$$[K]_i \{\bar{a}\}_i - \mu [T]_i \{\bar{a}\}_i = \{0\} \tag{10}$$

where $\{\bar{a}\}_i$ is any displacement vector of the kinematically admissible displacement field of the structure. Eq. (10) represents a set of homogeneous equations from which eigensolutions exist for special values of μ. If a plot of μ versus λ is generated a root loci diagram is obtained wherein regions of stable and unstable equilibrium can be established depending upon the sign of μ.

The function $\lfloor \bar{\Delta} \rfloor_i [T]_i \{\bar{\Delta}\}_i$ is defined as quadratic in terms of the same displacement functions as in $\lfloor \bar{\Delta} \rfloor_i [K]_i \{\bar{\Delta}\}_i$. However, as shown by Koiter $\lfloor \bar{\Delta} \rfloor_i [T]_i \{\bar{\Delta}\}_i$ can have a wider definition. If it is interpreted as the kinetic energy of the system with displacements replacing velocity, then Eq. (10) becomes simply a statement of Rayleigh's principle.

Eigensolutions $\{\bar{\Delta}_h\}_i$ and $\{\bar{\Delta}_k\}_i$ associated with different eigenvalues μ_h and μ_k are orthogonal with respect to $[T]_i$. That is

$$(\mu_h - \mu_k) \lfloor \bar{\Delta}_h \rfloor_i [T]_i \{\bar{\Delta}_k\}_i = 0 \qquad h \neq k \tag{11a}$$

Alternately

$$\lfloor \bar{\Delta}_h \rfloor_i [K]_i \{\bar{\Delta}_k\}_i = 0 \qquad h \neq k \tag{11b}$$

These conditions are derived from Eq. (10) in the established procedure of a Sturn-Liouville problem. Mode normalization also follows

$$\lfloor \bar{\Delta}_h \rfloor_i [T]_i \{\bar{\Delta}_h\}_i = 1 \tag{12a}$$

and

$$\lfloor \bar{\Delta}_h \rfloor_i [K]_i \{\bar{\Delta}_h\}_i = -\mu_h \tag{12b}$$

The case of multiple roots of Eq. (10) is treated in a straightforward manner, wherein eigenfunctions are determined which are mutually orthogonal as well as being orthogonal to modal functions of different roots (38).

Conditions for stability have been defined so far only in the fundamental State I. The condition expressed by Eq. (8)

is called the critical case of neutral equilibrium for which the stability limit from Eq. (9) is

$$\mu_1 = \min \frac{[\bar{\Delta}]_i [K]_i \{\bar{\Delta}\}_i}{[\bar{\Delta}]_i [T]_i \{\bar{\Delta}\}_i} = 0 \tag{13}$$

The eigenfunction corresponding to $\mu_1 = 0$ is called the critical buckling mode and is designated by $\{\Delta_1\}_i$. More than one eigenvalue may simultaneously be zero. In this case, eigenvectors corresponding to each value are determined by standard techniques. The linear combination of all of these vectors represents the general displacement field for which the second variation is zero.

To investigate the stability of the critical case of neutral equilibrium defined by a single buckling mode, a displacement state is assumed of the form

$$\{\Delta\}_i = a\{\Delta_1\}_i + \{\bar{\Delta}\}_i \tag{14}$$

where $\{\bar{\Delta}\}_i$ is any kinematically admissible displacement function which is orthogonal to $\{\Delta_1\}_i$ in the sense of Eq. (11), although $\{\bar{\Delta}\}_i$ need not be a higher order buckling mode of the system. In many problems it is convenient to assume a summation of higher order buckling modes to represent $\{\bar{\Delta}\}_i$, in which case each mode satisfies the characteristic equation

$$[K_0]_i \{\Delta_j\}_i + \lambda_1 [K_1]_i \{\Delta_j\}_i - \mu_j [T]_i \{\Delta_j\}_i = \{0\} \tag{15}$$

The basis for selecting Eq. (14) is that to resolve the question of stability the increment in potential energy must be

defined for a small displacement change from that at the critical point. Making $\{\bar{\Delta}\}_i$ orthogonal to $\{\Delta_1\}_i$ assures a characteristically different increment than simply a multiple of the fundamental buckling mode. Substituting Eq. (14) into Eq. (7)

$$
\begin{aligned}
P[a\Delta_1+\bar{\Delta}] = {} & a^3\left[\lfloor\Delta_1\rfloor_i[H_1]_i\{\Delta_1\}_i + \lambda_1\lfloor\Delta_1\rfloor_i[L_1]_i\{\Delta_1\}_i\right] + \\
& + a^4\left[\lfloor\Delta_1\rfloor_i[H_2]_i\{\Delta_1\}_i + \lambda_1\lfloor\Delta_1\rfloor_i[L_2]_i\{\Delta_1\}_i\right] + \\
& + a^2\left[\lfloor\Delta_1\rfloor_i[H_1]_i\{\bar{\Delta}\}_i + \lambda_1\lfloor\Delta_1\rfloor_i[L_1]_i\{\bar{\Delta}\}_i\right] + \\
& + a^3\left[\lfloor\Delta_1\rfloor_i[H_2]_i\{\bar{\Delta}\}_i + \lambda_1\lfloor\Delta_1\rfloor_i[L_2]_i\{\bar{\Delta}\}_i\right] + \\
& + \left[\lfloor\bar{\Delta}\rfloor_i[K_0]_i\{\bar{\Delta}\}_i + \lambda_1\lfloor\bar{\Delta}\rfloor_i[K_1]_i\{\bar{\Delta}\}_i\right] + \\
& + R_i[a\Delta_1, \bar{\Delta}]
\end{aligned}
\tag{16}
$$

Terms quadratic and higher order in $\{\bar{\Delta}\}_i$ are grouped in a remainder term $R_i[a\Delta_1, \bar{\Delta}]$ in Eq. (16). The magnitude of $\{\bar{\Delta}\}_i$ is variable and can be made arbitrarily small compared to $a\{\Delta_1\}_i$, in which the coefficient $\underline{a}$ can also be small, so that the remainder term becomes

$$
|R_i[a\Delta_1, \bar{\Delta}]| \le \varepsilon\left(\lfloor\bar{\Delta}\rfloor_i[K_0]_i\{\bar{\Delta}\}_i + \lambda_1\lfloor\bar{\Delta}\rfloor_i[K_1]_i\{\bar{\Delta}\}_i\right) \tag{17}
$$

where ε is less than unity. By this manipulation of parameters the remainder term can always be made negligible small. The coefficient of the a^3 term involving $\{\Delta_1\}$ must be zero, otherwise in the limit $\{\bar{\Delta}\} \to 0$ a signed value for $\underline{a}$ can be chosen

such that the energy increment is negative which infers instability. Apart from specified restrictions already placed on $\{\bar{\Delta}\}$ it is arbitrary. However, if an adjacent state is possible then the actual $\{\bar{\Delta}\}$ minimizes the energy increment. Thus, a solution for $\{\bar{\Delta}\}$ is sought that minimizes $\Psi[a\Delta_1+\bar{\Delta}]$. The variation of Eq. (16) with respect to $\{\bar{\Delta}\}_i$ is then

$$2\,[\delta\bar{\Delta}]_i[K_0]_i\{\bar{\Delta}\}_i + 2\lambda_1[\delta\bar{\Delta}]_i[K_1]_i\{\bar{\Delta}\}_i + a^2[\delta\bar{\Delta}]_i[H_1]_i\{\Delta_1\}_i$$

$$+ a^2\lambda_1[\delta\bar{\Delta}]_i[L_1]_i\{\Delta_1\}_i + a^3[\delta\bar{\Delta}]_i[H_2]_i\{\Delta_1\}_i +$$

$$+ a^3\lambda_1[\delta\bar{\Delta}]_i[L_2]_i\{\Delta_1\}_i + \cdots = 0 \tag{18}$$

Consider representing $\{\bar{\Delta}\}$ by a summation of higher order buckling modes of the form

$$\{\bar{\Delta}\}_i = a^2\xi_2\{\Delta_2\}_i + a^3\xi_3\{\Delta_3\}_i + \cdots \tag{19}$$

where ξ_2, ξ_3 . . . . are the amplitude or participation coefficients of each function, respectively. Doing this, the mode shape is known and Eq. (11) is satisfied. Substituting Eq. (19) into Eq. (18) and setting the coefficient of each power of $\underline{a}$ to zero independently yields

$$\xi_2 = \frac{-\left([\Delta_2]_i[H_1]_i\{\Delta_1\}_i + \lambda_1[\Delta_2]_i[L_1]_i\{\Delta_1\}_i\right)}{2\left([\Delta_2]_i[K_0]_i\{\Delta_2\}_i + \lambda_1[\Delta_2]_i[K_1]_i\{\Delta_2\}_i\right)} \tag{20a}$$

with $$[A_1]_i[T]_i\{\Delta_2\}_i = 0$$

$$\xi_3 = \frac{-\left(\langle \Delta_3 |_i [H_2]_i \{\Delta_1\}_i + \lambda_1 \langle \Delta_3 |_i [L_2]_i \{\Delta_1\}_i \right)}{2\left(\langle \Delta_3 |_i [K_0]_i \{\Delta_3\}_i + \lambda_1 \langle \Delta_3 |_i [K_1]_i \{\Delta_3\}_i \right)} \qquad (20b)$$

$$\text{with} \qquad \langle \Delta_1 |_i [T]_i \{\Delta_2\}_i = 0$$

and similar expressions for ξ_4, ξ_5, etc., if included.

With $\{\bar{\Delta}\}_i$ known to some order in $\underline{a}$ the increment in total potential energy can be evaluated by direct substitution into Eq. (16). Truncating $\{\bar{\Delta}\}_i$ at $\{\Delta_2\}_i$, where now ξ_2 is assumed contained in $\{\Delta_2\}_i$, and neglecting higher order terms in $\underline{a}$ in Eq. (16), the lowest order approximation for the increment in potential energy is

$$P[a\Delta_1 + \bar{\Delta}] = a^4 A_4 + a^5 A_5 + \cdots \qquad (21)$$

where

$$\begin{aligned} A_4 = {} & \langle \Delta_1 |_i [H_2]_i \{\Delta_1\}_i + \lambda_1 \langle \Delta_1 |_i [L_2]_i \{\Delta_1\}_i + \\ & + \langle \Delta_1 |_i [H_1]_i \{\Delta_2\}_i + \lambda_1 \langle \Delta_1 |_i [L_1]_i \{\Delta_2\}_i + \\ & + \langle \Delta_2 |_i [K_0]_i \{\Delta_2\}_i + \lambda_1 \langle \Delta_2 |_i [K_1]_i \{\Delta_2\}_i \end{aligned} \qquad (22)$$

The necessary condition for stability of the critical case of neutral equilibrium is

$$A_4 \geqq 0 \qquad (23)$$

and the sufficient condition for stability is

$$A_4 > 0 \tag{24}$$

Should it occur that $A_4=0$ then higher order terms must be considered in establishing the condition of stability.

It is not always possible or expeditious to evaluate the higher order buckling modes and an approximate function for $\{\Delta\}_i$ may be used instead. The solution for $\{\Delta\}_i$ from Eq. (18) will then not be representative of the true minimum of the energy increment. Continued use of $\{\Delta\}_i$ to evaluate A_4 will result in a value of A_4 greater than that for the true minimum. Thus, an approximate analysis results in an overestimation of the stability of the structure. A negative value for A_4 indicates instability, but a positive value does not necessarily indicate stable equilibrium. Interpretation of the theory for finite element applications is an approximating technique that will result in overestimation of the stability margin.

2.3 Displacement into Post-Buckling Domain.

Having the basic physical fact that a bifurcation occurs in the configuration space at $\lambda = \lambda_1$, we next examine response of the structure for loading through the critical point into the post-buckling domain. Of particular interest is the slope of the structural response path in the immediate vicinity of the bifurcation point. If the transition from State I to State II is smooth under quasi-static loading and the slope is

positive, then the structure is stable in the initial post-buckling state. However, if the transition is sudden then consideration of dynamic effects precludes a conclusive statement on stability even in the case of a static prediction of positive slope.

Apart from the physical considerations, the mathematical definition proceeds on the following assumption. It is assumed that the displacement state corresponding to the critical load λ_1 can be expanded in a Taylor series in ascending powers of $(\lambda-\lambda_1)$ in the neighborhood of the critical point--that is, we assume adjacent displacement states exist. The displacement from the fundamental state to an adjacent state is represented by

$$\{\Delta\} = a\{\Delta_1\} + \{\bar{\Delta}\} \tag{25}$$

where $\{\bar{\Delta}\}$ is small compared to $a\{\Delta_1\}$. Substituting Eq. (25) into a series expansion of Eq. (7) in powers of $(\lambda-\lambda_1)$ results in

$$\begin{aligned} P[a\Delta_1+\bar{\Delta}] = {} & a^3\left[L\Delta_1 J_i [H_1]_i \{\Delta_1\}_i + \lambda L\Delta_1 J_i [L_1]_i \{\Delta_1\}_i\right] + \\ & + a^4\left[L\Delta_1 J_i [H_2]_i \{\Delta_1\}_i + \lambda L\Delta_1 J_i [L_2]_i \{\Delta_1\}_i\right] + \\ & + L\bar{\Delta} J_i [K_0]_i \{\bar{\Delta}\}_i + \lambda L\bar{\Delta} J_i [K_1]_i \{\bar{\Delta}\}_i + \\ & + 3a^2\left[L\Delta_1 J_i [H_1]_i \{\bar{\Delta}\}_i + \lambda L\Delta_1 J_i [L_1]_i \{\bar{\Delta}\}_i\right] + \\ & + a^2\left[L\Delta_1 J_i [K_0]_i \{\Delta_1\}_i + \lambda L\Delta_1 J_i [K_1]_i \{\Delta_1\}_i\right] + \\ & + 2a\left[L\Delta_1 J_i [K_0]_i \{\bar{\Delta}\}_i + \lambda L\Delta_1 J_i [K_1]_i \{\bar{\Delta}\}_i\right] + \cdots \end{aligned} \tag{26}$$

Terms dropped are higher order in $\{\bar{\Delta}\}_i$, $\underline{a}$ and the load increment $(\lambda - \lambda_1)$, all assumed small quantities.

A particular expansion of the incremental displacement function is assumed of the form

$$\{\bar{\Delta}\} = a^2\{\Delta_2\} + a^3\{\Delta_3\} + \cdots \qquad (27)$$

where $\{\Delta_2\}$, $\{\Delta_3\}$, ... are kinematically admissible displacement functions which are orthogonal to $\{\Delta_1\}$ in the sense of Eq. (11), although the functions need not be higher order modes of Eq. (10).

Substituting Eq. (27) into Eq. (26) yields

$$\begin{aligned}
\mathcal{P}[a\Delta_1+\bar{\Delta}] = {} & a^2\left[L\Delta_1 J_i [K_0]_i \{\Delta_1\}_i + \lambda L\Delta_1 J_i [K_1]_i \{\Delta_1\}_i\right] + \\
& + a^3\left[L\Delta_1 J_i [H_1]_i \{\Delta_1\}_i + \lambda L\Delta_1 J_i [L_1]_i \{\Delta_1\}_i\right] + \\
& + a^4\left[L\Delta_1 J_i [H_2]_i \{\Delta_1\}_i + \lambda L\Delta_1 J_i [L_2]_i \{\Delta_1\}_i\right] + \\
& + a^4\left[L\Delta_2 J_i [K_0]_i \{\Delta_2\}_i + \lambda L\Delta_2 J_i [K_1]_i \{\Delta_2\}_i\right] + \\
& + 3a^4\left[L\Delta_1 J_i [H_1]_i \{\Delta_2\}_i + \lambda L\Delta_1 J_i [L_1]_i \{\Delta_2\}_i\right] + \\
& + 2a^3\left[L\Delta_1 J_i [K_0]_i \{\Delta_2\}_i + \lambda L\Delta_1 J_i [K_1]_i \{\Delta_2\}_i\right] + \\
& + 2a^4\left[L\Delta_1 J_i [K_0]_i \{\Delta_3\}_i + \lambda L\Delta_1 J_i [K_1]_i \{\Delta_3\}_i\right] + \\
& + 2a^5\left[L\Delta_2 J_i [K_0]_i \{\Delta_3\}_i + \lambda L\Delta_2 J_i [K_1]_i \{\Delta_3\}_i\right] + \\
& + a^6\left[L\Delta_3 J_i [K_0]_i \{\Delta_3\}_i + \lambda L\Delta_3 J_i [K_1]_i \{\Delta_3\}_i\right] + \\
& + 3a^5\left[L\Delta_1 J_i [H_1]_i \{\Delta_3\}_i + \lambda L\Delta_1 J_i [L_1]_i \{\Delta_3\}_i\right] +
\end{aligned}$$

$$+4a^6\left[\{\Delta_3\}_i[H_2]_i\{\Delta_1\}_i + \lambda\{\Delta_3\}_i[L_2]_i\{\Delta_1\}_i\right]+\cdots \qquad (28)$$

The unknown functions $\{\Delta_2\}$ and $\{\Delta_3\}$ are defined to minimize the increment in total potential energy. The variation with respect to $\{\Delta_2\}$ is

$$a^3\Big\{2a\left(\{\delta\Delta_2\}_i[K_0]_i\{\Delta_2\}_i+\lambda\{\delta\Delta_2\}_i[K_1]_i\{\Delta_2\}_i\right)+$$
$$+3a\left(\{\delta\Delta_2\}_i[H_1]_i\{\Delta_1\}_i+\lambda\{\delta\Delta_2\}_i[L_1]_i\{\Delta_1\}_i\right)+$$
$$+2\left(\{\delta\Delta_2\}_i[K_0]_i\{\Delta_1\}_i+\lambda\{\delta\Delta_2\}_i[K_1]_i\{\Delta_1\}_i\right)+$$
$$+2a^2\left(\{\delta\Delta_2\}_i[K_0]_i\{\Delta_3\}_i+\lambda\{\delta\Delta_2\}_i[K_1]_i\{\Delta_3\}_i\right)+\cdots\Big\}=0 \qquad (29a)$$

Variation with respect to $\{\Delta_3\}$ provides

$$a^4\Big\{2\left(\{\delta\Delta_3\}_i[K_0]_i\{\Delta_1\}_i+\lambda\{\delta\Delta_3\}_i[K_1]_i\{\Delta_1\}_i\right)+$$
$$+2a\left(\{\delta\Delta_3\}_i[K_0]_i\{\Delta_2\}_i+\lambda\{\delta\Delta_3\}_i[K_1]_i\{\Delta_2\}_i\right)+$$
$$+a^2\left(\{\delta\Delta_3\}_i[K_0]_i\{\Delta_3\}_i+\lambda\{\delta\Delta_3\}_i[K_1]_i\{\Delta_3\}_i\right)+$$
$$+3a\left(\{\delta\Delta_3\}_i[H_1]_i\{\Delta_1\}_i+\lambda\{\delta\Delta_3\}_i[L_1]_i\{\Delta_1\}_i\right)+$$
$$+4a^2\left(\{\delta\Delta_3\}_i[H_2]_i\{\Delta_1\}_i+\lambda\{\delta\Delta_3\}_i[L_2]_i\{\Delta_1\}_i\right)+\cdots\Big\}=0 \qquad (29b)$$

If $\lfloor A_2 \rfloor$ and $\lfloor A_3 \rfloor$ are kinematically admissible functions with only unknown amplitude coefficients, then we replace $\lfloor A_2 \rfloor$ by $\xi_2 \lfloor A_2 \rfloor$ and $\lfloor \delta A_2 \rfloor$ by $\delta \xi_2 \lfloor A_2 \rfloor$, etc. From the variational equations, Eq's. (29), we obtain

$$\left(\lfloor A_2 \rfloor_i [K_0]_i \{A_1\}_i + \lambda \lfloor A_2 \rfloor_i [K_1]_i \{A_1\}_i \right) +$$
$$+ a\xi_2 \left(\lfloor A_2 \rfloor_i [K_0]_i \{A_2\}_i + \lambda \lfloor A_2 \rfloor_i [K_1]_i \{A_2\}_i \right) +$$
$$+ \tfrac{3}{2} a \left(\lfloor A_2 \rfloor_i [H_1]_i \{A_1\}_i + \lambda \lfloor A_2 \rfloor_i [L_1]_i \{A_1\}_i \right) +$$
$$+ a^2 \xi_3 \left(\lfloor A_2 \rfloor_i [K_0]_i \{A_3\}_i + \lambda \lfloor A_2 \rfloor_i [K_1]_i \{A_3\}_i \right) + \ldots = 0 \qquad (30a)$$

and

$$\left(\lfloor A_3 \rfloor_i [K_0]_i \{A_1\}_i + \lambda \lfloor A_3 \rfloor_i [K_1]_i \{A_1\}_i \right) +$$
$$+ a\xi_2 \left(\lfloor A_3 \rfloor_i [K_0]_i \{A_2\}_i + \lambda \lfloor A_3 \rfloor_i [K_1]_i \{A_2\}_i \right) +$$
$$+ a^2 \xi_3 \left(\lfloor A_3 \rfloor_i [K_0]_i \{A_3\}_i + \lambda \lfloor A_3 \rfloor_i [K_1]_i \{A_3\}_i \right) +$$
$$+ \tfrac{3}{2} a \left(\lfloor A_3 \rfloor_i [H_1]_i \{A_1\}_i + \lambda \lfloor A_3 \rfloor_i [L_1]_i \{A_1\}_i \right) +$$
$$+ 2a^2 \left(\lfloor A_3 \rfloor_i [H_2]_i \{A_1\}_i + \lambda \lfloor A_3 \rfloor_i [L_2]_i \{A_1\}_i \right) + \ldots = 0 \qquad (30b)$$

A first approximation for coefficient ξ_2 is obtained if we set $\lambda = \lambda_1$, recognize orthogonality of the functions, and retain only the lower order terms. The result is

$$\xi_2 = - \frac{\frac{3}{2} \left(\lfloor A_2 \rfloor_i [H_1]_i \{A_1\}_i + \lambda_1 \lfloor A_2 \rfloor_i [L_1]_i \{A_1\}_i \right)}{\lfloor A_2 \rfloor_i [K_0]_i \{A_2\}_i + \lambda_1 \lfloor A_2 \rfloor_i [K_1]_i \{A_2\}_i} \qquad (31a)$$

In the absence of $[H_1]$ and $[L_1]$, $\xi_2 = 0$ and

$$\xi_3 = -\frac{2\left(\{A_3\}_i^T [H_2]_i \{A_1\}_i + \lambda_1 \{A_3\}_i^T [L_2]_i \{A_1\}_i\right)}{\{A_3\}_i^T [K_0]_i \{A_3\}_i + \lambda_1 \{A_3\}_i^T [K_1]_i \{A_3\}_i} \tag{31b}$$

These solutions are valid in the neighborhood of the bifurcation point. If the slope of the initial post-buckling response curve is negative, then no further refinement in ξ_2 or ξ_3 is required, as actual post-buckling structural response will not be along equilibrium paths predicted from static theory of deformation. However, for structures with stable post-buckling response a load-deflection estimate for finite loads beyond the critical load is of interest and can be obtained by forming solutions for ξ_2 and ξ_3 from Eq's. (30).

2.4 Extended Solution for Post-Buckling Stable Structure.

Direct solution of Eq. (30) is difficult because the amplitude coefficient $\underline{a}$ enters non-homogeneously. This difficulty can be eliminated in a second approximate solution if the modal functions are derived from the following simplified characteristic equation (rather than from Eq. (10)):

$$\left([K_0] + \lambda_i [K_1]\right) \{A_i'\} = \{0\} \tag{32a}$$

The orthogonality conditions are

$$\{A_j'\}^T [K_0] \{A_i'\} = \begin{cases} -\lambda_i & j = i \\ 0 & j \neq i \end{cases} \tag{32b}$$

$$\{A_j'\}^T [K_1] \{A_i'\} = \begin{cases} 1 & j = i \\ 0 & j \neq i \end{cases} \tag{32c}$$

Vectors $[A_2']$, $[A_3']$ . . . are now associated with higher order eigenvalues $\lambda_2, \lambda_3 \ldots$. Using these functions Eq's. (30) reduce to

$$\xi_2'\left([A_2']_i[K_0]_i\{A_2'\}_i + \lambda[A_2']_i[K_1]\{A_2'\}\right) + \frac{3}{2}\left([A_2']_i[H_1]_i\{A_1\}_i + \lambda[A_2']_i[L_1]_i\{A_1\}_i\right) = 0$$

$$a\xi_3'\left([A_3'][K_0]_i\{A_3'\}_i + \lambda[A_3'][K]_i\{A_3'\}\right) + \frac{3}{2}\left([A_3']_i[H_1]_i\{A_1\}_i + \lambda[A_3']_i[L_1]_i\{A_1\}_i\right) +$$

$$+ 2a\left([A_3']_i[H_2]_i\{A_1\}_i + \lambda([A_3']_i[L_2]_i\{A_1\}_i\right) = 0$$

These equations are of the same form as Eq's. (30), and correspondingly the solutions are

$$\xi_2' = -\frac{\frac{3}{2}\left([A_2']_i[H_1]_i\{A_1\}_i + \lambda[A_2']_i[L_1]_i\{A_1\}_i\right)}{[A_2']_i[K_0]_i\{A_2'\}_i + \lambda[A_2']_i[K_1]_i\{A_2'\}_i} \qquad (33a)$$

and if $[H_1] = [L_1] = [0]$

$$\xi_3' = -\frac{2\left([A_3']_i[H_2]_i\{A_1\}_i + \lambda[A_3']_i[L_2]_i\{A_1\}_i\right)}{[A_3']_i[K_0]_i\{A_3'\}_i + \lambda[A_3']_i[K_1]_i\{A_3'\}_i} \qquad (33b)$$

for $\lambda \geq \lambda_1$. As $\lambda \to \lambda_2$ the solution for $\xi_2' \to \infty$. This condition is analogous to the condition on $\{A_1\}$ as $\lambda \to \lambda_1$. Thus as $\lambda \to \lambda_2$ we take

$$\{A\} = a\{A_1\} + a^2\{A_2'\} + \{\bar{A}\} \qquad (34)$$

and represent $\{\bar{A}\}$ by higher order modal functions obtaining an equation for the increment in total potential energy similar to Eq. (26) except terms in $\{A_2'\}$ supplement those of $\{A_1\}$.

Eq's. (33) are uncoupled, again representing an approximate solution. A completely general solution (within assumptions on small strains, static theory, etc.) using Eq's. (32) requires solution of Eq's. (30) with $\underline{a}$ entering non-homogeneously. Under this circumstance Eq. (28) may be minimized with respect to $\underline{a}$ and solution for a, ξ_2, ξ_3 . . . carried out simultaneously. The set of coupled non-linear algebraic equations in coefficients a, ξ_2, ξ_3 . . . are difficult to solve, negating the numerical advantage of this method. As in the Rayleigh-Ritz method, rapid convergence with modal function content is to be expected for problems satisfying conditions for consideration by this method.

Using this extended solution technique, developed classically by Koiter (26), stable post-buckling structural equilibrium configurations can be evaluated for finite loads above the critical buckling load. In this calculation Eq. (28) is used directly for the increment in total potential energy.

2.5 Post-Buckling Equilibrium and Stability.

Returning to consideration of the simplified equations the increment in total potential energy, in the notation of Koiter (26) is

$$\mathcal{P}[aA_1+\bar{A}] = a^2(\lambda-\lambda_1)A_2' + a^3A_3 + a^4A_4 + a^5A_5 + \cdots \quad (35)$$

and setting $\lambda = \lambda_1$ the corresponding approximations for the A_i are:

$$A_2' = \lfloor A_1 \rfloor_i [K_1]_i \{A_1\}_i$$

$$A_3 = \lfloor A_1 \rfloor_i [H_1]_i \{A_1\}_i + \lambda_1 \lfloor A_1 \rfloor_i [L_1]_i \{A_1\}_i$$

$$A_4 = \lfloor A_1 \rfloor_i [H_2]_i \{A_1\}_i + \lambda_1 \lfloor A_1 \rfloor_i [L_2]_i \{A_1\}_i$$

$$+ \lfloor A_2 \rfloor_i [K_0]_i \{A_2\}_i + \lambda_1 \lfloor A_2 \rfloor_i [K_1]_i \{A_2\}_i$$

where the amplitude coefficient ξ_2 is contained in $\lfloor A_2 \rfloor_i$, and is evaluated by Eq. (31a). Because of the conditions imposed in order to obtain Eq. (31a), Eq. (35) is valid only in the neighborhood of the critical load. The post-buckling response computed next, then also is an estimate valid only in the immediate neighborhood of the critical load.

Representation of the total potential energy increment by Eq. (35) corresponds to truncation of Eq. (27) to

$$\{\bar{A}\}_i = a^2 \{A_2\}$$

If $A_3=0$, then $\{A_2\}_i = \{0\}$ and the criterion for stability is again associated with A_4.

So far the minimization of the potential energy increment has been with respect to kinematically admissible displacement functions with $\underline{a}$ held constant. The post-buckling equilibrium configurations are defined for values of $\underline{a}$ that minimize the energy as well. Therefore, setting

$$\frac{d}{da}\left(P[aA_1+\bar{A}]\right) = 2a(\lambda-\lambda_1)A_2' + n A_n a^{n-1} = 0 \,, \quad n \geq 3 \qquad (36)$$

the values of $\underline{a}$ that satisfy this polynomial equation for particular values of $(\lambda-\lambda_1)$ correspond to equilibrium configurations of the system. These configurations are stable or unstable depending upon whether the second variation of the energy increment evaluated at each point is respectively positive or negative

$$\frac{d^2}{da^2}\left(\mathcal{P}[a\phi_1+\bar{\Delta}]\right) = 2(\lambda-\lambda_1)A_2' + n(n-1)A_n a^{n-2}, \quad n\geq 3 \tag{37}$$

One solution to Eq. (36) is $\underline{a}=0$, which is a stable solution if $\lambda<\lambda_1$ (State I) and unstable for $\lambda>\lambda_1$ as determined from Eq. (37). Other possible solutions represent equilibrium states the stability of which are determined by substitution into Eq. (37). That is

$$\frac{d^2}{da^2}\left(\mathcal{P}[a\phi_1+\bar{\Delta}]\right) = -2(n-2)(\lambda-\lambda_1)A_2', \quad n\geq 3 \tag{38}$$

For A_2' negative, this result determines that for $\lambda>\lambda_1$ the adjacent states of equilibrium are stable, and for $\lambda<\lambda_1$ the equilibrium states are unstable.

The case of n odd or even must be treated separately in Eq. (38). For n odd a real solution exists for which the sign of $\underline{a}$ and of A_n correspond. A plot of the incremental load-deflection relation for the case $A_3>0$ is shown in Figure 1. As predicted by Eq. (38) for $\lambda-\lambda_1>0$ the equilibrium is stable (solid straight line path), and for $\lambda-\lambda_1<0$ the equilibrium is unstable (dashed line paths). For a structure

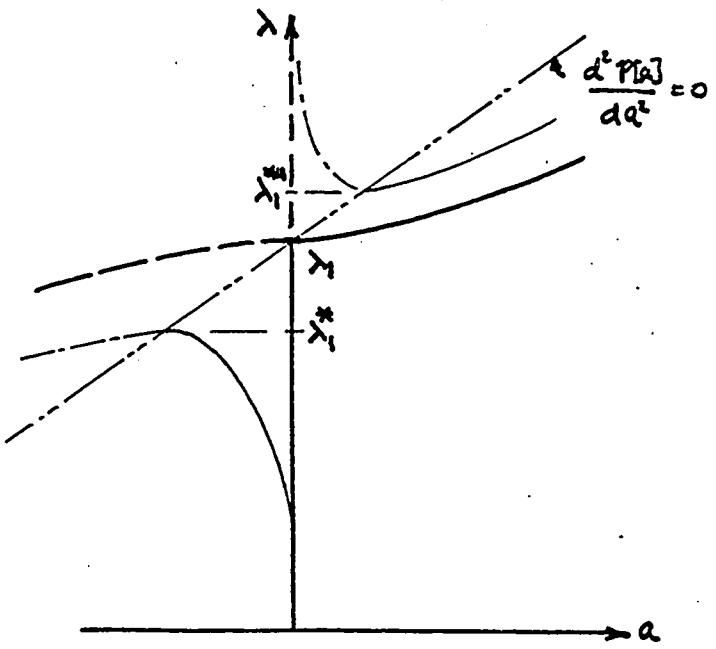

Figure II-1: Configuration Space: $A_3 > 0, \varepsilon > 0$

not constrained against $\underline{a} < 0$, the post-buckling response is unstable.

For n even in Eq. (37) real solutions for $\lambda - \lambda_1 > 0$ depend upon the sign of A_n. For A_n negative, in particular $A_3 = 0$ and $A_4 < 0$, the response is that shown in Figure 2, in which post-buckling equilibrium is unstable, i.e. $\lambda - \lambda_1 < 0$ as predicted by Eq. (36).

For A_n positive, in particular $A_3 = 0$, $A_4 > 0$, the response is that shown in Figure 3 in which post-buckling equilibrium is stable.

If $A_3 = A_4 = 0$ then the question of stability must be resolved by including higher order terms in Eq. (38).

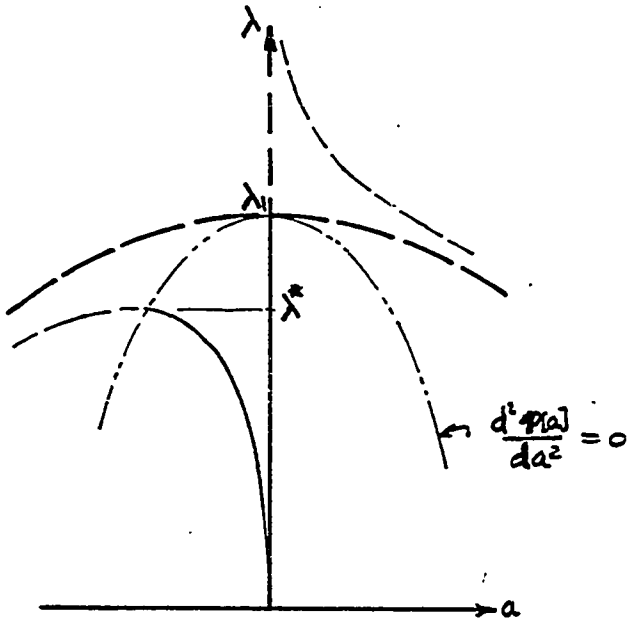

Figure II-2. Configuration Space: $A_3 = 0, A_4 < 0, \varepsilon > 0$

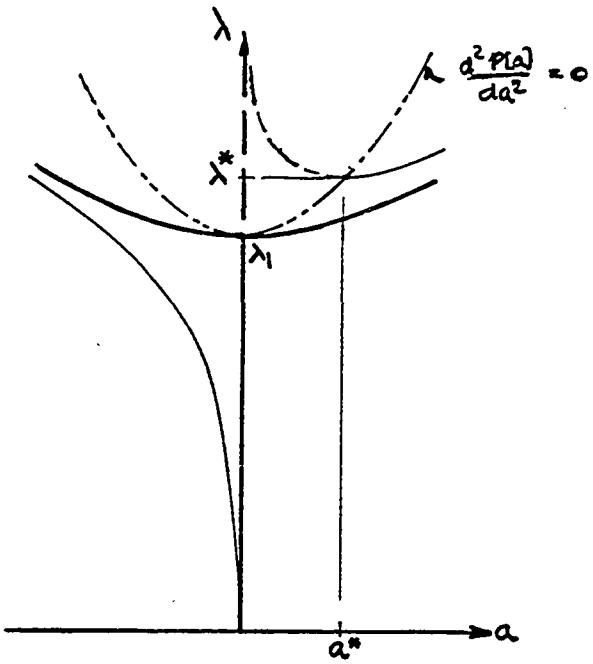

Figure II-3. Configuration Space: $A_3 = 0, A_4 > 0, \varepsilon > 0$

2.6 Response of the Imperfect Structure.

Two types of conditions produce deviations of the structure from otherwise perfect-structure bifurcation buckling. One is an initial shape imperfection and the second is load eccentricity. A geometric imperfection can be represented mathematically by a perturbation on the displacement function of magnitude ε :

$$\{\Delta\} = \{\Delta_0\} + \{\bar{\Delta}\} + \varepsilon\{\Delta_e\} \qquad (39)$$

Displacement $\{\Delta_0\}$ corresponds to initial state perfect structure displacement; $\{\bar{\Delta}\}$ is the displacement increment from higher order effects; and $\varepsilon\{\Delta_e\}$ is the amplitude and shape of the imperfection.

We assume the amplitude, ε , of the imperfection is small and structural response remains essentially linear up to loads approaching the critical load. The predominant energy addition is then the work done by the external load appearing as a bending moment, the moment caused by the geometric offset.

Under the same restriction of essentially linear prebuckling response, load eccentricity is accounted for in the external work integral by a dimensional misalignment of the load by, say, magnitude ε .

Introduction of either or both of these deviations into the expression for the total potential energy results in additional terms in ε , that is

$$\mathcal{P}[A] + \varepsilon\, Q[A] \tag{40}$$

replaces $\mathcal{P}[A]$ of Eq. (7). The expansion of Eq. (7) is to

$$\mathcal{P}[A] + \varepsilon Q[A] = \lambda \varepsilon \, [c]_i \{\Xi\}_i + \left[[\Xi]_i [K_0]_i \{\Xi\}_i + \lambda [\Xi]_i [K_1]_i \{\Xi\}_i \right] +$$
$$+ \left[[\Xi]_i [H_1]_i \{\Xi\}_i + \lambda [\Xi]_i [L_1]_i \{\Xi\}_i \right] +$$
$$+ \left[[\Xi]_i [H_2]_i \{\Xi\}_i + \lambda [\Xi]_i [L_2]_i \{\Xi\}_i \right] + \cdots \tag{41}$$

Only the predominant term in ε is retained in Eq. (41). Eq. (41) is an incremental energy equation as the perfect-structure axial deformation energies have been eliminated in the incrementation. For the case of a geometric eccentricity, $[c]$ contains $\{A_e\}$.

From this point forward the procedure parallels that developed for the perfect structure. We assume that the response can be represented by a superposition of buckling modes, Eq. (10), and evaluate the increment in total potential energy. We again can distinguish a first-approximation solution from a more general solution each having applicability dependent upon problem type.

Series expansion of the potential energy increment is

$$\mathcal{P}[\Xi,\lambda] + \varepsilon Q[\Xi,\lambda] = \left\{ \mathcal{P}[\Xi,\lambda] + \varepsilon Q[\Xi,\lambda] \right\}_{\lambda=\lambda_1} + (\lambda - \lambda_1) \frac{\partial}{\partial \lambda} \left\{ \mathcal{P}[\Xi,\lambda] + \varepsilon Q[\Xi,\lambda] \right\}_{\lambda=\lambda_1} \tag{42}$$

which results in an equation similar to Eq. (26). For the case of a single zero root of the determinantal equation an assumed incremental displacement function is

$$\{\Delta\} = a\{\Delta_1\} + a^2\{\Delta_2\} + \lambda\varepsilon\{\Delta_p\} + a^3\{\Delta_3\} + \cdots \qquad (43)$$

First order solutions for the coefficients of $\{\Delta_2\}$, $\{\Delta_3\}$ . . . are identical to Eq's. (31a,b).

First order approximation for the coefficient of $\{\Delta_p\}$ is obtained in like manner, in particular

$$\xi_p = \frac{\frac{1}{2}[C]_i\{\Delta_p\}_i}{[\Delta_p]([K_0] + \lambda_1[K_1])\{\Delta_p\}} \qquad (44)$$

$$\text{with} \qquad [\Delta_p][T]\{\Delta_1\} = 0$$

The simplifying assumptions entering into the derivation of Eq. (44) are that ξ_p, a, ξ_2, ξ_3 . . . are small quantities less than unity, and that for the solution applicable in the neighborhood of the bifurcation we take $\lambda \simeq \lambda_1$. Evaluation of Eq. (44) depends upon explicit definition of the type of imperfection in order to define $[C]$.

The final form of representation of the energy increment, similar to Eq. (35), is

$$\mathcal{P}[a] = a^2(\lambda-\lambda_1)A_2' + a^3A_3 + a^4A_4 + \cdots + a\varepsilon\lambda[C]_i\{\Delta_1\}_i + a^2\varepsilon\lambda[C]_i\{\Delta_2\}_i + \cdots \qquad (45)$$

First order truncation of Eq. (45) is simply

$$\mathcal{P}[a] = a^2(\lambda-\lambda_1)A_2' + a^nA_n + \varepsilon a B_1 \qquad (46)$$

where

$$B_1 = \lambda\,[C]_i\{\Delta_1\}_i \qquad (47)$$

Based upon this approximation of the increment in total potential energy the equilibrium states are given by

$$\frac{d}{da}\left(p[a]\right) = \varepsilon B_1 + 2a(\lambda-\lambda_1)A_2' + n a^{n-1} A_n = 0 \qquad (48)$$

In a first approximation solution we take

$$B_1 = \lambda_1 \, {}^{L}c_J{}_i \, \{\Delta_1\}_i \qquad (49)$$

The equilibrium state is stable only if the energy is at a relative minimum which is determined from the sign of

$$\frac{d^2}{da^2}\left(p[a]\right) = 2(\lambda-\lambda_1)A_2' + n(n-1)a^{n-2}A_n \;, \quad n \geq 3 \qquad (50)$$

For A_2' negative and the sense of εB_1 determined by ε (B_1 positive), then the question of stability depends upon the sign of ε and A_n, and whether n is odd or even.

For n odd an equilibrium value of $\underline{a}$ for values of ε and A_n will be the same as $-\underline{a}$ for values of $-\varepsilon$ and $-A_n$. Thus the distinct cases are:

$$\begin{aligned} &\text{i)} \quad n \text{ odd} \quad A_n > 0, \quad \varepsilon > 0 \\ &\text{ii)} \quad n \text{ odd} \quad A_n > 0, \quad \varepsilon < 0 \end{aligned} \qquad (51a)$$

For n even a solution for $\underline{a}$ corresponding to ε will be the same as $-\underline{a}$ for $-\varepsilon$. Thus it suffices to consider a, $\varepsilon > 0$ and A_n either sign, so that

$$\begin{aligned} &\text{iii)} \quad n \text{ even} \quad A_n < 0, \quad \varepsilon > 0 \\ &\text{iv)} \quad n \text{ even} \quad A_n > 0, \quad \varepsilon < 0 \end{aligned} \qquad (51b)$$

Each of these four cases is analyzed by Koiter (26) to determine the specific nature of the response.

In general the analysis shows either a perturbation or removal of critical load phenomena depending upon the case. For Case (i) roots λ_1^* and λ_1^{**} are obtained corresponding to branch response limits between stable (solid curved lines in Figure 1) and unstable (short-long dashed lines in Figure 1) depending upon the level of loading and value of a. As $\varepsilon \to 0$ the two curved branches connect at the bifurcation giving the perfect structure response.

Case (ii) is a perturbation on the same perfect structure response as Case (i). It is shown in Figure 4, where it is seen that no evidence of a limit load is obtained. The reduction to the perfect structure response as $\varepsilon \to 0$ is apparent.

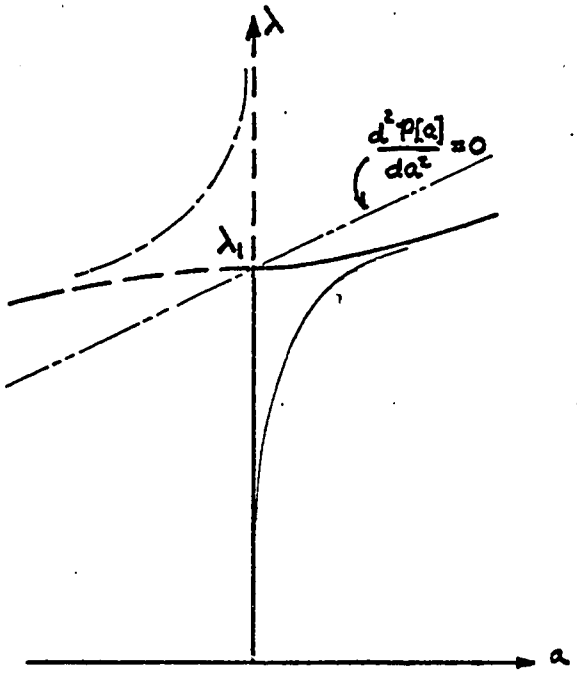

Figure II-4. Configuration Space: $A_3>0, \varepsilon<0$

The λ-$\underline{a}$ diagram for Case (iii) is shown in Figure 2. Response is stable for $\lambda < \lambda^*$ and $\underline{a}$ is negative. No load for any value of $\underline{a}$ corresponds to stable equilibrium above $\lambda = \lambda^*$.

Case (iv) is shown in Figure 3. For load gradually increasing the structure shows no buckling characteristic. A second stable branch can exist for $\lambda > \lambda^*$ and $\underline{a} > \underline{a}^*$. Actual placement on this equilibrium path would require loading of the structure while constrained, with subsequent release (34).

For structures that can be represented by an incremental energy equation of the form of Eq. (46), imperfect structure response will be characterized by one of the four cases described. The physically important branch in most structural applications is the one associated with the gradual increase of load from the no-load condition. It should be noted that information derived from Eq's. (48), (49), and (50) includes the limit load estimates λ^*, λ^{**} (when present) and estimate of the equilibrium paths in the nieghborhood of the perfect-structure buckling load.

2.7 Extended Solution for Imperfect Structure.

Extension of the imperfect theory for post-buckling stable structures is a valuable consideration as an estimate of the complete small-deflection response can be determined for finite loads beyond the critical load. Again, introducing the modified definition of the modal functions given by Eq. (32), the displacement expansion assumed is that of Eq. (43). Substituting into the potential function, Eq. (41), resultant variational

equations are:

with respect to ξ_2:

$$a^2\lambda\varepsilon\,[C]_i\{A_2'\}_i + 2a^4\xi_2\left[[A_2']_i[K_0]_i\{A_2'\}_i + \lambda\,[A_2']_i[K_1]_i\{A_2'\}_i\right] + \\ + 3a^4\left[[A_2']_i[H_1]_i\{A_1\}_i + \lambda\,[A_2']_i[L_1]_i\{A_1\}_i\right] + \\ + 4a^5\left[[A_2']_i[H_2]_i\{A_1\}_i + \lambda\,[A_2']_i[L_2]_i\{A_1\}_i\right] + \cdots = 0 \tag{52a}$$

with respect to ξ_3:

$$a^3\lambda\varepsilon\,[C]_i\{A_3'\}_i + 2a^6\xi_3\left[[A_3']_i[K_0]_i\{A_3'\}_i + \lambda\,[A_3']_i[K_1]_i\{A_3'\}_i\right] + \\ + 3a^5\left[[A_3']_i[H_1]_i\{A_1\}_i + \lambda\,[A_3']_i[L_1]_i\{A_1\}_i\right] + \\ + 4a^6\left[[A_3']_i[H_2]_i\{A_1\}_i + \lambda[A_3']_i[L_2]_i\{A_1\}_i\right] + \cdots = 0 \tag{52b}$$

with respect to ξ_p:

$$\lambda^2\varepsilon^2\,[C]_i\{A_p'\}_i + \\ + 2\lambda^2\varepsilon^2\xi_p\left[[A_p']_i[K_0]_i\{A_p'\}_i + \lambda\,[A_p']_i[K_1]_i\{A_p'\}_i\right] + \cdots = 0 \tag{52c}$$

If ε is assumed small and coupling of the higher order modes with the imperfection is assumed negligible, then Eq's. (52 a,b) provide solutions identical to Eq's. (33 a,b), respectively. The solution for ξ_p' is

$$\xi_p' = \frac{\frac{1}{2}\,[C]_i\{A_p'\}_i}{[A_p']_i\left([K_0]_i + \lambda[K_1]_i\right)\{A_p'\}} \tag{53}$$

and the increment in potential energy is

$$P[a]+\varepsilon Q[a] = a\varepsilon\lambda B_1 + a^2(\lambda-\lambda_1)A_2' + a^n A_n \tag{54}$$

where

$$A_2' = \{\Delta_1\}_i^T [K_1]_i \{\Delta_1\}_i$$

$$A_3 = \{\Delta_1\}_i^T [H_1]_i \{\Delta_1\}_i + \lambda \{\Delta_1\}_i^T [L_1]_i \{\Delta_1\}_i$$

$$A_4 = \{\Delta_1\}_i^T [H_2]_i \{\Theta_1\}_i + \lambda \{\Delta_1\}_i^T [L_2]_i \{\Delta_1\}_i$$

$$+ \{\Delta_2'\}^T [K_0] \{\Delta_2'\}_i + \lambda \{\Delta_2'\}^T [K_1]_i \{\Delta_2'\}_i$$

$$B_1 = \{C\}_i^T \{\Delta_1\}_i \tag{55}$$

all quantities functions of the load parameter λ. It is seen that in Eq. (54) as $\lambda \to 0$ an admissible solution is $\underline{a}=0$.

III. POST-BUCKLING RESPONSE OF COLUMNS

3.1 Nonlinear Strain-Displacement Equations.

Typical positive deformations of a line element under extension and flexure in the x-y plane are shown in Figure 1a. The position of a material point before deformation is given by

$$\vec{r} = \vec{r}_o + \eta \vec{n} \tag{1}$$

where $\vec{r}_o = x\vec{\imath}$ and η is the coordinate scalar along $\vec{n}$ measured from the neutral axis of the element. Assuming plane sections remain plane, the position of the material point after deformation is

$$\vec{R} = \vec{r}_o + u\vec{\imath} + v\vec{\jmath} + \Omega\eta\vec{\imath} \tag{2}$$

where change in the thickness dimension is assumed neglibible. Next, forming

$$d\vec{r} \cdot d\vec{r} = (dx)^2 + (d\eta)^2 \tag{3}$$

$$\begin{aligned} d\vec{R} \cdot d\vec{R} = {} & (dx)^2 + (du)^2 + \eta^2(d\Omega)^2 + \Omega^2(d\eta)^2 + \\ & + 2dxdu + 2\eta dx d\Omega + 2\Omega dx d\eta + \\ & + 2\eta du d\Omega + 2\Omega du d\eta + 2\eta\Omega d\Omega d\eta + \\ & + (dv)^2 + \eta^2(d\Omega)^2 + \Omega^2(d\eta)^2 \end{aligned} \tag{4}$$

the strain components are defined

$$2 e_{ij} dx_i dx_j = d\vec{R} \cdot d\vec{R} - d\vec{r} \cdot d\vec{r} \tag{5}$$

where i and j identify variables x and η, respectively. Thus

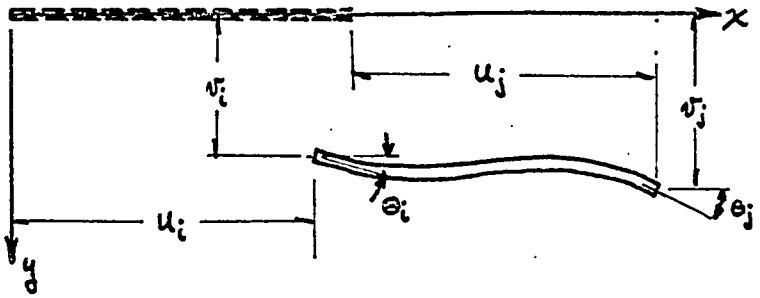

(a)

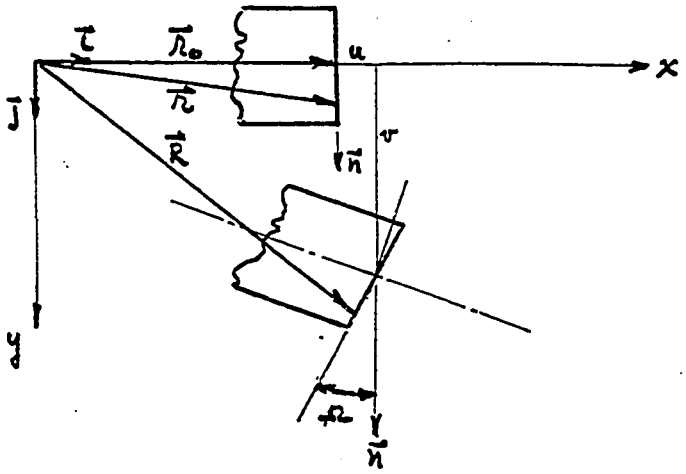

(b)

Figure III-1. Line Element Geometry and Deformation.

$$e_{xx} = \frac{du}{dx} + \eta \frac{d\Omega}{dx} + \frac{1}{2}\left(\frac{du}{dx}\right)^2 + \frac{1}{2}\eta^2\left(\frac{d\Omega}{dx}\right)^2 + \\ + \eta \frac{du}{dx}\frac{d\Omega}{dx} + \frac{1}{2}\left(\frac{dv}{dx}\right)^2 + \cdots \qquad (6)$$

$$2e_{x\eta} = \Omega + \Omega \frac{du}{dx} + \eta \Omega \frac{d\Omega}{dx} + \frac{dw}{dx} \qquad (7)$$

$$e_{\eta\eta} = \Omega^2 \qquad (8)$$

Transverse shear deformation is assumed negligible. Setting $e_{x\eta} = 0$ a relation between Ω and the neutral axis displacements is obtained as follows

$$\Omega = \frac{-\frac{dv}{dx}}{1 + \frac{du}{dx}} = -\frac{dv}{dx}\left[1 - \frac{du}{dx} + \frac{1}{2}\left(\frac{du}{dx}\right)^2 + \cdots\right] \qquad (9)$$

Substituting this relation into Eq. (6)

$$e_{xx} = \frac{du}{dx} + \frac{1}{2}\left(\frac{dv}{dx}\right)^2 + \frac{1}{2}\left(\frac{du}{dx}\right)^2 - \eta\left(\frac{d^2v}{dx^2}\right) + \frac{1}{2}\eta^2\left(\frac{d^2v}{dx^2}\right)^2 + \cdots \qquad (10)$$

Strains in the thickness direction were neglected initially so that Eq. (8) is incomplete and is dropped from subsequent development.

Two sets of nonlinear equations for the line element can be developed based upon extensibility or inextensibility of the element neutral axis. We consider the latter case first.

3.2 Total Potential Energy: Inextensional Case.

Inextensibility of the neutral axis requires $e_{xx}\big|_{\eta=0} = 0$,

and from Eq. (10) we find

$$\frac{du}{dx} = -\frac{1}{2}\left(\frac{dv}{dx}\right)^2 - \frac{1}{8}\left(\frac{dv}{dx}\right)^4 + \cdots \qquad (11)$$

so that

$$\epsilon_{xx} = -\eta \frac{d^2v}{dx^2} - \frac{\eta}{2}\left(\frac{dv}{dx}\right)^2 \frac{d^2v}{dx^2} + \cdots \qquad (12)$$

The displacement function selected for v(x) is the exact solution of the Bernoulli-Euler static flexure equation for a uniform beam,

$$v(x) = \begin{bmatrix} 1 & x & x^2 & x^3 \end{bmatrix} \begin{Bmatrix} b_0 \\ b_1 \\ b_2 \\ b_3 \end{Bmatrix} \qquad (13)$$

Boundary conditions are:

$$v(0) = v_i \;,\; v(\ell) = v_j \;,\; \left.\frac{dv}{dx}\right|_0 = \theta_i \;,\; \left.\frac{dv}{dx}\right|_\ell = \theta_j$$

Solving for the coefficients b_i:

$$v(x) = \begin{bmatrix} 1 & x & x^2 & x^3 \end{bmatrix} [B] \{\Delta\} \qquad (14)$$

where

$$[B] = \begin{bmatrix} 1 & 0 & 0 & 0 \\ 0 & 1/\ell & 0 & 0 \\ -3/\ell^2 & -2/\ell & 3/\ell^2 & -1/\ell \\ 2/\ell^3 & 1/\ell^2 & -2/\ell^3 & 1/\ell^2 \end{bmatrix} \qquad (15)$$

$$\begin{bmatrix} \Delta \end{bmatrix} = \begin{bmatrix} v_i & \theta_i \ell & v_j & \theta_j \ell \end{bmatrix}$$

Differentiating v(x) and substituting into Eq. (12)

$$\epsilon_{xx} = -\begin{bmatrix} 0 & 0 & 2 & 6x \end{bmatrix} [B] \{\Delta\} + -\frac{1}{2} \begin{bmatrix} \Delta \end{bmatrix} [B]^T [G] [B] \{\Delta\} \begin{bmatrix} 0 & 0 & 2 & 6x \end{bmatrix} [B] \{\Delta\} \qquad (16)$$

where

$$[G] = \begin{bmatrix} 0 & 0 & 0 & 0 \\ & 1 & 2x & 3x^2 \\ & & 4x^2 & 6x^3 \\ \text{SYM} & & & 9x^4 \end{bmatrix} \tag{17}$$

If the material of the member is isotropic then $\sigma_{xx} = E e_{xx}$ and the strain energy is

$$U = \frac{E}{2}\int_v e_{xx}^T e_{xx}\, dv \tag{18}$$

for corresponding zero stress and zero strain states. For the case of dead weight loading the work done is

$$W = \lambda P_j \int_0^l \left(\frac{du}{dx}\right) dx = -\frac{\lambda P_j}{2}\int_0^l \left(\frac{dv}{dx}\right)^2 dx - \frac{\lambda P_j}{8}\int_0^l \left(\frac{dv}{dx}\right)^4 dx \tag{19}$$

In the product λP_j, the P_j represents a reference or unit load, and λ the load intensity. The total potential energy is

$$P[v] = U[v] - W[v] \tag{20}$$

or

$$\begin{aligned} P[v] = {} & \frac{E}{2}\int_v \eta^2 \{a\}[B]^T[C][B]\{a\}\, dv + \\ & + \frac{E}{2}\int_v \eta \{a\}[B]^T \begin{Bmatrix} 0 \\ 0 \\ 2 \\ 6x \end{Bmatrix} \{a\}[B]^T[G][B]\{a\} \begin{bmatrix} 0 & 0 & 2 & 6x \end{bmatrix} [B]\{a\}\, dv + \\ & + \frac{E}{2}\int_v \eta^2 \{a\}[B]^T \begin{Bmatrix} 0 \\ 0 \\ 2 \\ 6x \end{Bmatrix} \{a\}[B]^T[G][B]\{a\} \{a\}[B]^T[G][B]\{a\} \begin{bmatrix} 0 & 0 & 2 & 6x \end{bmatrix} [B]\{a\}\, dv + \\ & + \frac{\lambda P_j}{2}\int_0^l \{a\}[B]^T[G][B]\{a\}\, dx + \\ & + \frac{\lambda P_j}{8}\int_0^l \{a\}[B]^T[G][B]\{a\} \{a\}[B]^T[G][B]\{a\}\, dx \end{aligned} \tag{21}$$

Retaining terms through fourth order in $\{\Delta\}$ the integrated expression for the total potential energy is

$$P[v] = \frac{EI}{2\ell^3}[\Delta][K_0]\{\Delta\} + \frac{\lambda P_j}{2\ell}[\Delta][K_1]\{\Delta\} + \frac{EI}{2\ell^5}[\Delta][H_2]\{\Delta\} + \frac{\lambda P_j}{8\ell^3}[\Delta][L_2]\{\Delta\} + \cdots \tag{22}$$

In the above equations

$$[K_0] = \begin{bmatrix} 12 & 6 & -12 & 6 \\ & 4 & -6 & 2 \\ & & 12 & -6 \\ \text{SYM} & & & 4 \end{bmatrix} \qquad [C] = \begin{bmatrix} 0 & 0 & 0 & 0 \\ & 0 & 0 & 0 \\ & & 4 & 12x \\ \text{SYM} & & & 36x^2 \end{bmatrix}$$

$$[K_1] = \begin{bmatrix} 6/5 & 1/10 & -6/5 & 1/10 \\ & 3/15 & -1/10 & -1/30 \\ & & 6/5 & -1/10 \\ \text{SYM} & & & 3/15 \end{bmatrix} \tag{23}$$

and $[H_2]$ and $[L_2]$, which contain $\{\Delta\}$ to second order, are derived in Appendix A.

Because of the assumption on inextensibility of the member no evidence of an initial load state appears in Eq. (22). Thus, Eq. (22) itself is an incremental energy equation with displacement v(x) occurring in the transition from a rigid State I to an adjacent State II.

3.3 Total Potential Energy: Extensional Case.

Development of an energy equation that includes extensional effects proceeds as above except the strain is defined

by Eq. (10). To establish an estimate of the order of terms in Eq. (16), we examine the physical transition to the buckled configuration. Just prior to buckling, if the axial load is $\bar{P}$, then the axial deformation is

$$u = \frac{\bar{P}\ell}{AE} \tag{24}$$

which does not change appreciably during buckling. After buckling the moment at any station in the column is characterized by

$$M = \bar{P}v = EI\frac{d^2v}{dx^2} \tag{25}$$

Combining Eq. (24) and (25) by eliminating $\bar{P}$

$$u = O\left(\frac{I\ell}{Av}\frac{d^2v}{dx^2}\right) \tag{26}$$

For h a characteristic thickness parameter in the plane of bending, appropriate non-dimensionalization is

$$\begin{aligned} \bar{v} &= \frac{v}{h} = O(1) \\ \bar{x} &= \frac{x}{\ell} = O(1) \\ \bar{\eta} &= \frac{\eta}{h} = O(1) \end{aligned} \tag{27}$$

Substituting into Eq. (26),

$$u = O\left(\frac{h^2}{\ell}\right) \quad \text{or} \quad \bar{u} = \frac{u\ell}{h^2} = O(1) \tag{28}$$

Non-dimensionalizing e_{xx} in terms of $\bar{x}$, $\bar{\eta}$, $\bar{u}$ and $\bar{v}$ yields

$$e_{xx} = \frac{h^2}{\ell^2}\left(\frac{d\bar{u}}{d\bar{x}}\right) + \frac{h^2}{\ell^2}\left(\frac{d\bar{v}}{d\bar{x}}\right)^2 + \frac{h^2}{\ell^2}\left(\bar{\eta}\,\frac{d^2\bar{v}}{d\bar{x}^2}\right) + \\ + \frac{h^4}{\ell^4}\left(\frac{d\bar{u}}{d\bar{x}}\right)^2 + \frac{h^4}{\ell^4}\left(\bar{\eta}\,\frac{d^2\bar{v}}{d\bar{x}^2}\right)^2 + O\left(\frac{h^5}{\ell^5}\right) \qquad (29)$$

where all terms in parentheses are O(1). For common engineering materials a criterion for elastic post-buckling response is

$$\text{slenderness ratio} = \sqrt{\frac{A\ell^2}{I}} > 150 \Rightarrow \frac{h}{\ell} < \frac{1}{6}$$

On this basis a reasonable approximation of the total potential energy is to retain terms through $O(\frac{h^4}{\ell^4})$. The strain energy and work integrals are, respectively

$$U = \frac{E}{2}\int_{\mathcal{V}} e_{xx}^T e_{xx}\, dx = \frac{E}{2}\int_{\mathcal{V}} \left(\frac{du}{dx}\right)^T\left(\frac{du}{dx}\right) d\mathcal{V} \\ + \frac{E}{2}\int_{\mathcal{V}} \left(\frac{du}{dx}\right)^T\left[\left(\frac{dv}{dx}\right)^T\left(\frac{dv}{dx}\right)\right] d\mathcal{V} + \frac{E}{8}\int_{\mathcal{V}} \left(\frac{dv}{dx}\right)^T\left(\frac{dv}{dx}\right)\left(\frac{dv}{dx}\right)\left(\frac{dv}{dx}\right)^T d\mathcal{V} \qquad (30) \\ + \frac{E}{2}\int_{\mathcal{V}} \eta^2\left(\frac{d^2v}{dx^2}\right)^T\left(\frac{d^2v}{dx^2}\right) d\mathcal{V} + O\left(\frac{h^5}{\ell^5}\right)$$

$$W = \lambda P_j \int_0^\ell e_{xx}\big|_{\eta=0}\, dx = \lambda P_j \int_0^\ell \left(\frac{du}{dx}\right) dx + \frac{\lambda P_j}{2}\int_0^\ell \left(\frac{dv}{dx}\right)^T\left(\frac{dv}{dx}\right) dx + \\ + \frac{\lambda P_j}{2}\int_0^\ell \left(\frac{du}{dx}\right)^T\left(\frac{du}{dx}\right) dx + O\left(\frac{h^5}{\ell^5}\right) \qquad (31)$$

where in Eq. (30) it is assumed that the neutral and centroidal axes are coincident. Superscript "T" indicates transpose in

the sense that displacement derivatives are expressed in matrix format. The integrated form of the total potential energy is then

$$P[\Delta,e] = -\lambda P_j \lfloor -1 \; 1 \rfloor \{e\} + \frac{EA}{2\ell} \lfloor e \rfloor [K_A] \{e\} +$$
$$+ \frac{EI}{2\ell^3} \lfloor \Delta \rfloor [K_0] \{\Delta\} - \frac{\lambda P_j}{2\ell} \lfloor \Delta \rfloor [K_1] \{\Delta\} +$$
$$+ \frac{EA}{2\ell^2} \lfloor -1 \; 1 \rfloor \{e\} \lfloor \Delta \rfloor [K_1] \{\Delta\} +$$
$$+ \frac{EA}{8\ell^3} \lfloor \Delta \rfloor [L_2] \{\Delta\} - \frac{\lambda P_j}{2\ell} \lfloor e \rfloor [K_A] \{e\} \qquad (32)$$

where terms are defined as in the inextensional case, with the addition of

$$\lfloor e \rfloor = \lfloor u_i \; u_j \rfloor \qquad (33)$$

$$[K_A] = \begin{bmatrix} 1 & -1 \\ -1 & 1 \end{bmatrix} \qquad (34)$$

Eq's. (22) and (32) are derived in terms of local coordinate variables. Transformation to a global coordinate system is not necessary for problems exhibiting bifurcation buckling characteristics since alignment of element neutral axes is required.

3.4 Geometric Nonlinearity -- Incremental Equilibrium Equations.

The types of structures under consideration are those that exhibit a sudden change in the deformation states at particular loads. In finite deformation problems, sudden changes of state need not occur, but in the large deflection of the structure each element may rotate or strain a finite amount.

Neglect of higher order nonlinear terms is then not permissible in accurate representation of the static response.

One method of solving the finite deformation problem is to trace the equilibrium configuration by stepwise linear load incrementation. To do this an incremental load-displacement equation is required. This type of equation can readily be derived using the strain energy expression from Eq. (30), but using a more general external work expression than Eq. (31). In particular at a point " I " in configuration space the total potential energy can be represented by:

$$P[\Delta,e] = \frac{EI}{2\ell_I^3} L\Delta J_I [K_0]\{\Delta\}_I + \frac{Ea}{2\ell_I} Le J_I [K_A]\{e\}_I +$$

$$+ \frac{Ea}{2\ell_I^2} L^{-1} U\{e\}_I L\Delta J_I [K_1]\{\Delta\}_I +$$

$$+ \frac{Ea}{8\ell^3} L\Delta J_I [L_2]\{\Delta\}_I - Le:\Delta J_I \{R\}_I \qquad (35)$$

where $\{R\}_I$ is the vector of applied external loads. In writing Eq. (35) only element length is incremented, but area a and second cross-section moment I likewise can be incremented if required. Minimizing the total potential energy with respect to the deformation state yields

$$L\delta e J_I \left\{ \frac{Ea}{\ell_I} [K_A]\{e\}_I + \frac{Ea}{2\ell_I^2} L\Delta J_I [K_1]\{\Delta\}_I \begin{Bmatrix} -1 \\ 1 \end{Bmatrix} \right\} +$$

$$+ L\delta\Delta J_I \left(\frac{EI}{\ell_I^3} [K_0]\{\Delta\}_I + \frac{Ea}{\ell_I^2} L^{-1} U\{e\}_I [K_1]\{\Delta\}_I \right) +$$

$$- L\delta e:\delta\Delta J_I \{R\}_I = 0 \qquad (36)$$

The variations are assumed kinematically admissible and independent so that two equilibrium equations are obtained from Eq. (36).

An increment in applied loading and deformation is represented by

$$\{R\} = \{R\}_I + \{\Delta R\}$$
$$\{e\} = \{e\}_I + \{\Delta e\} \qquad (37)$$
$$\{s\} = \{s\}_I + \{\Delta s\}$$

Replacing $\lfloor R \rfloor_I$, $\lfloor e \rfloor_I$ and $\lfloor s \rfloor_I$ in Eq. (35) by these incremented values an expression for the total potential energy in an adjacent state is obtained. Subtracting Eq. (35) from this the increment in total potential energy is obtained as follows:

$$\begin{aligned}
\Delta P = {} & \frac{EA}{l_I} \lfloor e \rfloor_I [K_A] \{\Delta e\} + \frac{EA}{2l_I} \lfloor \Delta e \rfloor [K_A] \{\Delta e\} + \frac{EI}{l_I^3} \lfloor s \rfloor_I [K_0] \{\Delta s\} + \\
& + \frac{EI}{2l_I^3} \lfloor \Delta s \rfloor [K_0] \{\Delta s\} + \frac{EA}{l_I^2} \lfloor -1 \ \ 1 \rfloor \{e\}_I \lfloor s \rfloor_I [K_1] \{\Delta s\} + \\
& + \frac{EA}{2l_I^2} \lfloor -1 \ \ 1 \rfloor \{e\}_I \lfloor \Delta s \rfloor [K_1] \{\Delta s\} + \frac{EA}{2l_I^2} \lfloor -1 \ \ 1 \rfloor \{\Delta e\} \lfloor s \rfloor_I [K_1] \{s\}_I + \\
& + \frac{EA}{l_I^2} \lfloor -1 \ \ 1 \rfloor \{\Delta e\} \lfloor s \rfloor_I [K_1] \{\Delta s\} + \frac{EA}{2l_I^2} \lfloor -1 \ \ 1 \rfloor \{\Delta e\} [K_1] \{\Delta s\} + \\
& - \lfloor \Delta e : \Delta s \rfloor \{R_I\} - \lfloor e : s \rfloor \{\Delta R\} + \\
& - \lfloor \Delta e : \Delta s \rfloor \{\Delta R\} \qquad (36) \\
& + \text{higher order terms}
\end{aligned}$$

The energy increment is minimized with respect to the displacement increments and in the process Eq. (36) is used to eliminate corresponding terms, leaving

$$\begin{aligned}
&\lfloor \delta \Delta e \rfloor \left(\frac{EA_i}{\ell_I} [K_A] \{\Delta e\} + \frac{EA_i}{\ell_I^2} \lfloor \Delta \rfloor_I [K_1] \{\Delta \Delta\} \begin{Bmatrix} -1 \\ 1 \end{Bmatrix} \right) + \\
&+ \lfloor \delta \Delta \Delta \rfloor \left(\frac{EI}{\ell_I^3} [K_0] \{\Delta \Delta\} + \frac{EA_i}{\ell_I^2} L^{-1} \rfloor \{e\}_I [K_1] \{\Delta \Delta\} + \right. \\
&\left. \frac{EA_i}{\ell_I^2} L^{-1} \rfloor \{\Delta e\} [K_1] \{\Delta\}_I \right) - \lfloor \delta \Delta e \vdots \delta \Delta \Delta \rfloor \{\Delta R\} = 0
\end{aligned} \tag{39}$$

where higher order terms in the displacements and displacement increments have been dropped. In its present form the equation can be written as follows:

$$\begin{aligned}
&\lfloor \delta \Delta e \vdots \delta \Delta \Delta \rfloor \left(\begin{bmatrix} \bar{K}_A & 0 \\ 0 & \bar{K}_0 \end{bmatrix} \begin{Bmatrix} \Delta e \\ \Delta \Delta \end{Bmatrix} + \frac{EA_i}{\ell_I^2} L^{-1} \rfloor \{e\}_I \begin{bmatrix} 0 & 0 \\ 0 & K_1 \end{bmatrix} \begin{Bmatrix} \Delta e \\ \Delta \Delta \end{Bmatrix} + \right. \\
&\left. + \frac{EA_i}{\ell_I^2} \begin{bmatrix} 0 & D \\ D^T & 0 \end{bmatrix} \begin{Bmatrix} \Delta e \\ \Delta \Delta \end{Bmatrix} \right) - \lfloor \delta \Delta e \vdots \delta \Delta \Delta \rfloor \{\Delta R\} = 0
\end{aligned} \tag{40}$$

where

$$[\bar{K}_A] = \frac{EA_i}{\ell_I} [K_A] \quad , \quad [\bar{K}_0] = \frac{EI}{\ell_I^3} [K_0] \tag{41}$$

and

$$[D] = \begin{bmatrix} -\lfloor \Delta \rfloor_I [K_1] \\ \lfloor \Delta \rfloor_I [K_1] \end{bmatrix} = \begin{bmatrix} -d_1 & -d_2 & -d_3 & -d_4 \\ d_1 & d_2 & d_3 & d_4 \end{bmatrix} \tag{42}$$

where the d_i are the individual row-column products of $\lfloor \Delta \rfloor_I [K_1]$.

Eq. (40) is the variational form for an approximation of the incremental equilibrium equation. It is expressed in terms of element variables and transformation to global coordinates is required in usage. The term in the equation containing matrix [D] is referred to as the "initial displacement matrix" by Marcal (36) where its significance in large deflection analyses is evaluated.

3.5 Stability of a Uniform Cantilever Column.

The inextensional form of the energy equation is developed for a uniform cantilever column to demonstrate application of the theory. The column has length ℓ, cross-sectional area a, material modulus E, and second cross-sectional moment I. It is loaded axially by load λP_j where P_j is a reference load state and λ is the load intensity factor. Results obtained for this case are compared to an exact inextensional solution. Studied also are sensitivity of the governing equations to round-off error and rate of convergence of the solution.

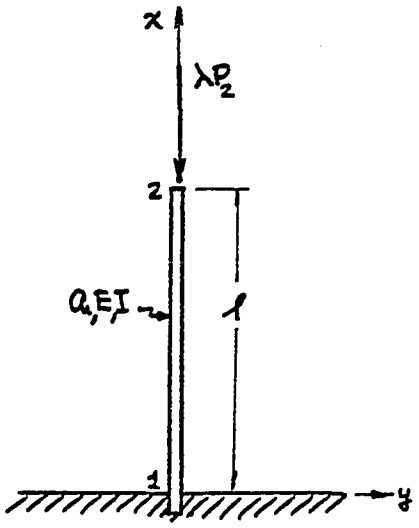

Figure III-2. Cantilever Column, Single Element Idealization.

The increment in total potential energy is given by Eq. (22). Imposing displacement boundary conditions on a single element representation of the column (Figure 2), the potential energy is

$$P[\Delta] = \frac{EI}{2\ell^3} \begin{bmatrix} v_2 & \theta_2\ell \end{bmatrix} \begin{bmatrix} 12 & -6 \\ -6 & 4 \end{bmatrix} \begin{Bmatrix} v_2 \\ \theta_2\ell \end{Bmatrix} - \frac{\lambda}{2\ell} \begin{bmatrix} 6/5 & -1/10 \\ -1/10 & 2/15 \end{bmatrix} \begin{Bmatrix} v_2 \\ \theta_2\ell \end{Bmatrix} +$$

$$- \frac{\lambda}{8\ell^3} \begin{bmatrix} v_2 & \theta_2\ell \end{bmatrix} \begin{bmatrix} 9\frac{\ell_4}{\ell} - 12\frac{\ell_5}{\ell^2} + 4\frac{\ell_6}{\ell^3} & -3\frac{\ell_4}{\ell} + 5\frac{\ell_5}{\ell^2} - 2\frac{\ell_6}{\ell^3} \\ \text{SYM} & \frac{\ell_4}{\ell} - 2\frac{\ell_5}{\ell^2} + \frac{\ell_6}{\ell^3} \end{bmatrix} \begin{Bmatrix} v_2 \\ \theta_2\ell \end{Bmatrix}$$

$$+ \frac{EI}{2\ell^5} \begin{bmatrix} v_2 & \theta_2\ell \end{bmatrix} \begin{bmatrix} 9\ell h_4 - 12h_5 + 4\frac{h_6}{\ell} & -3\ell h_4 + 5h_5 - 2\frac{h_6}{\ell} \\ \text{SYM} & \ell h_4 - 2h_5 + \frac{h_6}{\ell} \end{bmatrix} \begin{Bmatrix} v_2 \\ \theta_2\ell \end{Bmatrix} \qquad (43)$$

The ℓ_i and h_i are defined in Appendix A. The reference loading factor $P_j = -1$.

The critical load condition is obtained from a solution to Eq. (II-10) in which $T_2[\Delta]$ is any positive definite quadratic form in terms of the variables of $P[\Delta]$. Possible choices for $T_2[\Delta]$ are

$$T_2[\Delta] = \begin{bmatrix} v_2 & \theta_2\ell \end{bmatrix} \begin{bmatrix} 1 & 0 \\ 0 & 1 \end{bmatrix} \begin{Bmatrix} v_2 \\ \theta_2\ell \end{Bmatrix}$$

$$T_2[\Delta] = \frac{m}{12} \begin{bmatrix} v_2 & \theta_2\ell \end{bmatrix} \begin{bmatrix} 12 & 0 \\ 0 & 1 \end{bmatrix} \begin{Bmatrix} v_2 \\ \theta_2\ell \end{Bmatrix}$$

$$T_2[\Delta] = \frac{m}{420} \begin{bmatrix} v_2 & \theta_2\ell \end{bmatrix} \begin{bmatrix} 156 & -22 \\ -22 & 4 \end{bmatrix} \begin{Bmatrix} v_2 \\ \theta_2\ell \end{Bmatrix} \qquad (44)$$

The second and third forms are kinetic energy expressions used in dynamic analyses (37). Continuing with the first form, we investigate the roots of Eq. (II-10).

$$\left\{\frac{EI}{\ell^3}\begin{bmatrix}12 & -6\\ -6 & 4\end{bmatrix} - \frac{\lambda}{\ell}\begin{bmatrix}6/5 & -1/10\\ -1/10 & 2/15\end{bmatrix} - \mu\begin{bmatrix}1 & 0\\ 0 & 1\end{bmatrix}\right\}\begin{Bmatrix}v_2\\ \theta_2\ell\end{Bmatrix} = \{0\} \qquad (45$$

Denoting $\lambda^* = \frac{\lambda\ell^2}{EI}$ and $\mu^* = \frac{\mu\ell^3}{EI}$, of interest is the case where at least one value of $\mu^*=0$, but no values are negative. Setting $\mu^*=0$, two values found for λ^* are 2.48596 and 32.1813. The second roots for μ^* corresponding to these values of λ^* are $\mu^*=12.69$ and -26.8. Thus, $\lambda^*=32.1813$ is an unstable load state. It is seen also that $\mu^*=0$ is a single pole so that only one critical buckling mode is obtained. The normalized modal functions are

$$\{A_1\} = \begin{Bmatrix}0.537768\\ 0.843093\end{Bmatrix} \quad \mu^*=0.0,\ \lambda^*=2.48596 \qquad (46a)$$

and

$$\{A_2\} = \begin{Bmatrix}-0.843093\\ 0.537768\end{Bmatrix} \quad \mu^*=12.69,\ \lambda^*=2.48596 \qquad (46b)$$

Stability of the structure at the critical point of neutral equilibrium ($\lambda^*=2.486$, $\mu^*=0$) is established by evaluating Eq. (II-22). Since the higher order modal functions are known, $\{\bar{x}\}_i$ can be represented by Eq. (II-19). However, since $[H_1]$ and $[L_1]$ are zero in the present example the only possible solution for $\{\bar{x}\}_i$ from Eq's. (II-20) is $\{\bar{x}\}_i = \{0\}$.

The equation for A_4 then reduces simply to

$$A_4 = \{A_1\}_1^T [H_2]_1 \{A_1\}_1 - \lambda_1 \{A_1\}_1^T [L_2]_1 \{A_1\}_1$$

Numerical expansion of this equation is

$$A_4 = \frac{EI}{2\ell^5} \{A_1\}^T \begin{bmatrix} 4.1993 & -2.9281 \\ \text{SYM} & 2.2294 \end{bmatrix} \{A_1\} +$$

$$-\frac{\lambda_1}{8\ell^3} \{A_1\}^T \begin{bmatrix} 0.42213 & 0.00862 \\ \text{SYM} & 0.07182 \end{bmatrix} \{A_1\}$$

from which, for $\lambda_1 = 2.4860 \frac{EI}{\ell^2}$,

$$A_4 = 0.0158 \frac{EI}{l^5} \tag{47}$$

Since $A_4 > 0$, the structure is stable at the critical point of neutral equilibrium.

The first step in obtaining an equation for the post-buckling response is to evaluate $\xi_2, \xi_3 \ldots$. Since $[H_1]$ and $[L_1]$ are zero, $\xi_2 = 0$ by Eq. (II-31a).

The only remaining non-zero low order coefficient is

$$A_2' = -\frac{1}{2\ell} \{A_1\}_1^T [K_1]_1 \{A_1\}_1 = -0.17556 \frac{1}{\ell}$$

Substituting A_2' and A_4 into Eq. (II-36) and solving for $\underline{a}$

$$a = \pm 2.358 \sqrt{\lambda^* - \lambda_1^*}\, \ell \tag{48}$$

The complete response equation, corresponding to Eq's. (II-25) and (II-27), is

$$\begin{Bmatrix} \sqrt{2} \\ \theta_2 \ell \end{Bmatrix} = \pm 2.358 \sqrt{\lambda^* - \lambda_1^*}\ \ell \begin{Bmatrix} 0.538 \\ 0.843 \end{Bmatrix} \qquad (49)$$

This solution is the total series solution due to the limitation on number of modal functions. Further refinement of solution requires the use of additional elements in the structural representation.

The exact inextensional solution is obtained by evaluating the elliptic integral of first kind for small value of argument (38). The result obtained is

$$\sqrt{2} = 1.148 \sqrt{\lambda^* - \lambda_1^*}\ \ell \qquad (50)$$

$$\lambda_1^* = \frac{\pi^2}{4} = 2.467$$

and $$\sqrt{2} = \frac{2}{\pi} \theta_2 \ell = 0.638\, \theta_2 \ell$$

The comparison, then, between the exact inextensional solution and a single element finite element solution is

$$\sqrt{2}_{(\text{EXACT})} = 1.148 \sqrt{\lambda^* - \lambda_1^*}\ \ell$$

$$\sqrt{2}_{(\text{APPROX})} = 1.270 \sqrt{\lambda^* - \lambda_1^*}\ \ell$$

The finite element solution is in error by 10.6% and indicates greater flexibility than the exact solution. The error is small and suggests rapid convergence of this approximate method.

To complete the investigation on convergence, results for 2, 3, and 4 element representations show rapid convergence to the exact value (Figure 3). The displacement contribution from $\{\Delta_3\}$ is negligibly small in all cases.

The numerical procedure was repeated for the case of a pin-ended column and results are summarized in Figure 4.

The displacement polynomial selected to represent the deflected shape of both the cantilever and pinned columns is not the exact function for either case. Thus, in evaluating and subsequently minimizing the potential energy with respect to the displacement parameters we expect monotonic and bounded convergence as predicted by the Rayleigh-Ritz method. However, in obtaining the post-buckling response two minimization procedures are used, the second a minimization of already approximate results. Proved by Koiter (26) the results of the second minimization need not show monotonic or bounded convergence properties, and this is substantiated by the results shown in Figures 3 and 4.

The rapid convergence of the solutions in these simple cases suggests the possibility of important utility of this method in more complex problems.

3.6 Evaluation of Truncation Errors.

The results shown in Figures 3 and 4 were obtained using structural stiffness matrices and eigenfunctions having 6 to 8 significant figure element values. To measure the sensitivity of the solution technique to accuracy in the structural representation the four-element cantilever column case is considered further. Of particular concern are two possible error sources. One is error introduced in the

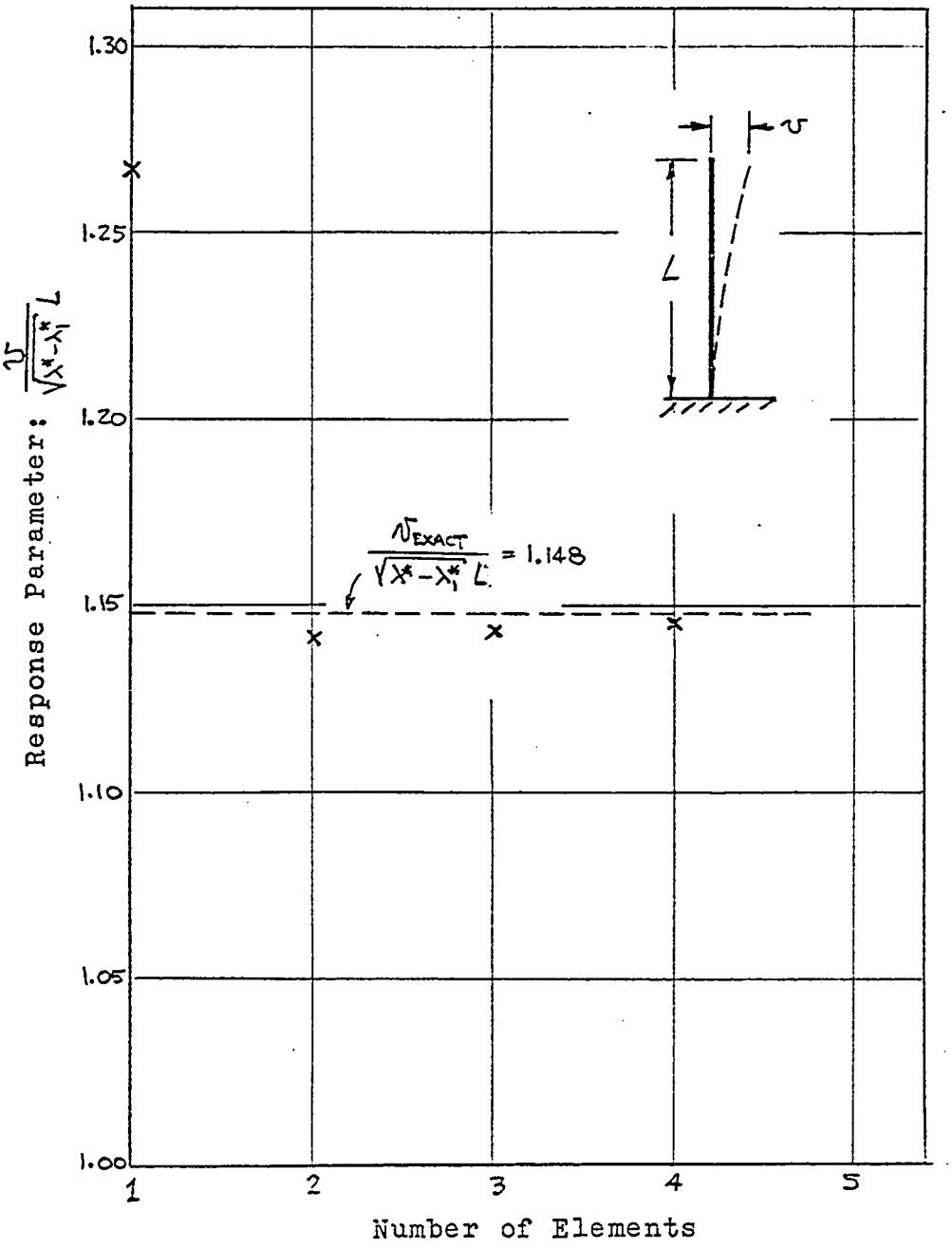

Number of Elements	Eigenvalue λ_1
1	2.4860
2	2.4685
3	2.4675
4	2.4674

$\lambda_{1(EXACT)} = 2.4674$

Figure III-3: Cantilever Column, Inextensional Theory Response

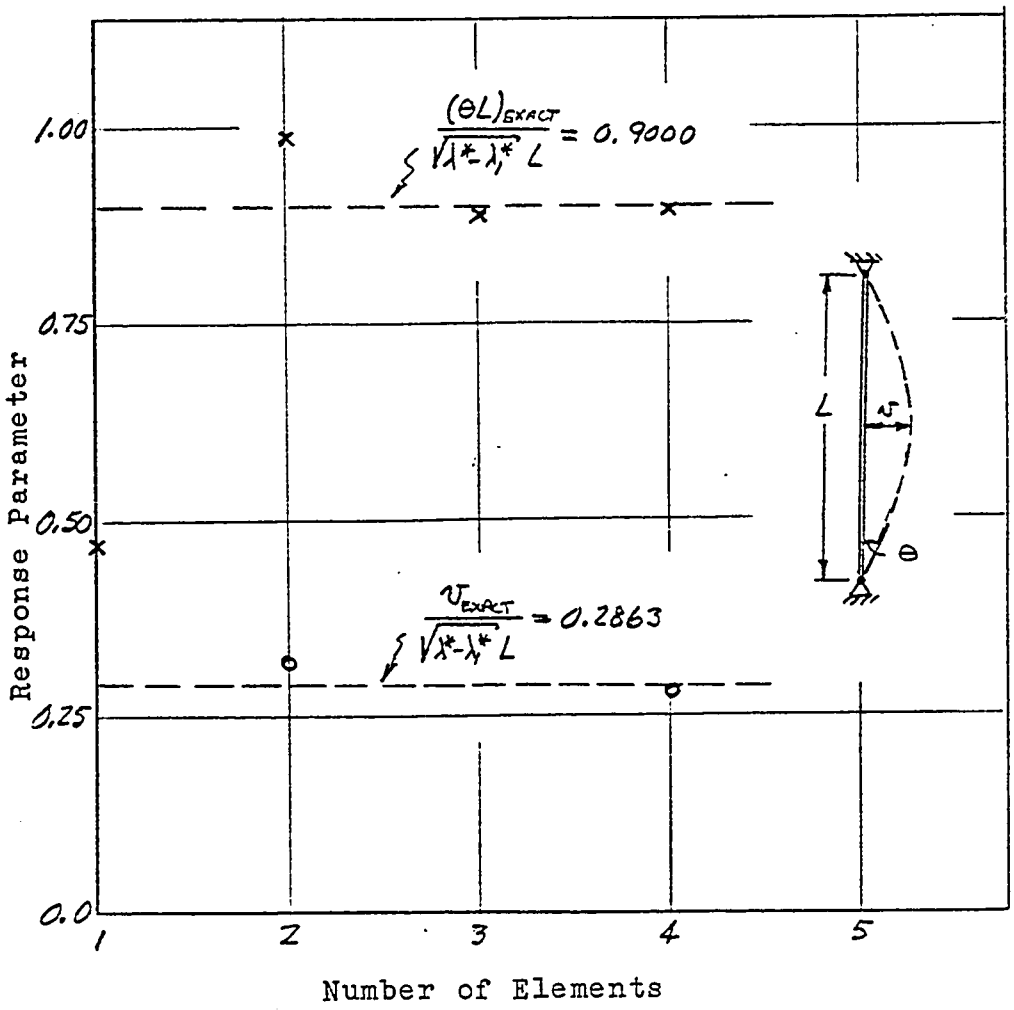

Number of Elements	Eigenvalue λ_1
1	12.003
2	9.944
3	9.885
4	9.874

$\lambda_{1EXACT} = 9.8696$

Figure III-4: Pin-Ended Column, Inextensional Theory Response

eigenfunction and eigenvalue by round-off or truncation, and the second is the same type of error introduced in the fourth degree stiffness matrices (inextensional case). To assess these types of errors the four-element cantilever representation was rerun with the following changes:

Case I: Eigenfunction values and eigenvalue successively single digit truncated, maintaining 6 to 8 figure accuracy on all stiffness matrices.

Case II: Fourth degree stiffness matrix values successively single digit truncated, maintaining 6 figure accuracy on eigenvalue and eigenfunction values.

The error in the transverse end displacement of the cantilever for Cases I and II is reported in Figure 5.

The results show that the solution technique is more sensitive to errors in the fourth degree stiffness matrices than to errors in the eigenfunction and eigenvalue. For the line element structures considered the total error is small even with large truncation.

3.7 Cantilever Column with Geometric Imperfection.

The external work integral for the inextensional theory is given by Eq. (19). Using Eq. (14) and integrating

$$W = \frac{\lambda}{2\ell} \{\Delta\}_i^T [K_1]_i \{\Delta\}_i + \frac{\lambda}{8\ell^3} \{\Delta\}_i^T [K_2]_i \{\Delta\}_i \qquad (51)$$

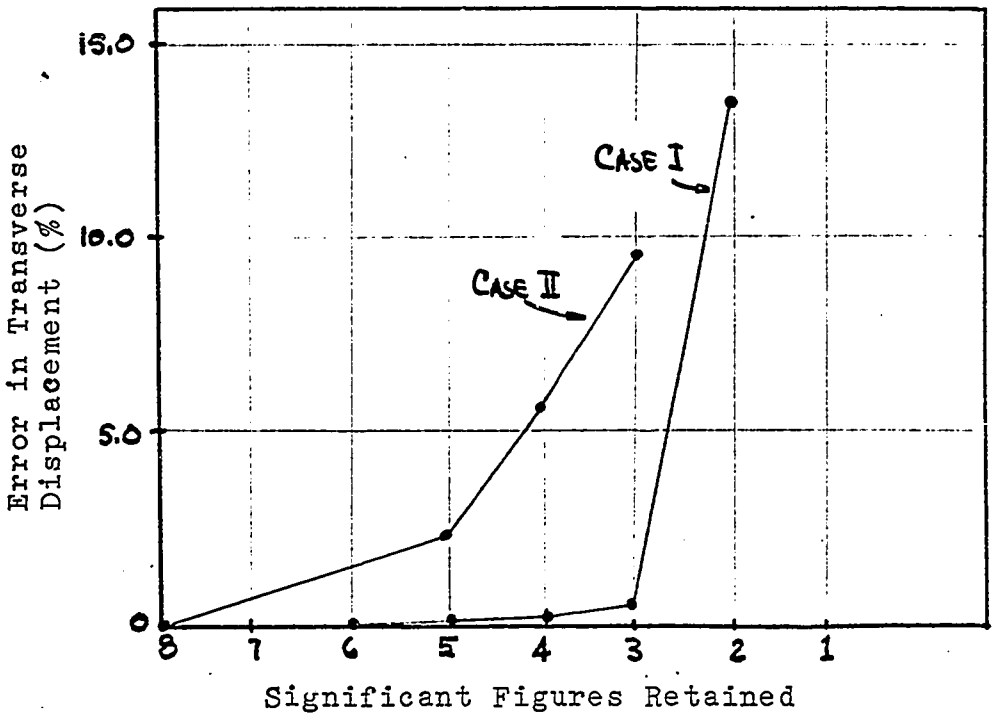

Figure III-5. Cantilever Column, Error in Transverse Displacement vs. Significant Figure Truncation.

Introducing a geometric imperfection of shape $\{\delta e\}$ and magnitude ε the total transverse displacement of the column is

$$\{\Delta\} = \varepsilon\{\delta e\} + \{\bar{\Delta}\}$$

which substituted into Eq. (51) yields

$$W = \frac{\lambda}{2\ell}\lfloor\bar{\Delta}\rfloor_i[K_1]_i\{\bar{\Delta}\}_i + \frac{\lambda\varepsilon}{\ell}\lfloor\delta e\rfloor_i[K_1]_i\{\bar{\Delta}\}_i$$

$$+\frac{\lambda}{8\ell^3}\lfloor\bar{\Delta}\rfloor_i[L_2]_i\{\bar{\Delta}\}_i + \frac{\lambda\varepsilon}{2\ell^3}\lfloor\delta e\rfloor_i[L_2]_i\{\bar{\Delta}\}_i + \ldots$$

Neglecting all but the lowest order term in ε, we determine that

$$\lfloor C\rfloor_i = \frac{1}{\ell}\lfloor\delta e\rfloor_i[K_1]_i \qquad (52)$$

for use in Eq. (II-41).

Consider the case of the imperfection in the shape of the critical buckling mode, then $\{\Delta_e\} = \{A_1\}$ and the first-approximation post-buckling response equation (Eq. (II-48)) for the four element representation of the column is:

$$-\frac{E}{L}\lambda_1^* \left[A_1 J_i\right]\left[K_1\right]_i \{A_1\}_i - \frac{a}{L}(\lambda^* - \lambda_1^*)\left[A_1 J_i\right]\left[K_1\right]_i \{A_1\}_i + \\ +8\frac{a^3}{L^3}\left[4\left[A_1 J_i\right]\left[H_2\right]_i \{A_1\}_i - \lambda_1^* \left[A_1 J_i\right]\left[L_2\right]_i \{A_1\}_i\right] = 0 \tag{53}$$

where $i=1,2,3,4$, $L=4\ell$, $\lambda = \lambda^* \frac{EI}{\ell^2} = 16\lambda^* \frac{EI}{L^2}$, $\lambda_1^* = 0.154207$ and

$$\{A_1\} = \begin{Bmatrix} v_2 \\ \theta_2 \ell \\ v_3 \\ \theta_3 \ell \\ v_4 \\ \theta_4 \ell \\ v_5 \\ \theta_5 \ell \end{Bmatrix} = \begin{Bmatrix} .05564 \\ .11024 \\ .21486 \\ .20370 \\ .45286 \\ .26615 \\ .73359 \\ .28808 \end{Bmatrix}$$

The extended theory equilibrium equation, determined from Eq. (II-54) is

$$-\frac{E}{L}\lambda^* \left[A_1 J_i\right]\left[K_1\right]_i \{A_1\}_i - \frac{a}{L}(\lambda^* - \lambda_1^*)\left[A_1 J_i\right]\left[K_1\right]_i \{A_1\}_i + \\ +8\frac{a^3}{L^3}\left[4\left[A_1 J_i\right]\left[H_2\right]_i \{A_1\}_i - \lambda^* \left[A_1 J_i\right]\left[L_2\right]_i \{A_1\}_i\right] = 0 \tag{54}$$

on the basis $\xi_2' = 0$ since $[H_1]$ and $[L_1]$ are zero, and the third mode contribution negligible. If the imperfection were in the shape of a higher order mode then higher order terms in the series expansion should also be considered.

For either approximation since ξ_p and ξ_p' are zero

the estimate of total displacement is

$$\{\Delta\} = (a + \varepsilon)\{\Delta_1\}$$

where a is determined from Eq's. (53) or (54) upon specification of the magnitude, ε , of the imperfection and value of the load λ^* . Eq. (53) applies only for λ near λ^* while Eq. (54) is applicable for $\lambda > 0$. Solution to Eq's. (53) and (54) determine three possible values for a/L. Generally the root loci of physical interest is that one corresponding to incremental loading from the no-load state although Eq's. (53) and (54) admit solutions for other branches as well.

A numerical example is considered in which $\varepsilon/L=0.01$. Root loci of the two approximate solutions are shown in Figure 6. The extended theory solution corresponds well with the exact inextensional solution for lateral deflections up to about 0.2 of the column length. Beyond this point the neglect of geometric change in the extended theory solution results in gradual divergence from the large deflection solution.

3.8 Extensional Theory Applied to the Cantilever Column.

Important differences between the inextensional and extensional theories can be assessed by considering further the cantilever column. The extensional solution is based upon the first approximation theory outlined in Section II. Extension to finite post-buckling response prediction is similar to that outlined for the inextensional case.

Equations for a two element representation of a

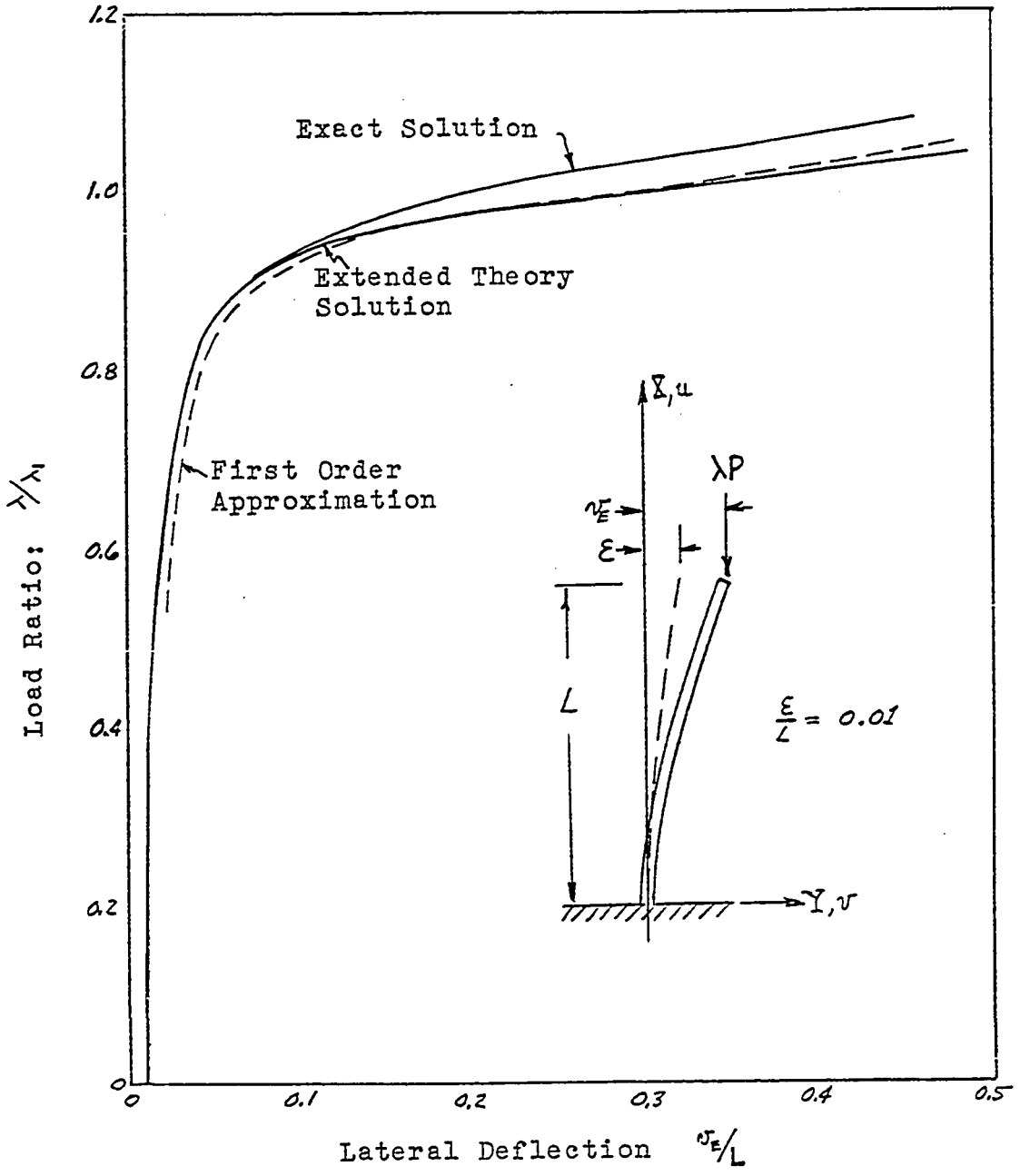

Figure III-6: Cantilever Column, Imperfect Structure Response

cantilever column are considered (Figure 7). The axial and flexural displacement vector components are separated and represented as follows:

$$[e] = [u_2 \quad u_3]$$

$$[A] = [v_2 \quad \theta_2 l \quad v_3 \quad \theta_3 l]$$

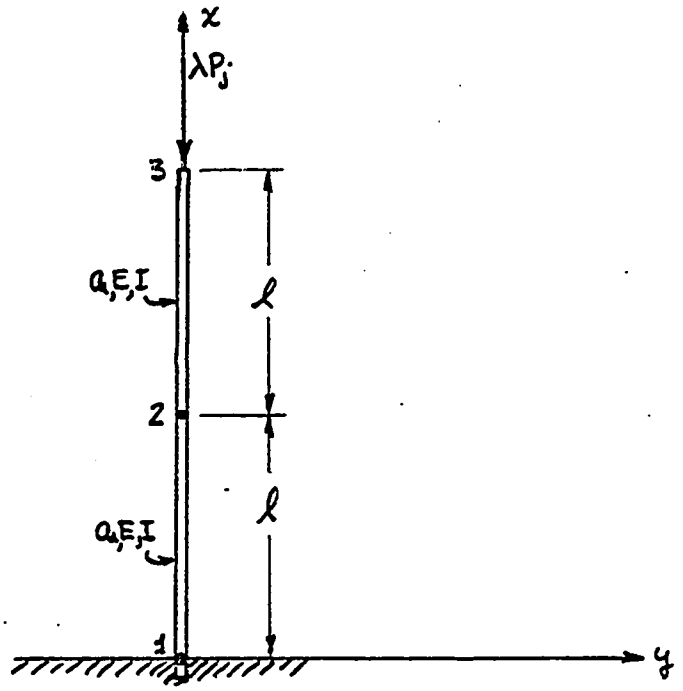

Figure III-7. Cantilever Column, Two Element Idealization.

Using Eq. (32) the total potential energy in a general state of deformation is

$$P[e,A] = \lambda^{-1} U\{e\}_1 + \lambda^{-1} U\{e\}_2 + \frac{Ea}{2l}[e]_1[K_A]_1\{e\}_1 +$$

$$+ \frac{Ea}{2l}[e]_2[K_A]_2\{e\}_2 + \frac{EI}{2l^3}[A]_1[K_0]_1\{A\}_1 + \frac{EI}{2l^3}[A]_2[K_0]_2\{A\}_2 +$$

$$+ \frac{\lambda}{2l}[A]_1[K_1]_1\{A\}_1 + \frac{\lambda}{2l}[A]_2[K_1]_2\{A\}_2 + \frac{Ea}{2l^2}\lambda^{-1} U\{e\}_1[A]_1[K_1]_1\{A\}_1 +$$

$$+\frac{EA}{2\ell^2}\begin{bmatrix}-1 & 1\end{bmatrix}\{e\}_2\begin{bmatrix}\Delta\end{bmatrix}_2[K_1]_2\{\Delta\}_2+\frac{EA}{8\ell^3}\begin{bmatrix}\Delta\end{bmatrix}_1[L_2]_1\{\Delta\}_1+\frac{EA}{8\ell^3}\begin{bmatrix}\Delta\end{bmatrix}_2[L_2]_2\{\Delta\}_2+$$

$$+\frac{\lambda}{2\ell}\begin{bmatrix}e\end{bmatrix}_1[K_A]_1\{e\}_1+\frac{\lambda}{2\ell}\begin{bmatrix}e\end{bmatrix}_2[K_A]_2\{e\}_2 \qquad (56)$$

where $P_2=P_3=-1$. Accounting for boundary conditions

$$\begin{bmatrix}e\end{bmatrix}_1=\begin{bmatrix}0 & u_2\end{bmatrix} \qquad \begin{bmatrix}\Delta\end{bmatrix}_1=\begin{bmatrix}0 & 0 & v_2 & \theta_2\ell\end{bmatrix}$$
$$\begin{bmatrix}e\end{bmatrix}_2=\begin{bmatrix}u_2 & u_3\end{bmatrix} \qquad \begin{bmatrix}\Delta\end{bmatrix}_2=\begin{bmatrix}v_2 & \theta_2\ell & v_3 & \theta_3\ell\end{bmatrix} \qquad (57)$$

Structure response in the fundamental state is axial and assumed linear so that

$$\begin{bmatrix}e\end{bmatrix}=\begin{bmatrix}e_0\end{bmatrix}$$
$$\begin{bmatrix}\Delta\end{bmatrix}=\begin{bmatrix}0\end{bmatrix} \qquad (58)$$

and

$$P_I[e_0]=\lambda\begin{bmatrix}0 & 1\end{bmatrix}\{e_0\}+\frac{EA}{2\ell}\begin{bmatrix}e_0\end{bmatrix}[K_A]\{e_0\} \qquad (59)$$

Minimizing $P_I[e_0]$ with respect to $\{e_0\}$ defines the condition for equilibrium, namely

$$\{e_0\}=\begin{Bmatrix}u_2\\u_3\end{Bmatrix}=-\frac{\lambda\ell}{EA}[K_A]^{-1}\begin{Bmatrix}0\\1\end{Bmatrix} \qquad (60)$$

where $\lambda > 0$.

The critical case of neutral equilibrium is determined from the quadratic terms in $\begin{bmatrix}e\end{bmatrix}$ and $\begin{bmatrix}\Delta\end{bmatrix}$ in Eq. (56). Defining displacement variables as $\begin{bmatrix}e_1\end{bmatrix}$ and $\begin{bmatrix}\Delta_1\end{bmatrix}$, the corresponding characteristic equations are

$$\frac{EA}{2\ell}\begin{bmatrix}e_1\end{bmatrix}[K_A]\{e_1\}+\frac{\lambda}{2\ell}\begin{bmatrix}e_1\end{bmatrix}[K_A]\{e_1\}-\mu\begin{bmatrix}e_1\end{bmatrix}[\tau_A]\{e_1\}=0 \qquad (61a)$$

$$\frac{EI}{2\ell^3}\,\lfloor \delta_1 \rfloor [K_0]\{\delta_1\} + \frac{\lambda}{2\ell}\,\lfloor \delta_1 \rfloor [K_1]\{\delta_1\} - \mu\,\lfloor \delta_1 \rfloor [T_B]\{\delta_1\} = 0 \qquad (61b)$$

where the axial and bending terms uncouple. The critical case corresponds to $\mu = 0$, which under arbitrary variation $\lfloor \delta e_1 \rfloor$ and $\lfloor \delta \delta_1 \rfloor$ requires

$$\left(\frac{EA}{\ell} + \frac{\lambda}{\ell}\right)[K_A]\{e_1\} = \{0\} \qquad (62a)$$

$$\frac{EI}{\ell^3}[K_0]\{\delta_1\} + \frac{\lambda}{\ell}[K_1]\{\delta_1\} = \{0\} \qquad (62b)$$

Solutions for λ are

$$\lambda_1^A = -EA \qquad (63a)$$

$$\lambda_1^B = -.61714\,\frac{EI}{\ell^2} \qquad (63b)$$

However, $\lambda_1^A = O\left(\frac{A\ell^2}{I}\lambda_1^B\right)$ where $\frac{A\ell^2}{I}$ is the square of the slenderness ratio, a large number for elastic post-buckling response. For $\lambda_1 = \lambda_1^B$ the equilibrium is neutral so that for $\lambda_1 = \lambda_1^A$ the system is unstable. Thus the physically meaningful solution to Eq. (62a) is $\lfloor e_1 \rfloor = \lfloor 0 \rfloor$. This result means that axially the response to loading does not exhibit a bifurcation, but is continuous. Thus, axial deformation in the post-buckling domain is defined simply by $\lfloor e \rfloor = \lfloor e_0 \rfloor$ for $\lfloor \delta \rfloor = a \lfloor \delta_1 \rfloor$ and terms of thte total potential energy involving $\lfloor e_0 \rfloor$ are

$$P_I[e_o,A] = \lambda \lfloor 0\ 1 \rfloor \{e_o\}_1 + \lambda \lfloor L^{-1}\ 1 \rfloor \{e_o\}_2 + \frac{EA}{2\ell} \lfloor e_o \rfloor_1 [K_A]_1 \{e_o\}_1 +$$

$$+ \frac{EA}{2\ell} \lfloor e_o \rfloor_2 [K_A]_2 \{e_o\}_2 + \frac{EA}{2\ell^2} a^2 \lfloor A_1 \rfloor_1 [K_1]_1 \{A_1\}_1 \lfloor 0\ 1 \rfloor \{e_o\}_1 +$$

$$+ \frac{EA}{2\ell^2} \lfloor A_1 \rfloor_2 [K_1]_2 \{A_1\}_2 \lfloor L^{-1}\ 1 \rfloor \{e_o\}_2 \qquad (64)$$

Minimizing $P_I[e_o, A_1]$ with respect to $\lfloor e_o \rfloor$ yields

$$\{e_o\} = \begin{Bmatrix} u_2 \\ u_3 \end{Bmatrix} = -\frac{\lambda \ell}{EA} [K_A]^{-1} \begin{Bmatrix} 0 \\ 1 \end{Bmatrix} - \frac{a^2}{2\ell^2} [K_A]^{-1} \begin{Bmatrix} \lfloor A_1 \rfloor_1 [K_1]_1 \{A_1\}_1 - \lfloor A_1 \rfloor_2 [K_1]_2 \{A_1\}_2 \\ \lfloor A_1 \rfloor_2 [K_1]_2 \{A_1\}_2 \end{Bmatrix} \qquad (65)$$

This solution for $\{e_o\}$ is the total axial displacement of the structure for loading into the post-buckling range for which bending displacement has maximum amplitude $\underline{a}$. Since $\{e_o\}$ represents the total displacement, particularly at gridpoint 3 where the external load acts, any additional nonlinear axial displacement must occur with $u_3 = 0$. To evaluate the post-buckling response, set

$$\lfloor e \rfloor = \lfloor \bar{e} \rfloor \qquad (\bar{u}_3 = 0) \qquad (66)$$

and

$$\lfloor A \rfloor = a \lfloor A_1 \rfloor + a^2 \lfloor A_2 \rfloor + \cdots \qquad (67)$$

where $\lfloor A_2 \rfloor$ is the second mode from Eq. (61b) corresponding to $\mu = 0$. Looking only at the increment in total potential energy in State II, we have

$$P[\bar{e}, A] = \frac{EA}{2\ell} \lfloor \bar{e} \rfloor [K_A] \{\bar{e}\} + \frac{EI}{2\ell^3} \lfloor A_1 \rfloor [K_0] \{A_1\} + \frac{\lambda a^2}{2\ell} \lfloor A_1 \rfloor [K_1] \{A_1\} +$$

$$+\frac{EI}{\ell^3}a^3\,[A_1]^T[K_0]\{A_2\}+\frac{\lambda}{\ell}a^3\,[A_1]^T[K_1]\{A_2\}+\frac{EI}{2\ell^3}a^4\,[A_2]^T[K_1]\{A_2\}+$$

$$+\frac{\lambda}{2\ell}a^4\,[A_2]^T[K_1]\{A_2\}+\frac{EA}{2\ell^2}[A_1]_1^T[K_1]_1\{A_1\}_1{}^{[0\ 1]}\{\bar{e}\}_1+$$

$$+\frac{EA}{2\ell^2}[A_1]_2^T[K_1]_2\{A_1\}_2{}^{[-1\ 1]}\{\bar{e}\}_2+\frac{EA}{\ell^2}a^3\,[A_1]_1^T[K_1]_1\{A_2\}_1{}^{[0\ 1]}\{\bar{e}\}_1+$$

$$+\frac{EA}{\ell^2}a^3\,[A_1]_2^T[K_1]_2\{A_2\}_2{}^{[-1\ 1]}\{\bar{e}\}_2+\frac{EA}{2\ell^2}a^4\,[A_2]_1^T[K_1]_1\{A_2\}_1{}^{[0\ 1]}\{\bar{e}\}_1+$$

$$+\frac{EA}{2\ell^2}a^4\,[A_2]_2^T[K_1]_2\{A_2\}_2{}^{[-1\ 1]}\{\bar{e}\}_2+\frac{EA}{8\ell^3}a^4\,[A_1]_1^T[L_2]_1\{A_1\}_1+$$

$$+\frac{EA}{8\ell^3}a^4\,[A_1]_2^T[L_2]_2\{A_1\}_2+O(a^5) \tag{68}$$

Minimization of the energy with respect to $[\bar{e}]$ yields

$$\frac{EA}{\ell}[K_A]\{\bar{e}\}+\frac{EA}{2\ell^2}a^2\begin{Bmatrix}[A_1]_1^T[K_1]_1\{A_1\}_1-[A_1]_2^T[K_1]_2\{A_1\}_2\\ [A_1]_2^T[K_1]_2\{A_1\}_2\end{Bmatrix}+$$

$$+\frac{EA}{2\ell^2}a^3\begin{Bmatrix}[A_1]_1^T[K_1]_1\{A_2\}_1-\{A_1\}_2^T[K_1]_2\{A_2\}_2\\ [A_1]_2^T[K_1]_2\{A_2\}_2\end{Bmatrix}+O(a^4)=0 \tag{69}$$

Imposing the condition $\bar{u}_3=0$, we have remaining

$$\frac{EA}{\ell}[Z]\{\bar{u}_2\}+\frac{EA}{2\ell^2}a^2\left\{[A_1]_1^T[K_1]_1\{A_1\}_1-[A_1]_2^T[K_1]_2\{A_1\}_2\right\}+$$

$$+\frac{EA}{2\ell^2}a^3\left\{[A_1]_1^T[K_1]_1\{A_2\}_1-[A_1]_2^T[K_1]_2\{A_2\}_2\right\}+$$

$$+\ O(a^4)=0 \tag{70}$$

From this equation it is seen that $[\bar{e}]$ is $O(\underline{a}^2)$ and higher. Since third order terms in $[\Delta]$ are absent (Eq. (II-31a)),

$$\xi_2 = 0 \tag{71}$$

and this result then requires, from Eq. (70)

$$\bar{u}_2 = -\frac{a^2}{4\ell}\left[\lfloor\Delta_1\rfloor_1[K_1]_1\{\Delta_1\}_1 - \lfloor\Delta_1\rfloor_2[K_1]_2\{\Delta_1\}_2\right] \tag{72}$$

and

$$\{\bar{e}\} = -\frac{a^2}{4\ell}\{e^*\} = -\frac{a^2}{4\ell}\begin{Bmatrix}\lfloor\Delta_1\rfloor_1[K_1]_1\{\Delta_1\}_1 - \lfloor\Delta_1\rfloor_2[K_1]_2\{\Delta_1\}_2 \\ 0\end{Bmatrix} \tag{73}$$

Using the result given by Eq. (71), the energy increment reduces to

$$\begin{aligned}\mathcal{P}[\bar{e},\Delta] = {} & \frac{Eq_1}{2\ell}\lfloor\bar{e}\rfloor[K_A]\{\bar{e}\} + \frac{\lambda-\lambda_1}{2\ell}a^2\lfloor\Delta_1\rfloor[K_1]\{\Delta_1\} + \\ & + \frac{Eq_1}{2\ell^2}a^2\left[\lfloor\Delta_1\rfloor_1[K_1]_1\{\Delta_1\}_1 - \lfloor\Delta_1\rfloor_2[K_1]_2\{\Delta_1\}_2 \quad \lfloor\Delta_1\rfloor_2[K_1]_2\{\Delta_1\}_2\right]\{\bar{e}\} + \\ & + \frac{Eq_1}{8\ell^3}a^4\left[\lfloor\Delta_1\rfloor_1[L_2]_1\{\Delta_1\}_1 + \lfloor\Delta_1\rfloor_2[L_2]_2\{\Delta_1\}_2\right] + O(a^5)\end{aligned} \tag{74}$$

The remaining step is to minimize $\mathcal{P}[\bar{e},\Delta]$ with respect to $\underline{a}$, which provides the condition for equilibrium in the post-buckled state. Doing this, we obtain

$$a^2 = \frac{2(\lambda_1-\lambda)\ell^2\lfloor\Delta_1\rfloor[K_1]\{\Delta_1\}}{Eq_1\left[\lfloor\Delta_1\rfloor_1[L_2]_1\{\Delta_1\}_1 + \lfloor\Delta_1\rfloor_2[L_2]_2\{\Delta_1\}_2 - \frac{1}{2}\lfloor\bar{e}^*\rfloor\{\bar{e}^*\}\right]} \tag{75}$$

The results given by Eq's. (70) and (74) are general in the sense that expansion for refined element approximations is straightforward. The terms in square brackets in the denominator of Eq. (75) correspond to the quantity A_4, the sign of which establishes the type of stability at the critical point of neutral equilibrium (Eq. (II-22)).

The total displacement state in the post-buckled configuration is then

$$\{e\} = \{e_0\} + \{\bar{e}\} \tag{77a}$$

$$\{A\} = a\{A_1\} \tag{77b}$$

where equations for all terms involved have been developed.

In addition to the two-element case, one, three and four element representations were evaluated to determine the convergence characteristics of the extensional representation. Results are compared with the exact extensional solution (derived using the procedure outlined for plates in (38)) in Figure 8. Convergence of the extensional solution is slower than the corresponding solution for the inextensional case (Figure 3). The lateral deflection at the end of the cantilever predicted by the two theories is

Inextensible: $v = 1.148\sqrt{\lambda^* - \lambda_1^*}\, L$

Extensible: $v = 1.273\sqrt{\lambda^* - \lambda_1^*}\, L \sqrt{\frac{I}{a_4 L^2}}$

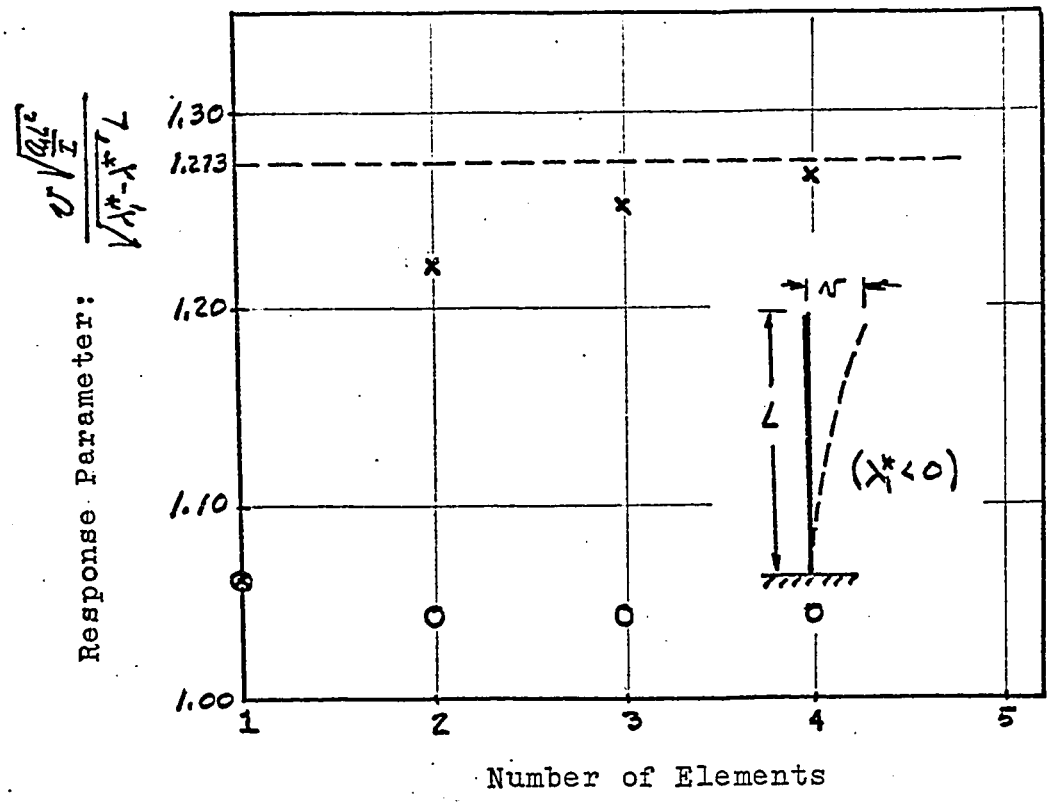

Figure III-8. Cantilever Column -- Extensional Theory Response

The difference between the two solutions is approximately the value of the slenderness ratio, with the extensional theory predicting stiffer post-buckling response. Qualitatively this result is predictable, as the strain energy of bending is less in the extensional case for equal total strain energy content for both theories. For elastic post-buckling response the slenderness ratio is large (> 150) so that significant differences in post-buckling response are obtained.

The extensional solution, which accounts for axial deformation, is the more exact theory and; therefore, should be used in predicting post-buckling response. It should be noted that

the extensional equations are more difficult to set up and solve. Furthermore, the minimization procedure for finding $[\bar{e}]$ couples the element equations so that in applications to large order systems large order matrix equations must be manipulated. This is in contrast to the inextensional theory which was treated on a per-element basis in calculations following the eigenvalue-eigenvector calculation. If the calculation of $[\bar{e}]$ is suppressed, thereby establishing a "per-element" basis of evaluation of the response, the circle point values in Figure 7 are obtained. Convergence is to 1.04 rather than 1.273 which is in 18% error.

IV. GEOMETRICALLY NONLINEAR EQUATIONS FOR THE FLAT PLATE ELEMENT

4.1 Strain-Displacement and Constitutive Equations.

Matrices of the total potential energy for the plate element for the prediction of initial post-buckling response can be derived following the procedure as in Section III for the line element. Requiring a material fiber normal to the plate neutral surface to remain normal to the surface after deformation (Kirchhoff hypothesis) results in the following nonlinear strain displacement relations truncated to consistent, common order

$$e_{xx} = \frac{\partial u}{\partial x} + \frac{1}{2}\left(\frac{\partial w}{\partial x}\right)^2 - z\left(\frac{\partial^2 w}{\partial x^2}\right) \tag{1}$$

$$e_{yy} = \frac{\partial v}{\partial y} + \frac{1}{2}\left(\frac{\partial w}{\partial y}\right)^2 - z\left(\frac{\partial^2 w}{\partial y^2}\right) \tag{2}$$

$$2\,e_{xy} = \frac{\partial u}{\partial y} + \frac{\partial v}{\partial x} + \frac{\partial w}{\partial x}\frac{\partial w}{\partial y} - 2z\frac{\partial^2 w}{\partial x \partial y} \tag{3}$$

Displacement components u,v,w are positive in positive coordinate directions as shown in Figure 1. It is noted that the strain displacement relations account for extensional deformation of the element as required based upon inaccuracy of the inextensional theory as determined in Section III.

The three dimensional linear strain-stress relationship for an adiabatic process is

$$e_{ij} = D_{ijkl}\,\sigma_{kl} + \alpha_{ij}\,\Delta T, \quad i,j,k,l = 1,2,3 \tag{4}$$

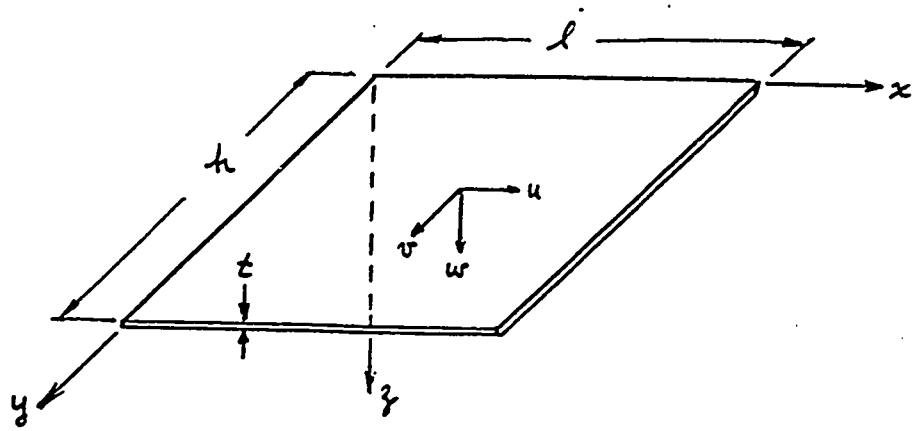

Figure IV-1. Plate Geometry.

where the indices refer specifically to rectangular cartesian components. The fourth order tensor components D_{ijkl} have symmetrices as a result of symmetrices of the stress and strain tensors so that only 36 of the coefficients D_{ijkl} are independent. Symmetry of the strain energy function reduces the number to 21. The symmetric second order tensor coefficients α_{ij} are the coefficients of thermal expansion of the material. Several simplifying assumptions based upon material symmetrices can be made to reduce further the number of independent coefficients. In the following development the restriction to material isotropy provides the greatest simplification and will be used. Any orthotropic approximation requires the same development that follows, but fewer terms combine.

With the assumption of isotropy and linear material behavior the three-dimensional constitutive equation becomes

$$\sigma_{ij} = \frac{E}{1+\nu}\left[e_{ij} + \frac{\nu}{1-2\nu} e_{kk}\delta_{ij}\right] - \beta(T-T_o)\delta_{ij} \qquad (5)$$

where $\beta = \frac{E\alpha}{1-2\nu}$ and α is the coefficient of thermal expansion. The plate is in a loaded state of plane stress, so that

$$e_{33} = -\frac{\nu}{1-\nu} e_{\rho\gamma} + \alpha \frac{(1+\nu)}{(1-\nu)}(T-T_0) \tag{6}$$

Setting subscripts ρ and γ = 1,2, then for the plane stress case

$$\sigma_{\rho\gamma} = \frac{E}{1+\nu}\left[e_{\rho\gamma} + \frac{\nu}{1-\nu} e_{ss}\,\delta_{\rho\gamma}\right] - E\alpha(T-T_0)\delta_{\rho\gamma} \tag{7}$$

$$\sigma_{\rho 3} = \frac{E}{1+\nu} e_{\rho 3} \quad ; \quad \sigma_{33} = 0 \tag{8}$$

4.2 Strain Energy and Work Functions.

The strain energy in terms of the strain components for the plane stress case is obtained by direct substitution into Clapeyron's formula. The result is

$$U = \frac{E}{2(1-\nu^2)} \iiint_V \left[(e_{xx} + e_{yy})^2 - 2(1-\nu)(e_{xx}e_{yy} - e_{xy}^2)\right] dv$$

$$- E\alpha(T-T_0) \iiint_V \left[e_{xx} + e_{yy}\right] dv \tag{9}$$

The work done by edge resultants is

$$W = \iint_a \left(N_x e_{xx_0} + N_y e_{yy_0} + 2N_{xy} e_{xy_0}\right) da \tag{10}$$

where the strains are the neutral surface strains. The total potential energy, using Eq's. (1), (2) and (3), is

$$P[u,v,w] = \frac{Et}{2(1-\nu^2)}\iint_{a_e}\left[u_x^2 + u_y^2 + 2u_x u_y + u_x w_x^2 + u_x w_y^2 + v_y w_x^2 + v_y w_y^2 + \right.$$
$$\left. + \frac{1}{4} w_x^4 + \frac{1}{4} w_y^4 + \frac{1}{2} w_x^2 w_y^2\right] dx\,dy +$$
$$+ \frac{Et^3}{24(1-\nu^2)}\iint_{a_e}\left[w_{xx}^2 + w_{yy}^2 + 2w_{xx}w_{yy} - 2(1-\nu)w_{xx}w_{yy} + 2(1-\nu)w_{xy}w_{xy}\right] dx\,dy +$$
$$+ \frac{Et}{(1+\nu)}\iint_{a_e}\left[\frac{1}{4} u_y^2 + \frac{1}{4} v_x^2 + \frac{1}{2} u_y v_x - u_x v_y + \frac{1}{2} u_y w_x w_y + \right.$$
$$\left. + \frac{1}{2} v_x w_x w_y - \frac{1}{2} u_x w_y^2 - \frac{1}{2} v_y w_x^2\right] dx\,dy +$$
$$- N_x\iint_{a_e}\left[u_x + \frac{1}{2} w_x^2\right] dx\,dy - N_y\iint_{a_e}\left[v_y + \frac{1}{2} w_y^2\right] dx\,dy +$$
$$- N_{xy}\iint_{a_e}\left[u_y + v_x + w_x w_y\right] dx\,dy +$$
$$- E\alpha t(T-T_0)\iint_{a_e}\left[u_x + v_y + \frac{1}{2} w_x^2 + \frac{1}{2} w_y^2\right] dx\,dy \qquad (11)$$

where integration over the thickness of the plate has been carried out. To further evaluate these integrals it is necessary to select displacement functions to represent the deformation state of the state element.

4.3 Finite Element Displacement Functions.

For structures exhibiting bifurcation buckling, required element alignment precludes the necessity for equivalent orthogonal displacement functions since preferential axes of deformation exist. Transverse displacement of the structure is represented by a sixth order mixed variable polynomial of the form

$$
\begin{aligned}
w(\xi,\eta) = {} & (A_1+1)(B_1+1)w_1 + (A_1+1)B_2\theta_{\xi_1} - A_2(B_1+1)\theta_{\eta_1} + A_2B_2\psi_{\xi\eta_1} + \\
& - A_1(B_1+1)w_2 - A_1B_2\theta_{\xi_2} - A_3(B_1+1)\theta_{\eta_2} + A_3B_2\psi_{\xi\eta_2} + \\
& - (A_1+1)B_1w_3 + (A_1+1)B_3\theta_{\xi_3} + A_2B_1\theta_{\eta_3} + A_2B_3\psi_{\xi\eta_3} + \\
& + A_1B_1w_4 - A_1B_3\theta_{\xi_4} + A_3B_1\theta_{\eta_4} + A_3B_3\psi_{\xi\eta_4}
\end{aligned} \tag{12}
$$

where

$$
\begin{aligned}
A_1 &= 2\xi^3 - 3\xi^2 & B_1 &= 2\eta^3 - 3\eta^2 & \theta_{\eta i} &= -l\left(\frac{\partial w}{\partial x}\right)_i & \xi &= \frac{x}{l} \\
A_2 &= \xi^3 - 2\xi^2 + \xi & B_2 &= \eta^3 - 2\eta^2 + \eta & \theta_{\xi i} &= h\left(\frac{\partial w}{\partial y}\right)_i & \eta &= \frac{y}{h} \\
A_3 &= \xi^3 - \xi^2 & B_3 &= \eta^3 - \eta^2 & \psi_{\xi\eta i} &= lh\left(\frac{\partial^2 w}{\partial x \partial y}\right)_i
\end{aligned} \tag{13}
$$

Positive definition of grid point variables and grid point numbering sequence is shown in Figure 2.

In-plane displacements are of lesser order in the independent variables having the form:

$$
\begin{pmatrix} u(\xi,\eta) \\ v(\xi,\eta) \end{pmatrix} = (1-\xi)(1-\eta)\begin{pmatrix} u_1 \\ v_1 \end{pmatrix} + \xi(1-\eta)\begin{pmatrix} u_2 \\ v_2 \end{pmatrix} + \eta(1-\xi)\begin{pmatrix} u_3 \\ v_3 \end{pmatrix} + \xi\eta\begin{pmatrix} u_4 \\ v_4 \end{pmatrix} \tag{14}
$$

We set

$$
\begin{aligned}
[A] &= [w_1\ \theta_{\xi_1}\ \theta_{\eta_1}\ \psi_{\xi\eta_1} \vdots w_2\ \theta_{\xi_2}\ \theta_{\eta_2}\ \psi_{\xi\eta_2} \vdots w_3\ \theta_{\xi_3}\ \theta_{\eta_3}\ \psi_{\xi\eta_3} \vdots w_4\ \theta_{\xi_4}\ \theta_{\eta_4}\ \psi_{\xi\eta_4}] \\
[e] &= [u_1\ v_1\ u_2\ v_2\ u_3\ v_3\ u_4\ v_4]
\end{aligned} \tag{15}
$$

It is readily verified that the superposition of Hermitean polynomials originally developed to obtain the above displacement functions assures interelement compatibility of displacement and slope and representation of rigid body modes. (Reference 39)

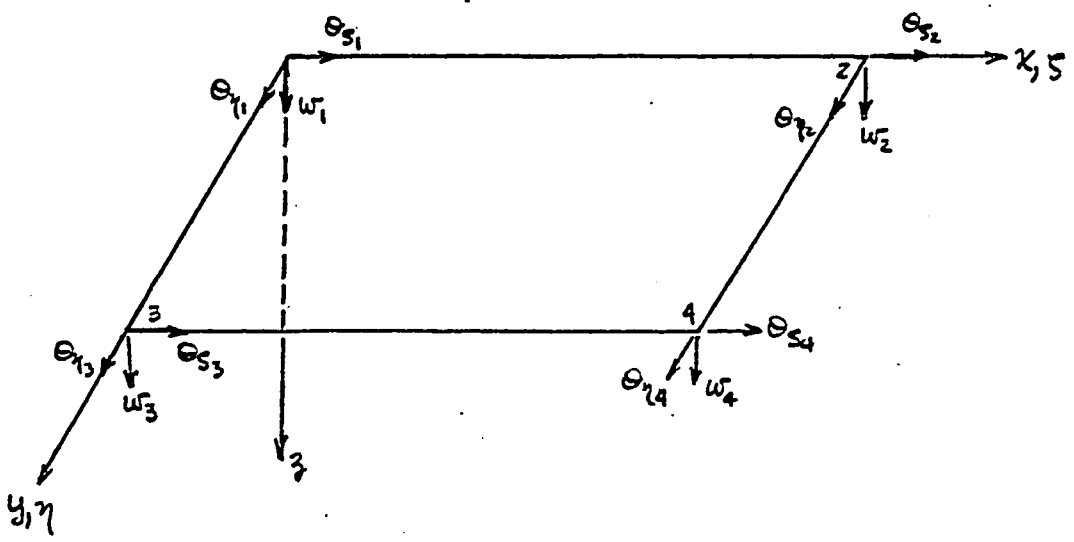

Figure IV-2. Rectangular Plate: Gridpoint Variables.

4.4 Total Potential Energy in Terms of Generalized Variables.

Using Eq's. (12) and (14) the terms in the total potential energy given by Eq. (11) can be integrated to obtain an algebraic expression in terms of unknown gridpoint displacements $\lfloor \delta \rfloor$ and $\lfloor e \rfloor$. Eq. (11) for the total potential energy is written in the following matrix form:

$$P[u,v,w] = \frac{Et}{2(1-\nu^2)} \left\{ \lfloor e \rfloor [K_A]_1 \{e\} + \lfloor e_j \rfloor \left\{ \lfloor \delta \rfloor [K_{1j}] \{\delta\} \right\} + \right.$$

$$\left. + \frac{1}{4} \lfloor \delta \rfloor [H_{ss_2}] \{\delta\} + \frac{1}{4} \lfloor \delta \rfloor [H_{\eta\eta_2}] \{\delta\} + \frac{1}{4} \lfloor \delta \rfloor [H_{s\eta_2}] \{\delta\} \right\} +$$

$$+ \frac{Et^3}{24(1-\nu^2)} \left\{ \lfloor \delta \rfloor [K_{ssss_0}] \{\delta\} + \lfloor \delta \rfloor [K_{\eta\eta\eta_0}] \{\delta\} + \right.$$

$$\left. + 2\nu \lfloor \delta \rfloor [K_{ss\eta\eta_0}] \{\delta\} + 2(1-\nu) \lfloor \delta \rfloor [K_{s\eta s\eta_0}] \{\delta\} \right\} + \qquad (16)$$

$$+\frac{Et}{4(1+\nu)}\left\{\lfloor e\rfloor[K_{A_2}]\{e\}+2\lfloor e_j\rfloor\left\{\lfloor A\rfloor[K_{2j}]\{A\}\right\}\right\}+$$

$$-N_\xi\left\{\lfloor C_{\xi_0}\rfloor\{e\}+\tfrac{1}{2}\lfloor A\rfloor[K_{\xi\xi_1}]\{A\}\right\}+$$

$$-N_\eta\left\{\lfloor C_{\eta_0}\rfloor\{e\}+\tfrac{1}{2}\lfloor A\rfloor[K_{\eta\eta_1}]\{A\}\right\}+$$

$$-N_{\xi\eta}\left\{\lfloor C_{\xi\eta_0}\rfloor\{e\}+\lfloor A\rfloor[K_{\xi\eta_1}]\{A\}\right\}+$$

$$-E\alpha t(T-T_0)\left\{\lfloor C_{\xi_0}\rfloor\{e\}+\lfloor C_{\eta_0}\rfloor\{e\}+\tfrac{1}{2}\lfloor A\rfloor[K_{\xi\xi_1}]\{A\}+\tfrac{1}{2}\lfloor A\rfloor[K_{\eta\eta_1}]\{A\}\right\}$$

The matrices shown in Eq. (16) are listed in Appendix C. The third order terms are explicit in the displacement vector content, however, the fourth order terms are not. These are indicated by $[H_{\xi\xi_2}]$, $[H_{\eta\eta_2}]$ and $[H_{\xi\eta_2}]$ in which each element of these matrices is a triple matrix product of the form $\lfloor A\rfloor[H]\lfloor A\rfloor$ (Appendix C).

4.5 Example Plate Problem.

Finite element formulation of plate post-buckling response is computed and compared to a corresponding Fourier series solution (38). The plate configuration is shown in Figure 3. The pinned edges at $\eta = \pm 1$ are subjected to in-plane stress resultant $N_\eta = \lambda\cdot(1)$. The pinned edges $\xi = \pm 1$ can contract vertically ($N_{\xi\eta} = 0$) but with no horizontal expansion so that $N_\xi = \nu N_\eta = \nu\lambda\cdot(1)$. Thus the center of the plate has no in-plane displacements. A single and four element representations of one-quarter of the plate are evaluated. The

four element array is dashed outlined in Figure 3.

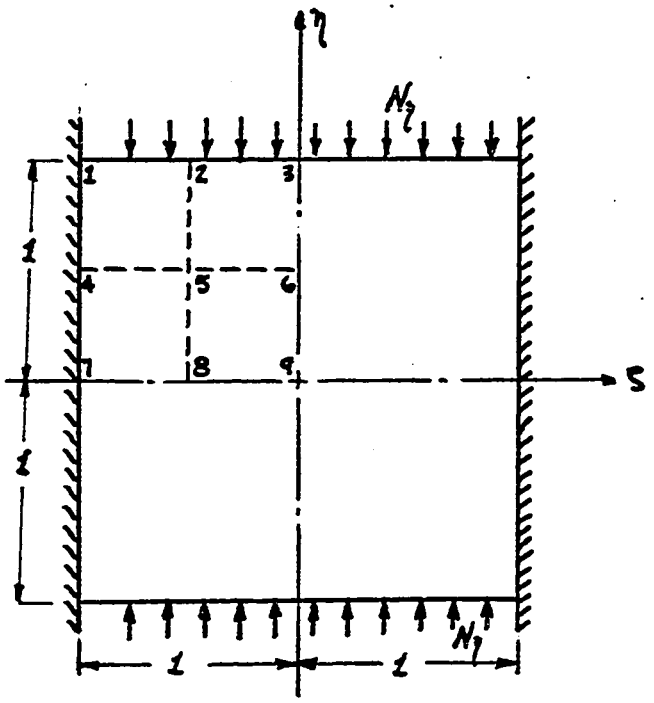

Figure IV-3. Plate Detail of Numerical Example.

For this case boundary conditions are

$$w_1 = \theta_{s_1} = \theta_{\eta_1} = \psi_{s\eta_1} = 0 \;,\quad w_2 = \theta_{\eta_2} = \psi_{s\eta_2} = 0 \;,\quad w_3 = \theta_{\eta_3} = \psi_{s\eta_3} = 0 \;,$$

$$w_4 = \theta_{s_4} = \psi_{s\eta_4} = 0 \;,\quad \theta_{\eta_6} = \psi_{s\eta_6} = 0 \;,\quad w_7 = \theta_{s_7} = \psi_{s\eta_7} = 0 \;, \tag{17}$$

$$\theta_{s_8} = \psi_{s\eta_8} = 0 \;,\quad \theta_{s_9} = \theta_{\eta_9} = \psi_{s\eta_9} = 0$$

This leaves 13 degrees-of-freedom (three degrees-of-freedom for single element case) in the critical buckling mode which is evaluated by standard techniques. The modes are

$$\lfloor \theta_{s_2} \;\; \theta_{\eta_3} \;\; w_4 \rfloor = \lfloor .65486 \;\; -.64298 \;\; .39385 \rfloor \tag{18}$$

for the single element representation, and

$$\lfloor \theta_{s_2} \;\; \theta_{s_3} \;\; \theta_{\eta_4} \;\; w_5 \;\; \theta_{s_5} \;\; \theta_{\eta_5} \;\; \psi_{s\eta_5} \;\; w_6 \;\; \theta_{s_6} \;\; \theta_{\eta_7} \;\; w_8 \;\; \theta_{\eta_8} \;\; w_9 \rfloor =$$

$$\lfloor -.24968 \quad -.34872 \quad .24928 \quad -.21894 \quad -.17743 \quad .17794 \quad -.08713$$
$$-.31039 \quad -.25155 \quad .34750 \quad -.31003 \quad .25197 \quad -.44201 \rfloor \tag{19}$$

for the four element representation.

If the total potential energy is evaluated for the plate using Eq. (16) it is seen that a quadratic term in the axial deformation $\lfloor e \rfloor$ with coefficient N_ξ or N_η does not exist. Thus, as in the case of the line element, the axial deformation is continuous through the point of bifurcation and no axial buckling mode develops at $\lambda = \lambda_1$. The k^{th} component of the axial deformation into the post-buckling state is then given by

$$\left\{ \frac{Et}{2(1-\nu^2)} [K_{A_1}]_i \{e_0\}_i + \frac{Et}{4(1+\nu)} [K_{A_2}]_i \{e_0\}_i + \frac{Eta^2}{2(1-\nu^2)} \{\lfloor A_1 \rfloor_i [K_{1k}]_i \{A_1\}_i\} + \right.$$
$$\left. + \frac{Eta^2}{2(1+\nu)} \{\lfloor A_1 \rfloor_i [K_{2k}]_i \{A_1\}_i\} - \lambda \nu \{C_{\xi_0}\}_i - \lambda \{C_{\eta_0}\}_i \right\}_k = 0 \tag{20}$$

where $\lfloor A_1 \rfloor$ is the critical buckling mode (Eq. 19), and $\underline{a}$, the amplitude coefficient of this mode, is unknown.

Deflection into the post-buckling state is assumed of the form

$$\lfloor e \rfloor = \lfloor \bar{e} \rfloor$$
$$\lfloor a \rfloor = a \lfloor A_1 \rfloor + a^2 \lfloor A_2 \rfloor + \cdots \tag{21}$$

where $\lfloor \bar{e} \rfloor$ is an admissible in-plane displacement function which, however, does not contribute to the in-plane displacements at the edges of the plate, since total boundary displacements are

contained in $\lfloor e_o \rfloor$. Assuming all elements identical in stiffness and geometric properties, the increment in total potential energy, based upon Eq. (21), is then

$$\mathcal{P}[\bar{e}, A] = \frac{Et}{2(1-\nu^2)} \Big(\lfloor \bar{e} \rfloor_i [K_{A_1}]_i \{\bar{e}\}_i + a^2 \lfloor \bar{e}_j \rfloor_i \left\{ \lfloor A_1 \rfloor_i [K_{1j}]_i \{A_1\}_i \right\} +$$

$$+ \frac{a^4}{4} \lfloor A_1 \rfloor_i [H_{SS_2}]_i \{A_1\}_i + \frac{a^4}{4} \lfloor A_1 \rfloor_i [H_{\eta\eta_2}] \{A_1\}_i + \frac{a^4}{4} \lfloor A_1 \rfloor_i [H_{S\eta_2}]_i \{A_1\}_i \Big) +$$

$$+ \frac{Et}{4(1+\nu)} \Big(\lfloor \bar{e} \rfloor_i [K_{A_2}]_i \{\bar{e}\}_i + 2a^2 \lfloor \bar{e}_j \rfloor_i \left\{ \lfloor A_1 \rfloor_i [K_{2j}]_i \{A_1\}_i \right\} \Big) +$$

$$- \nu(\lambda - \lambda_1) \left(\frac{a^2}{2} \lfloor A_1 \rfloor_i [K_{SS_1}]_i \{A_1\}_i \right) +$$

$$- (\lambda - \lambda_1) \left(\frac{a^2}{2} \lfloor A_1 \rfloor_i [K_{\eta\eta_1}]_i \{A_1\}_i \right) \qquad (22)$$

where higher order terms in $\lfloor A_2 \rfloor$ are neglected. Minimization of the energy increment with respect to $\lfloor \bar{e} \rfloor$ for the four element case defines $\lfloor \bar{e} \rfloor$ as a function of the amplitude coefficient $\underline{a}$ ($\lfloor \bar{e} \rfloor = \lfloor 0 \rfloor$ for single element case). Only interior gridpoint displacement components can be included in $\lfloor \bar{e} \rfloor$, in particular, $\lfloor \bar{e} \rfloor = \lfloor u_5 \;\; v_5 \;\; v_6 \;\; u_8 \rfloor$ with symmetry restrictions included.

The equation for the k^{th} component of $\lfloor \bar{e} \rfloor$ is

$$\Big(\frac{Et}{1-\nu^2} [K_{A_1}]_i \{\bar{e}\}_i + \frac{Et}{2(1+\nu)} [K_{A_2}]_i \{\bar{e}\}_i + \frac{Eta^2}{2(1-\nu^2)} \left\{ \lfloor A_1 \rfloor_i [K_{1k}]_i \{A_1\}_i \right\} +$$

$$+ \frac{Eta^2}{2(1+\nu)} \left\{ \lfloor A_1 \rfloor_i [K_{1k}]_i \{A_1\}_i \right\}_k = \{0\} \qquad (23)$$

where k identifies a component of $\lfloor \bar{e} \rfloor$ and i is summed on all elements that contain the k^{th} component as a generalized displacement. Since $\lfloor e_1 \rfloor = \lfloor 0 \rfloor$ any kinematically admissible displacement function is orthogonal to $\lfloor e_1 \rfloor$. In evaluating $\lfloor \bar{e} \rfloor$ minimization is imposed on each component due to the simplicity of the particular calculation and because any finite solution satisfies orthogonality. Alternately a mode shape could be selected consistent with the displacement constraints and minimization of an amplitude coefficient performed as outlined in the general theory.

For the four element representation ($\nu = 0.3$)

$$a^2 \lfloor \bar{e} \rfloor = a^2 \lfloor .008613 \quad .012695 \quad .048128 \quad .038862 \rfloor \tag{24}$$

This result is substituted into Eq. (22), then Eq. (22) is minimized with respect to $\underline{a}$. The resulting expression is

$$a^2 = \frac{\nu(\lambda-\lambda_1)\frac{h}{2}\lfloor A_1 \rfloor_i [K_{SS_1}]_i \{A_1\}_i + (\lambda-\lambda_1)\frac{l}{h}\lfloor A_1 \rfloor_i [K_{\gamma\gamma_1}]_i \{A_1\}_i}{4 A_4} \tag{25}$$

where

$$A_4 = \frac{Et}{8(1-\nu^2)} \left\{ \frac{h}{l^3} \lfloor A_1 \rfloor_i [H_{SS_2}]_i \{A_1\}_i + \frac{l}{h^3} \lfloor A_1 \rfloor_i [H_{\gamma\gamma_2}] \{A_1\}_i + \right.$$

$$+ \frac{2}{hl} \lfloor A_1 \rfloor_i [H_{S\gamma_2}] \{A_1\}_i - 4 \lfloor \bar{e} \rfloor_i [K_{A_1}]_i \{\bar{e}\}_i +$$

$$\left. - 2(1-\nu) \lfloor \bar{e} \rfloor_i [K_{A_2}]_i \{\bar{e}\}_i \right\} \tag{26}$$

Upon evaluation of $\underline{a}$, the complete displacement state as a function of load $\lambda > \lambda_1$ is determined for the plate. Equation (25) is the solution corresponding to the extended theory. Setting $[\bar{e}] = [0]$ we obtain the first approximation solution.

Results of these calculations are shown in Figure 4. Including the coupling expressed by $[\bar{e}] \neq 0$, the solution for the transverse displacement at the center of the plate for the four element case is

$$w = 0.810 \frac{\pm\sqrt{\lambda-\lambda_1}}{\sqrt{\lambda_1}} \tag{27}$$

compared to the Fourier series solution

$$w = 0.845 \frac{\pm\sqrt{\lambda-\lambda_1}}{\sqrt{\lambda_1}} \tag{28}$$

This is a difference of 4.1% between the two values with the finite element prediction stiffer than the series solution. It is noted that the single element prediction is off only 9.3%; thus convergence is slow but accuracy of coarse element prediction is high. Neglecting $[\bar{e}]$ in the four element case we get

$$w = 0.710 \frac{\pm\sqrt{\lambda-\lambda_1}}{\sqrt{\lambda_1}} \tag{29}$$

which is 16% off the series solution.

Preliminary to the post-buckling response calculation is calculation of the critical buckling modes. Values determined for the two element representations are

$$\lambda_1 = 0.70 \frac{Et^2}{(1-\nu^2)} \left(\begin{matrix}\text{one}\\ \text{element}\end{matrix}\right), \quad \lambda_1 = 0.668 \frac{Et^2}{(1-\nu^2)} \left(\begin{matrix}\text{four}\\ \text{element}\end{matrix}\right) \tag{30}$$

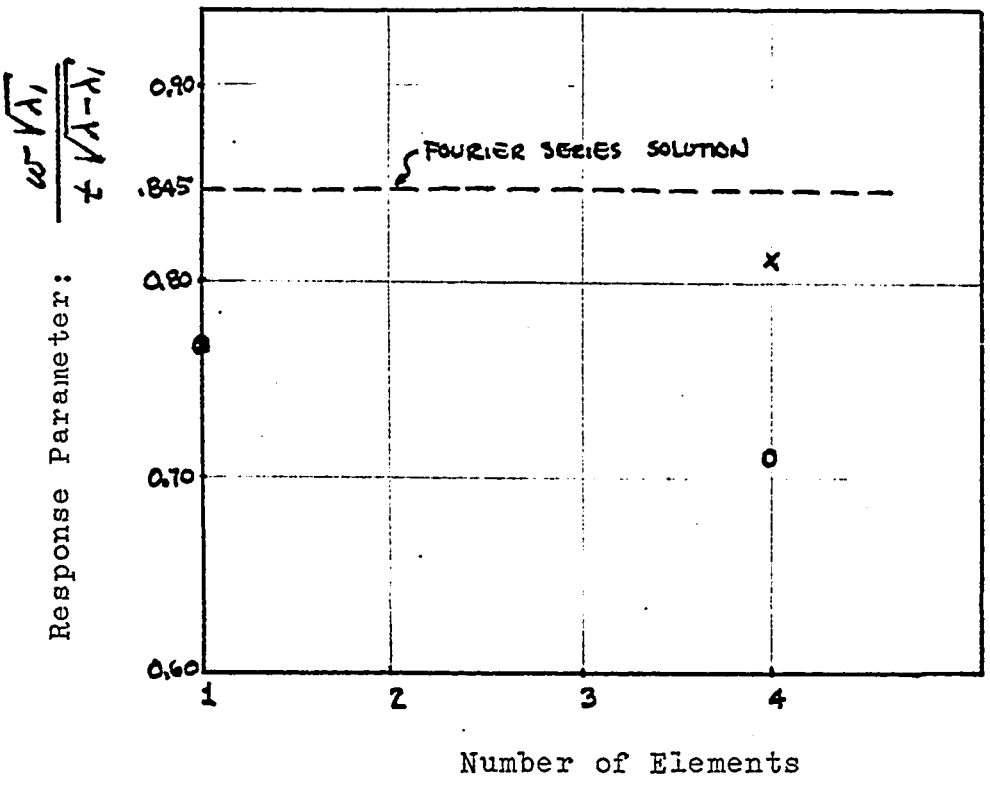

Figure IV-4. Plate-Response Prediction

as compared to $\lambda_1 = 0.632 \frac{Eh^2}{(1-\nu^2)}$ from the series solution, or differences of 10.7% and 5.7%, respectively. Thus, differences in the eigenvalue prediction are a guide to differences to be expected in the response prediction, as would be expected. The same trend is observed in the column problems treated in Section III.

V. ADDITIONAL APPLICATIONS OF THE GENERAL THEORY

5.1 The Uniform Shallow Arch.

So far example problems have been of structural configurations that are post-buckling stable. Consider next a case in which post-buckling response is unstable resulting in snap-through. The point of bifurcation is a singularity predicted from the nonlinear equations of equilibrium, and application of the perturbation method to the perfect structure idealization results in prediction of a negative-sloped post-buckling response path. The slope estimate is a qualitative measure of the sensitivity of the structure to imperfections. A small negative slope indicates relative insensitivity to imperfections and the load will approach the bifurcation value before imperfections cause buckling from the fundamental state. A large negative slope means the unstable post-buckling path (state) is in close proximity to the loading path and in the presence of small imperfections a jump may occur at loads appreciably below the theoretical buckling load. With this behavior, correlation between theory and experiment is difficult. Assumed forms of imperfections can be evaluated theoretically; however, this may not relate to physical conditions. Approaches used are statistical estimates of the expected range of imperfections (40) or exact control of the size and nature of the imperfection (34,41).

A number of perfect-structure arch configurations with different types of boundary conditions have been analyzed classically (42,43,44) as well as by the finite element

method (36,45). Classical results for a pin ended arch with sinusoidal shape and distributed load typlify the general characteristics of arch response (43). Under transverse loading a bifurcation point may or may not occur on the loading path, depending upon the specific geometric configuration of the arch. Define $\xi_o = a_o/R_g$ where a_o is the midspan height of the arch and $R_g = \sqrt{I/a}$ is the radius of gyration. For $\xi_o < 2.0$ (an extremely shallow arch) no decrease in load occurs as the arch deforms into a reverse curvature configuration. For $\xi_o < 4.0$ the structure buckles in a symmetric mode with axial load close to the Euler buckling load. For $\xi_o > 4.0$ the assumption of an asymmetric mode admits the condition for a point of bifurcation. For $\xi_o > 4.67$ change of state into the asymmetric mode occurs at loads Q* which are smaller in value than loads Q_c corresponding to horizontal tangency. The larger the value of ξ_o the greater the difference in the two loads (Figure 1). For large values of ξ_o, structural response up to the point of bifurcation is essentially linear.

5.1.1 Finite Element Formulation of the Shallow Arch Equations.

A modified development of the total potential energy is followed in light of admission of geometric imperfections. The work integral for a distributed transverse load per unit length $q(x) = q_o \bar{v}(x)$ for an element of length ℓ under transverse displacement $v(x)$ is

$$W = \int_0^{\ell} q(x)\, v(x)\, dx \qquad (1)$$

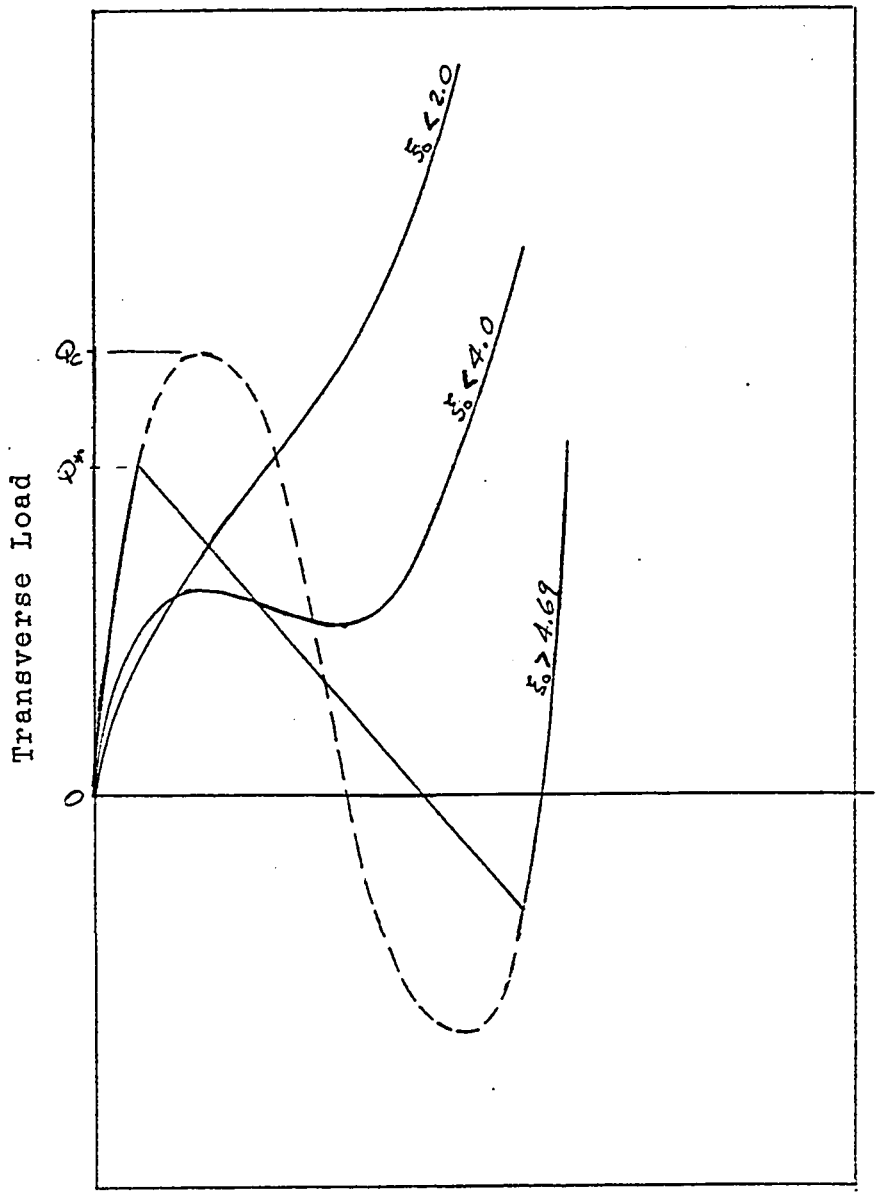

Figure V-1: Arch, Qualitative Response Characteristics

Substituting from Eq. (III-14) and integrating

$$W = \frac{q_o l}{420} \{\tilde{a}\}[M]\{a\} \tag{2}$$

where

$$[M] = \begin{bmatrix} 156 & 22 & 54 & -13 \\ & 4 & 13 & -3 \\ & & 156 & -22 \\ \text{SYM.} & & & 4 \end{bmatrix} \tag{3}$$

and $\{\tilde{a}\}$ is the column of normalized shape coefficients of the transverse load distribution.

The extensional form of the total potential energy for a straight column, Eq. (III-32), including the external work, Eq. (3), summed over all elements i, is

$$P[a,e] = \lambda^{1-1} U\{e\}_i + \frac{EA}{2l}\{e\}_i[K_A]_i\{e\}_i + \frac{EI}{2l^3}\{a\}_i[K_0]_i\{a\}_i +$$
$$-\frac{\lambda P_i}{2l}\{a\}_i[K_1]_i\{a\}_i - \frac{q_o l}{420}\{\tilde{a}\}_i[M]_i\{a\}_i +$$
$$+\frac{EA_i}{2l^2}\lambda^{1-1} U\{e\}_i\{a\}_i[K_1]_i\{a\}_i + \frac{EA_i}{8l^2}\{a\}_i[L_i]_i\{a\}_i + \cdots \tag{4}$$

Starting at this point in the finite element development already admits certain approximations that are made in the shallow arch formulation. Parameter λ represents the in-plane load intensity factor, and taking it constant for all elements implies a shallow arch with uniform material and geometric properties. If this cannot be assumed then a more general formulation of the problem is required.

The initial arched shape is introduced by assuming an initial shape function $a_o\{a_o\}$, where a_o is the midspan

height and $\{A_o\}$ are the normalized displacement coefficients. Transverse displacement from the initial state is represented by $\{\bar{A}\}$ so that "total" displacement is

$$\{A\} = a_o\{A_o\} + \{\bar{A}\} \tag{5}$$

and the total potential energy is

$$\begin{aligned}
\Phi[A,e] = {} & \lambda \underline{L-1\ U}\{e\}_i + \frac{Ea}{2\ell} \underline{Le}\underline{J}_i [K_o]_i \{e\}_i + \\
& + \frac{EI}{2\ell^3} \underline{L\bar{A}}\underline{J}_i [K_o]_i \{\bar{A}\}_i - \frac{\lambda P_i}{2\ell} \underline{L\bar{A}}\underline{J}_i [K_1]_i \{\bar{A}\}_i + \\
& - \frac{\lambda P_i}{\ell} a_o \underline{LA_o}\underline{J}_i [K_1]_i \{\bar{A}\}_i - \underline{\frac{\lambda P_i}{2\ell} a_o^2 \underline{LA_o}\underline{J}_i [K_1]_i \{A_o\}_i} + \\
& - \underline{\frac{q_o \ell}{420} a_o \underline{L\bar{A}}\underline{J}_i [M]_i \{A_o\}_i} - \frac{q_o \ell}{420} \underline{L\bar{A}}\underline{J}_i [M]_i \{\bar{A}\}_i + \\
& + \frac{Ea}{\ell^2} a_o \underline{L-1\ U}\{e\}_i \underline{LA_o}\underline{J}_i [K_1]_i \{\bar{A}\}_i + \\
& + \frac{Ea}{2\ell^2} \underline{L-1\ U}\{e\}_i \underline{L\bar{A}}\underline{J}_i [K_1]_i \{\bar{A}\}_i + \\
& + \frac{Ea}{8\ell^3} \underline{L\bar{A}}\underline{J}_i [L_2]_i \{\bar{A}\}_i + \frac{Ea}{2\ell^3} \underline{LA_o}\underline{J}_i [L_2]_i \{\bar{A}\}_i + \cdots .
\end{aligned} \tag{6}$$

where it is assumed the column in its initial arched shape is stress free. Variation is on $\underline{Le}\underline{J}$ and $\underline{L\bar{A}}\underline{J}$, thus the dash underlined terms can be dropped without loss of generality. For a kinematically admissible but arbitrary variation in the j^{th} component of $\underline{L\bar{A}}\underline{J}$ the following equilibrium equation is obtained

$$\lfloor \delta\bar{a}_j \rfloor \left\{ \frac{EI}{\ell^3} [K_0]_i \{\bar{a}\}_i + \frac{\lambda}{\ell} [K_1]_i \{\bar{a}\}_i + \frac{\lambda}{\ell} a_0 [K_1]_i \{A_0\}_i - \frac{q_0 \ell}{420} [M]_i \{\ddot{\bar{a}}\}_i + \right.$$

$$\left. + \frac{Ea_1}{\ell^2} \lfloor -1 \; 1 \rfloor \{e\}_i [K_1]_i \{A_0\}_i + \frac{3Ea_1}{2\ell^3} [L_2]_i \{A_0\}_i + \cdots \right\}_j = 0 \qquad (7)$$

where i is summed on all elements that contain the j^{th} coefficient. It is seen that both constant and quadratic terms in $\lfloor \bar{a} \rfloor$ remain in truncation to quadratic terms. This inhomogeneity negates an eigenvalue form, obtaining instead a nonlinear response equation.

One method of solution is suggested by the form of Eq. (7), that eigenvalues and vectors can be evaluated from the quadratic terms in $\lfloor \bar{a} \rfloor$. These are simply the straight-column functions and values which are designated by λ_1, λ_2, λ_3 ----and A_1, A_2, A_3----respectively. The initial shape and load distribution functions are assumed expressible in terms of a finite sequence of these functions as follows

$$\lfloor A_0 \rfloor = a_{0j} \lfloor A_j \rfloor \qquad j = 1,3, \ldots m$$
$$\lfloor \ddot{\bar{a}} \rfloor = a_{Lj} \lfloor A_j \rfloor \qquad j = 1,3, \ldots n \qquad (8)$$

where the a_{0j} and a_{Lj} are specified constants. Only symmetric distributions are admitted in order that a bifurcation can potentially occur on the loading path. Any assumed asymmetry results simply in a nonlinear loading to a point of horizontal tangency. For $\lfloor \bar{a} \rfloor$ we take

$$\lfloor \bar{a} \rfloor = a_j \lfloor A_j \rfloor \qquad j = 1,3,5 \ldots \qquad (9)$$

while for the in-plane displacements $[e]$, which must be symmetric, variation with respect to each modal displacement component yields a set of equilibrium equations that when summed result in an additional relation between λ and the bending deflection $[\Delta]$. This result is a consequence of the assumption on constant λ and uniform structure properties.

Assuming $n > m$ in Eq. (8), and substituting Eqs. (8) and (9) into Eq. (6), variation of Eq. (6) with respect to the a_j yields

$$\frac{EI}{\ell^3} a_j [A_j]_i [K_0]_i \{A_j\}_i + \frac{\lambda}{\ell} a_j [A_j]_i [K_1]_i \{A_j\}_i +$$

$$+ \frac{\lambda}{\ell} a_0 [A_0]_i [K_1]_i \{A_j\}_i - \frac{q_0 \ell}{420} a_{1j} [A_j]_i [M]_i \{A_j\}_i +$$

$$+ \text{higher order terms in } a_j = 0 \quad (j = 1, 3, \ldots n) \qquad (10)$$

Recognizing that λ varies with q_o and a_j in Eq. (10), the total nonlinear response is obtained by summation of modal contributions. The response curves obtained by this procedure are slope-continuous curves as shown in Figure 1.

If a bifurcation occurs in the loading path then the symmetric solution described above represents the pre-buckled displacement state. With $[A_o]$ and $[\Delta]$ expressed in terms of symmetric functions in Eq. (10), the first asymmetric mode, $[A_2]$, is obtained from a homogeneous quadratic form from Eq. (10). This function, orthogonal to the symmetric modes that define the pre-buckling deflection of the arch, is

examined for specifications of a possible adjacent state corresponding to a point of bifurcation.

To simplify further work we introduce a specific arch configuration that is representative of the general case. We consider a finite element formulation with arch shape and load distribution proportional to the fundamental buckling mode of a straight column having the same span length as the arch. The initial shape is then $a_0 \{A_1\}$, where a_0 is the midspan height and $\{A_1\}$ are the vector coefficients of the fundamental buckling mode. Deviation from this zero stress state is represented by $a_{1I} \{A_1\}$ and $a_2 \{A_2\}$ for, respectively, possible first mode symmetric and second mode asymmetric deflections. The initial shape function may be interpreted as an initial state imperfection from the straight column geometry. Thus a_0 must be considered small consistent with the shallow arch approximation. Total displacement from the straight column configuration is then

$$\{A\} = a_0\{A_1\} + a_{1I}\{A_1\} + a_2\{A_2\} \tag{11}$$

where a_{1I} and a_2 are variables for the arch geometry. If imperfections are admitted in the shape of the first and second buckling modes then the displacement function is expanded to

$$\{A\} = a_0\{A_1\} + a_{1I}\{A_1\} + a_2\{A_2\} + \bar{a}_1\{A_1\} + \bar{a}_2\{A_2\} \tag{12}$$

where $\bar{a}_1$ and $\bar{a}_2$ are numerical coefficients. Substituting for $[A]$ from Eq. (12) and retaining terms only of lowest order in the imperfections on the basis that the imperfections are of

small amplitude

$$\begin{aligned}\Phi[A,e] = {} & \lambda^{L-1}U\{e\}_i + \frac{EA}{2\ell}\,Le\rfloor_i[K_A]_i\{e\}_i + \\ & + \frac{EI}{2\ell^3}a_{1I}^2\,\lfloor A_1\rfloor_i[K_0]_i\{A_1\}_i + \frac{EI}{2\ell^3}a_2^2\,\lfloor A_2\rfloor_i[K_0]_i\{A_2\}_i + \\ & + \frac{\lambda}{2\ell}a_{1I}^2\,\lfloor A_1\rfloor_i[K_1]_i\{A_1\}_i + \frac{\lambda}{2\ell}a_2^2\,\lfloor A_2\rfloor_i[K_1]_i\{A_2\}_i + \\ & + \frac{\lambda}{\ell}a_0a_{1I}\,\lfloor A_0\rfloor_i[K_1]_i\{A_1\}_i + \frac{\lambda}{\ell}\bar{a}_1a_{1I}\,\lfloor A_1\rfloor_i[K_1]_i\{A_1\}_i + \\ & + \frac{\lambda}{\ell}\bar{a}_2a_2\,\lfloor A_2\rfloor_i[K_1]_i\{A_2\}_i + \frac{EA}{\ell^2}a_0a_{1I}\,\lfloor A_0\rfloor_i^{L-1}U\{e\}_i\,\lfloor A_0\rfloor_i[K_1]_i\{A_1\}_i + \\ & + \frac{EA}{\ell^2}a_0a_2\,\lfloor A_0\rfloor_i^{L-1}U\{e\}_i\,\lfloor A_0\rfloor_i[K_1]_i\{A_1\}_i + \frac{EA}{2\ell^2}a_{1I}^2\,\lfloor A_1\rfloor_i^{L-1}U\{e\}_i\,\lfloor A_1\rfloor_i[K_1]_i\{A_1\}_i + \\ & + \frac{EA}{2\ell^2}a_2^2\,\lfloor A_2\rfloor_i^{L-1}U\{e\}_i\,\lfloor A_2\rfloor_i[K_1]_i\{A_2\}_i + \\ & + \frac{EA}{8\ell^3}a_{1I}^4\,\lfloor A_1\rfloor_i[L_2]_i\{A_1\}_i - \frac{\rho_0\ell}{420}a_{1I}\,\lfloor\hat{A}\rfloor_i[M]_i\{A_1\}_i + \cdots \end{aligned} \tag{13}$$

where the displacement functions of Eq. (11) are orthogonal by

$$\lfloor A_n\rfloor[K_0]\{A_m\} = \begin{cases} -\frac{\lambda_n\ell^2}{EI} & m=n \\ 0 & m\neq n \end{cases} \qquad \lfloor A_n\rfloor[K_1]\{A_m\} = \begin{cases} 1 & m=n \\ 0 & m\neq n \end{cases} \tag{14}$$

The total potential energy is first minimized with respect to the j^{th} component of $Le\rfloor_i$ holding all other displacement variables constant. The resulting equation is

$$\begin{aligned}\Big\{ & \lambda^{L-1}U\{\delta e\}_i + \frac{EA}{\ell}\,Le\rfloor_i[K_A]_i\{\delta e\}_i + \lfloor\delta e\rfloor_i^{L-1}U\Big[\frac{EA}{2\ell^2}a_{1I}^2\,\lfloor A_1\rfloor_i[K]_i\{A_1\}_i + \\ & + \frac{EA}{2\ell^2}a_2^2\,\lfloor A_2\rfloor_i[K_1]_i\{A_2\}_i + \frac{EA}{\ell^2}a_0a_{1I}\,\lfloor A_1\rfloor_i[K_1]_i\{A_1\}_i\Big]\Big\}_j = 0 \end{aligned} \tag{15}$$

where i is summed on all elements containing the j^{th} component.

The variation is assumed arbitrary, so setting the coefficient equations to zero and summing these equations over all elements of the arch, the sum of the second terms is zero and λ is expressed in terms of the transverse displacement variables by

$$\lambda = \frac{EA}{L}\left[\frac{a_{1I}^2}{2\ell}\{A_1\}[K_1]\{A_1\} + \frac{a_2^2}{2\ell}\{A_2\}[K_1]\{A_2\} + \frac{a_0 a_{1I}}{\ell}\{A_1\}[K_1]\{A_1\}\right] \quad (16)$$

Defining the non-dimensionalization

$$Q_0 = \frac{q_0 L^4}{\pi^4 EI R_1}, \quad \xi_n = \frac{a_n}{R_1}, \quad \lambda^* = \frac{\lambda L^2}{EI} \quad (17)$$

Eq. (16) becomes

$$\lambda^* = \frac{N}{2}\left[\xi_{1I}^2 + \xi_2^2 + 2\xi_0\xi_1\right] \quad (18)$$

where N is the number of elements of the arch (Figure 2). The third term in Eq. (18) corresponds to the strain of initial curvature $\frac{v}{R}$ which for shallow geometry is approximated by $\frac{dv}{dx}\frac{dy}{dx}$ (Reference 21).

Minimizing the total potential energy with respect to a_{1I} and a_2, and non-dimensionalizing, the following equilibrium equations are obtained

$$\xi_{1I}(\lambda^* - \lambda_1^*) + \xi_0\lambda^* + \bar{\xi}_1\lambda^* - \frac{Q_0\pi^4}{420N^2}\left(\{\bar{A}\}_i[M]_i\{A_1\}_i\right) + \cdots = 0 \quad (19)$$

$$\xi_2(\lambda^* - \lambda_2^*) + \bar{\xi}_2\lambda^* = 0 \quad (20)$$

In Eq. (19) the term $\xi_0\lambda^*$ representing the moment due to the initial curved shape is assumed large compared to third and fourth order terms in ξ_{1I} and ξ_2 obtained from Eq. (14).

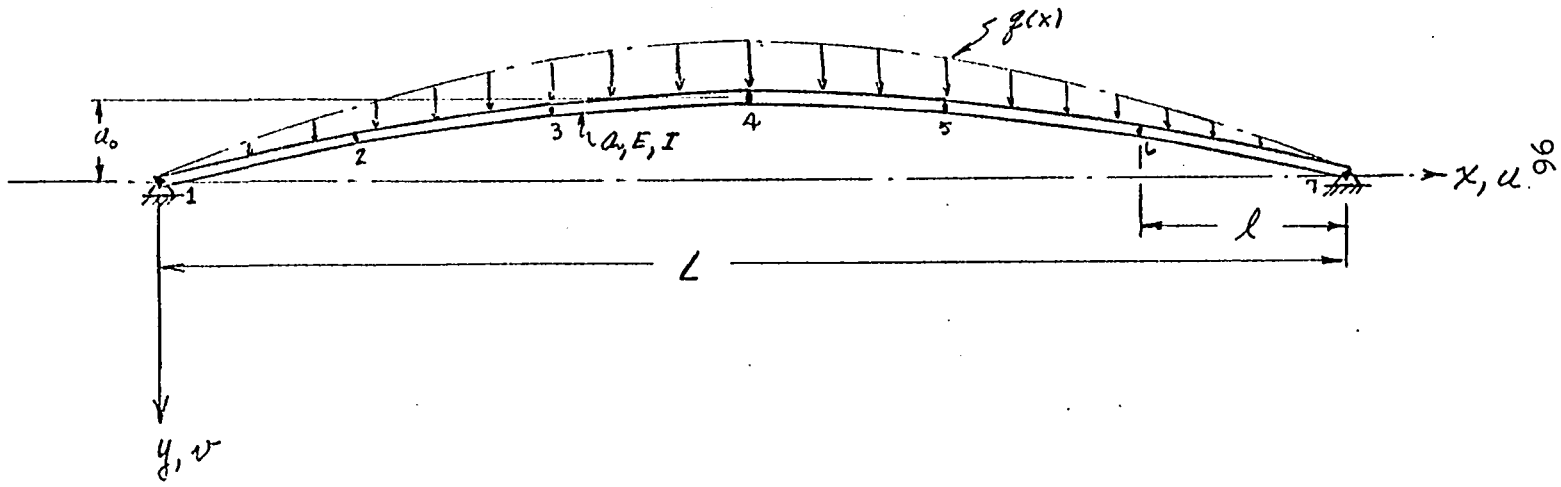

Figure V-2: Arch, Finite Element Idealization

5.1.2 Numerical Evaluation of Arch Response.

There is adequate documentation of the shallow arch problem depicting the various possible equilibrium paths in its configuration space (34,42,43,44). Concern here is accurate prediction of perfect structure and imperfect structure response using a simple finite element representation of the arch. To evaluate this, the structure initially omitting initial imperfections ($\bar{\xi}_1 = \bar{\xi}_2 = 0$) is idealized by 4, 6 and 8 element representations, and response from zero load is evaluated. Two arch geometries are considered, defined by $\xi_0 = 6$ and 50, which respectively represent extreme and moderate shallowness and/or member thinness.

In the absence of the imperfection $\bar{\xi}_2$, Eq. (20) reduces to $\xi_2(\lambda^* - \lambda_2^*) = 0$ so that

i) $\xi_2 = 0$ and λ^* is arbitrary or

ii) $\lambda = \lambda_2^*$ and ξ_2 is arbitrary.

Condition (i) corresponds to the prebuckling state of symmetric deformation. Condition (ii) corresponds to admittance of the asymmetric second mode which occurs when the average in-plane load $\lambda^* = \lambda_2^*$ (second mode buckling load for the straight column) and sudden change of state of deformation into the second mode causes instability. The amplitude coefficient ξ_2 is not specified directly from its minimization condition; however, with λ^* specified, ξ_2 can be calculated from Eq. (18) for parameterization on ξ_{1I}. Finally, from Eq. (19) we obtain the value of the transverse load Q_o. The response curves for increasing load from zero-load are

shown in Figures 3 and 4. For the four-element case

$$\lfloor A_1 \rfloor = \lfloor \Theta_1 \ell \quad v_2 \quad \Theta_2 \ell \quad v_3 \quad \Theta_3 \ell \quad v_4 \quad \Theta_4 \ell \quad \Theta_5 \ell \rfloor =$$

$$\lfloor .70714 \quad .63693 \quad .50024 \quad .90076 \quad 0.0 \quad .63693 \quad .50024 \quad .70714 \rfloor$$

and

$$\lfloor \hat{x} \rfloor = \lfloor 0.0 \quad -.70599 \quad 0.0 \quad -1.0 \quad 0.0 \quad -.70599 \quad 0.0 \quad 0.0 \rfloor$$

To summarize, in the prebuckled initial state $(\lambda^* < \lambda_2^*)$ the governing equations for the perfect arch are

$$\frac{1}{R_j} \{A\} = \xi_0 \{A_1\} + \xi_{1_I} \{A_1\}$$

$$\lambda^* = \frac{N}{2} \left(\xi_{1_I}^2 + \xi_0 \xi_{1_I} \right)$$

$$\xi_{1_I} (\lambda^* - \lambda_1^*) + \xi_0 \lambda^* - \frac{Q_0 \pi^4}{420 N^2} \left(\lfloor \hat{x} \rfloor_i [M]_i \{A_1\}_i \right) + \ldots = 0$$

$$\xi_2 = 0$$

At the point of bifurcation $(\lambda^* = \lambda_2^*)$

$$\frac{1}{R_j} \{A\} = \xi_0 \{A_1\} + \xi_{1_{I_c}} \{A_1\}$$

$$\lambda_2^* = \frac{N}{2} \left(\xi_{1_{I_c}}^2 + 2 \xi_0 \xi_{1_{I_c}} \right)$$

$$\xi_{1_{I_c}} (\lambda_2^* - \lambda_1^*) + \xi_0 \lambda_2^* - \frac{Q_{0c} \pi^4}{420 N^2} \left(\lfloor \hat{x} \rfloor_i [M]_i \{A_1\}_i \right) + \ldots = 0$$

$$\xi_2 = 0$$

If displacement into the post buckled state is defined by

$$\{A\} = a_0 \{A_1\} + (a_{1_{I_c}} + a_{1_{II}}) \{A_1\} + a_2 \{A_2\}$$

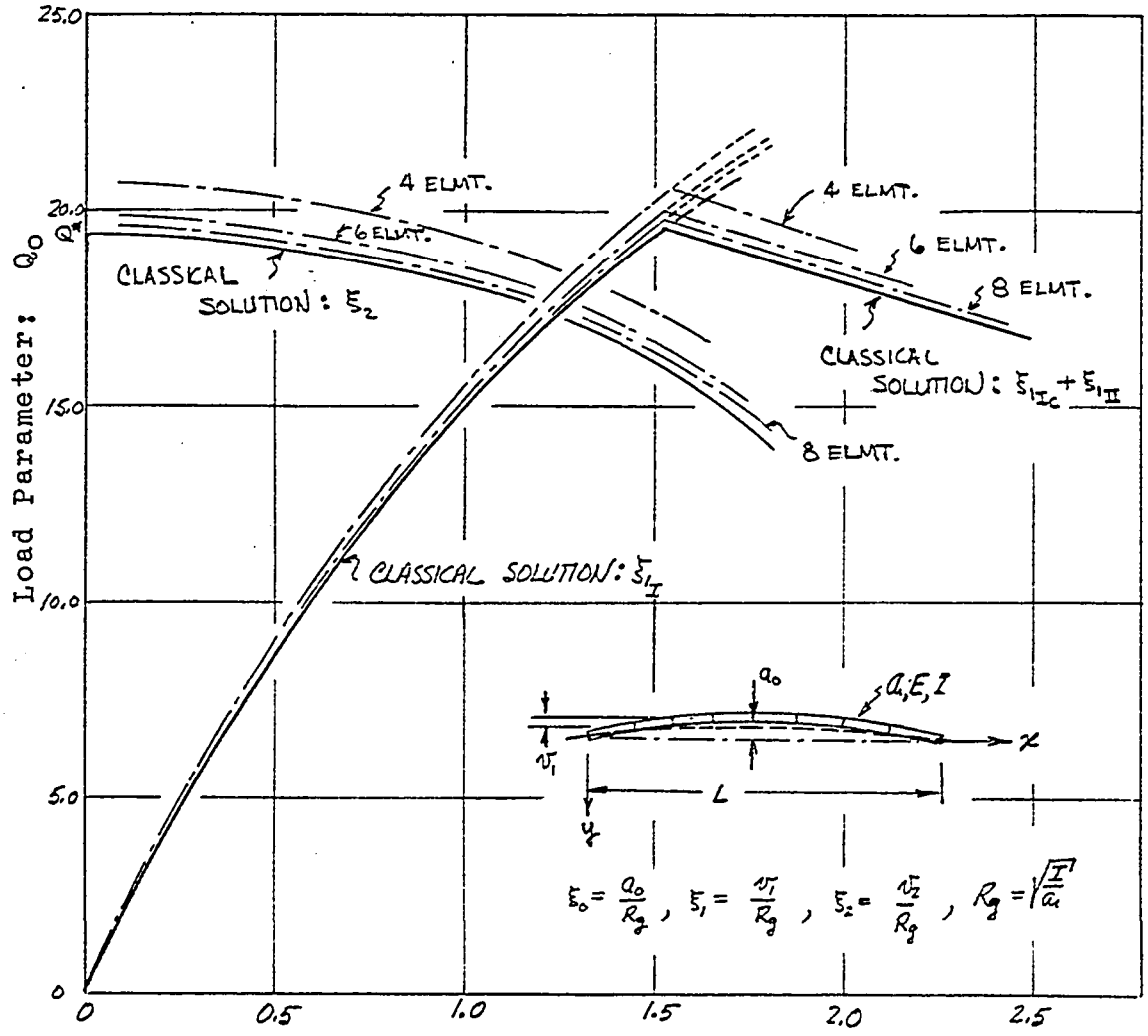

Figure V-3: Arch Response for $\xi_0 = 6$

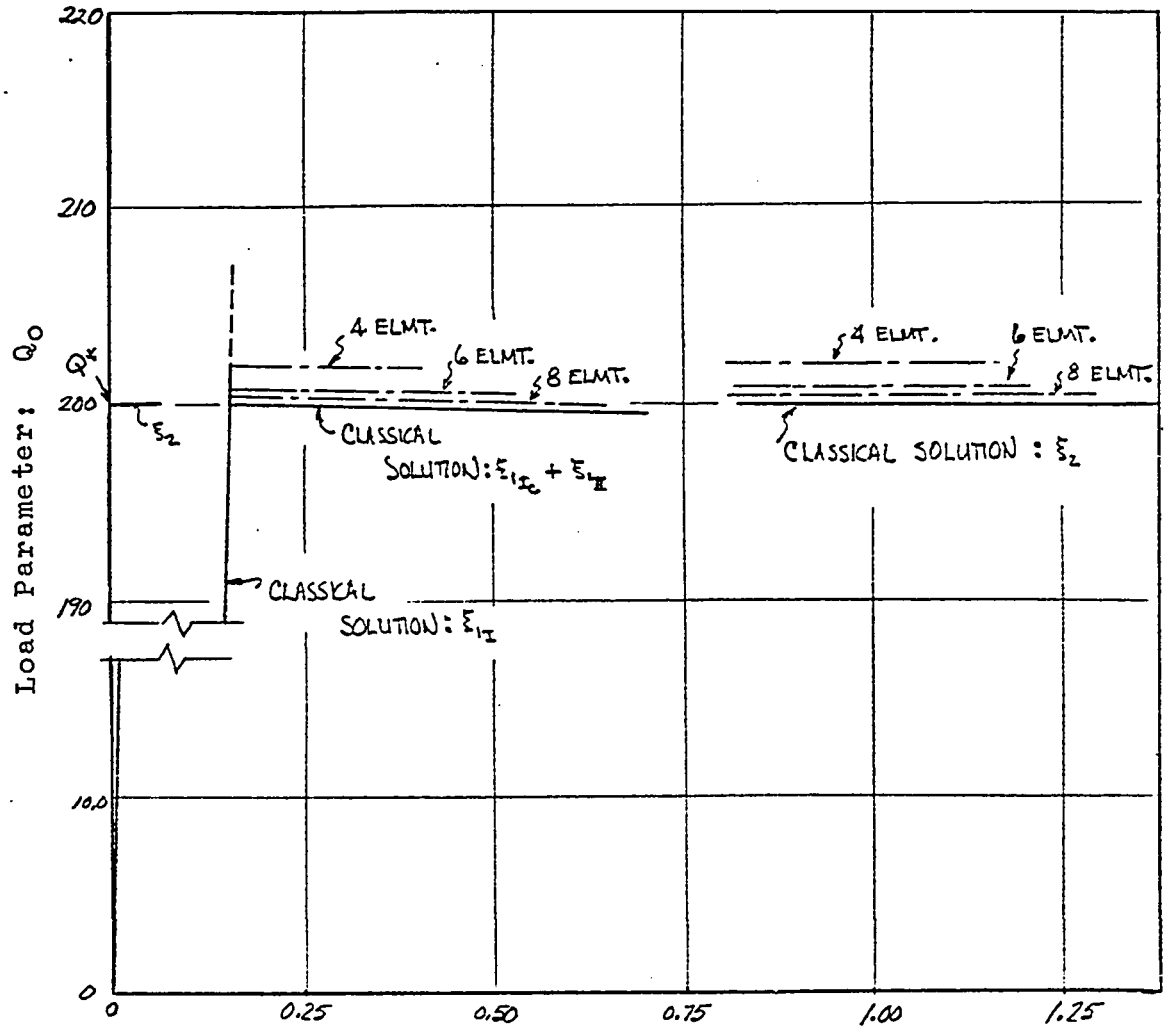

Figure V-4: Arch Response for $\xi_0 = 50$

then the increment in total potential energy is

$$P[\Delta] = \frac{EI}{2\ell^3}\left(a_{1II}^2 + 2a_{1II}a_{1Ic}\right)\{\Delta_1\}_i^T[K_0]_i\{\Delta_1\}_i +$$
$$+ \frac{\lambda}{2\ell}\left(a_{1II}^2 + 2a_{1II}a_{1Ic}\right)\{\Delta_1\}_i^T[K_1]_i\{\Delta_1\}_i +$$
$$+ \frac{EI}{2\ell^3}a_2^2\{\Delta_2\}_i^T[K_0]_i\{\Delta_2\}_i + \frac{\lambda}{2\ell}a_2^2\{\Delta_2\}_i^T[K_1]_i\{\Delta_2\}_i +$$
$$+ \frac{\lambda}{\ell}a_0a_{1II}\{\Delta_1\}_i^T[K_1]_i\{\Delta_1\} - \frac{\Delta q_0\ell}{420}a_{1Ic}\{\tilde{\Delta}\}_i^T[M]_i\{\Delta_1\}_i +$$
$$- \frac{(q_{0c}+\Delta q_0)\ell}{420}a_{1II}\{\tilde{\Delta}\}_i^T[M]_i\{\Delta_1\}_i + \ldots.$$

and the non-dimensionalized incremental equations of equilibrium are $(\lambda^* = \lambda_2^*)$

$$2\xi_{1Ic}\xi_{1II} + \xi_{1II}^2 + \xi_2^2 + 2\xi_0\xi_{1II} = 0$$
$$(\xi_{1Ic} + \xi_{1II})(\lambda_2^* - \lambda_1^*) + \xi_0\lambda_2^* - \frac{Q_0\pi^4}{420N^2}\{\tilde{\Delta}\}_i^T[M]_i\{\Delta_1\}_i = 0 \qquad (21)$$

Displacements into the post buckled state corresponding to solution of Eqs. (21) are shown in Figures 3 and 4.

5.1.3 Arch Response with Initial Geometric Imperfections.

With introduction of the symmetric imperfection $(\bar{\xi}_1 \neq 0, \bar{\xi}_2 = 0)$ the principal effect is a lowering of the critical buckling load, Q^*, without any change in the form of the load-deflection curve. This imperfection can be interpreted as simply an increasing of the shallowness of the arch prior to loading. With ξ_0 specifying the reference configu-

ration (buckling pressure Q^*) the effect of $\bar{\xi}_1$ on reduction of the buckling load to $\bar{Q}^*$ is shown in Figures 5 and 6 for $\xi_0 = 6$ and 50 respectively. The eight-element representation of the arch is used in this evaluation.

The assumption of an initial imperfection in the shape of the fundamental asymmetric mode results in reduction of the maximum load, and also a change in the characteristics of the load-deflection response. The fractional change in maximum load versus size of imperfection $\bar{\xi}_2$ (relative to ξ_0) is plotted in Figures 5 and 6. Typical load-deflection curves versus size of imperfection are shown in Figure 7.

In Figures 5 and 6 curves are given showing the decrease in critical pressure versus size of imperfection. The slopes of these curves are of interest, particularly the slopes of the curves for $\bar{\xi}_2 \neq 0$, $\bar{\xi}_1 = 0$ as $\bar{\xi}_2 \to 0$.

The critical load Q^* corresponding to $\bar{\xi}_1 = \bar{\xi}_2 = 0$ is determined from Eq's. (18), (19) and (20). From Eq. (20)

$$\lambda^* = \lambda_2^*$$

next, from Eq. (18)

$$\xi_{1_{I_c}} = -\xi_0 \pm \sqrt{\xi_0^2 - \left(\xi_2^2 - \frac{2\lambda_2^*}{N}\right)}$$

however, ξ_0 is large compared to the remaining terms under the radical so that from the binomial expansion

$$\xi_{1_{I_c}} \simeq \frac{\lambda_2^*}{N\xi_0^2} - \frac{1}{2}\,\frac{\xi_2^2}{\xi_0^2} + \cdots$$

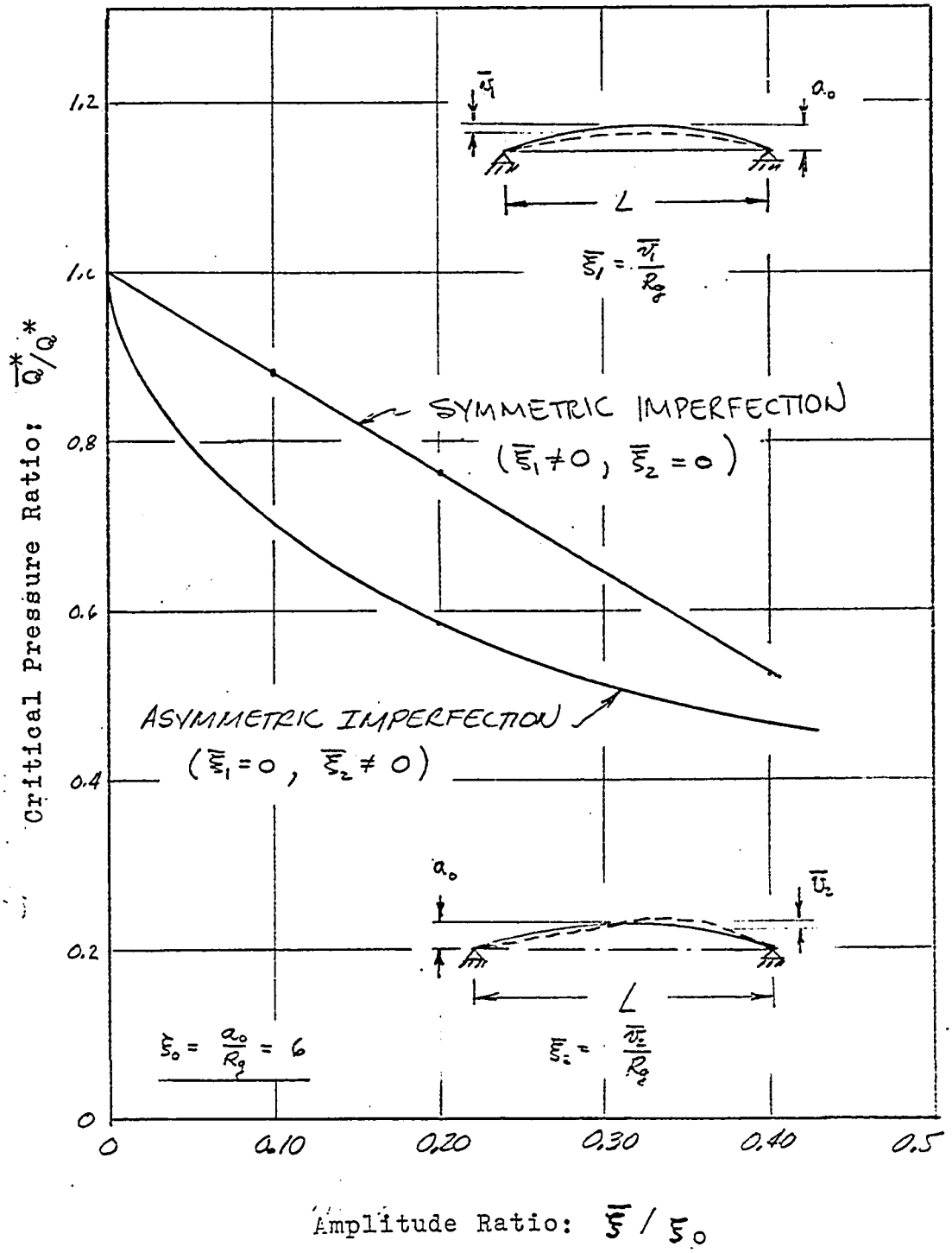

Figure V-5: Arch-Buckling Load of Imperfect Structure, $\xi_0 = 6$

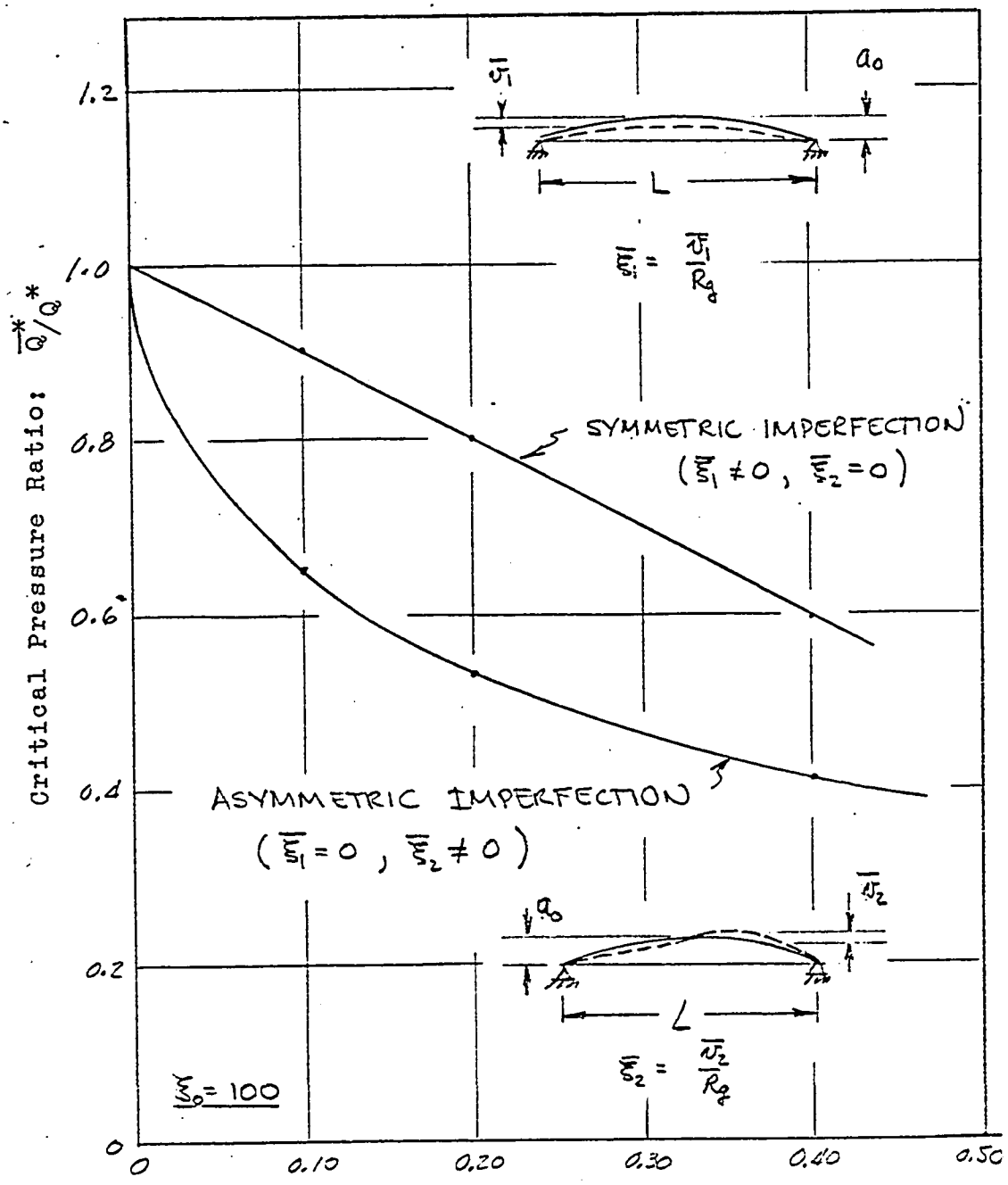

Figure V-6: Arch-Buckling Load of Imperfect Structure, $\xi_0 = 50$

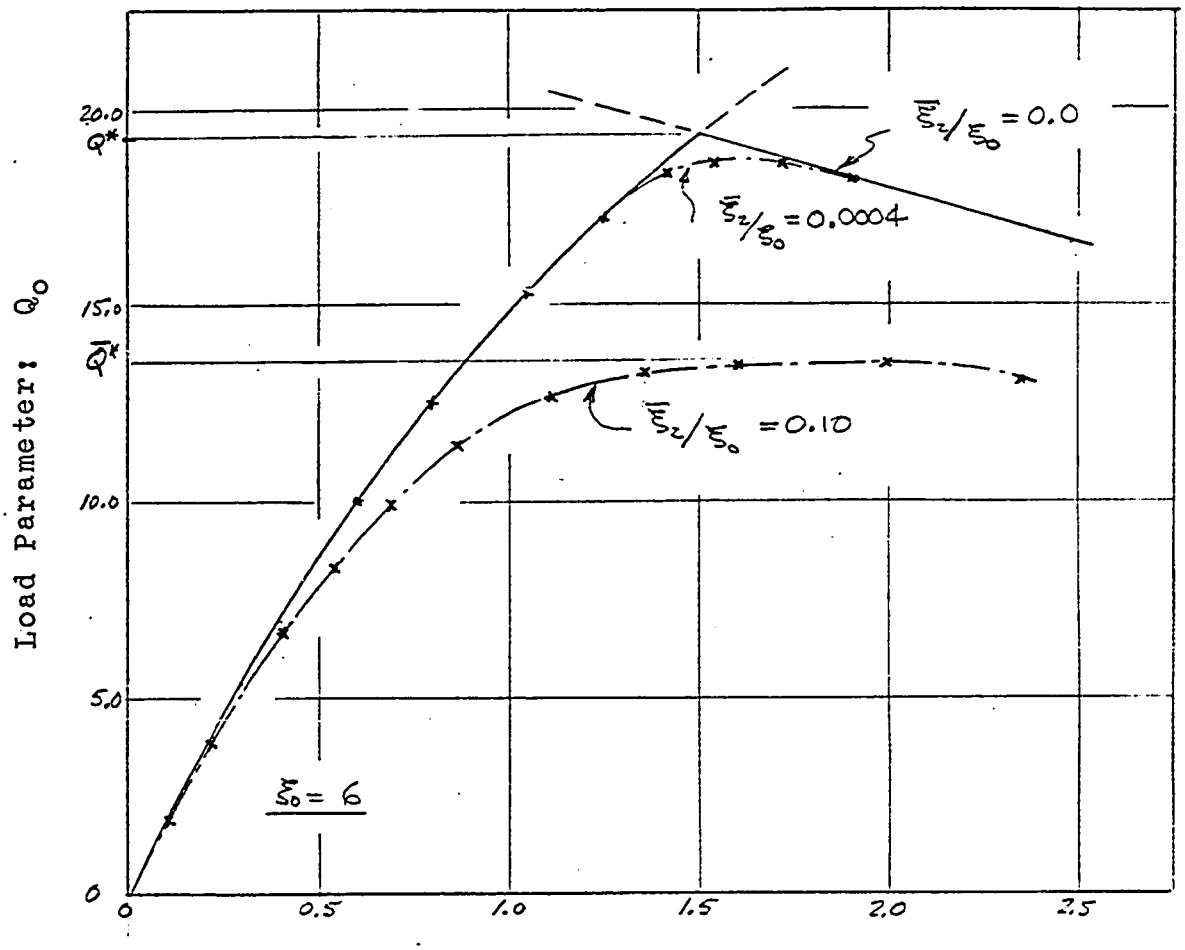

Figure V-7: Arch-Load-Deflection Response with Asymmetric Imperfection

Substituting these results into Eq. (19) and taking the limit $\xi_2 \to 0$

$$\frac{\pi^4}{420N^2} Q^* \{\bar{x}\}_i [M]_i \{\phi\}_i = \xi_0 \lambda_2^* + \frac{\lambda_2^*}{\xi_0^2 N} (\lambda_2^* - \lambda_1^*)$$

With $\bar{\xi}_1 \neq 0$ the equation for $\bar{Q}^*$ is

$$\frac{\pi^4}{420N^2} \bar{Q}^* \{\bar{x}\}_i [M]_i \{\phi\}_i = \xi_0 \lambda_2^* + \xi_1 \bar{\xi}_1 \lambda_2^* + \left(\frac{\lambda_2^*}{N} - \frac{1}{2}\xi_2^2\right) \frac{(\lambda_2^* - \lambda_1^*)}{\xi_0^2} + \cdots$$

thus

$$\frac{\bar{Q}^*}{Q^*} = \frac{\xi_0^2 N (\xi_0 + \bar{\xi}_1) + \left(1 - \frac{1}{2} N \xi_2^2\right)(\lambda_2^* - \lambda_1^*)}{\xi_0^3 N + (\lambda_2^* - \lambda_1^*)}$$

The term with ξ_2 is negligibly small (e.g., $\xi_0 = -6$, N=8, $\xi_2 < 1$, $\lambda_1^* \approx \pi^2$, $\lambda_2^* \approx 4\pi^2$) , so that

$$\frac{\partial \bar{Q}^*/Q^*}{\partial \bar{\xi}_1} \approx \frac{\xi_0^2 N}{\xi_0^3 N + (\lambda_2^* - \lambda_1^*)} \qquad (22)$$

Consider next $\bar{\xi}_2 > 0$ and $\bar{\xi}_1 = 0$. From Eq. (20)

$$\lambda^* = \frac{\xi_2 \lambda_2^*}{\xi_2 + \bar{\xi}_2}$$

and ξ_{11} is unchanged. Substituting into Eq. (19)

$$\frac{\bar{Q}^*}{Q^*} = \frac{\left(\lambda_2^* - \tfrac{1}{2} N \xi_2^2\right)\left[\xi_2 \lambda_2^* - \lambda_1^*\left(\xi_2 + \bar{\xi}_2\right) + \xi_0^3 N \xi_2 \lambda_2^*\right]}{\lambda_2^*\left(\xi_2 + \xi_2^*\right)\left(\xi_0^3 N + \lambda_2^* - \lambda_1^*\right)}$$

thence

$$\frac{\partial\left(\bar{Q}^*/Q^*\right)}{\partial \bar{\xi}_2} = -\frac{\xi_2\left(\lambda_2^* - \tfrac{1}{2} N \xi_2^2\right)\left(1 + \xi_0^3 N\right)}{\left(\xi_2 + \bar{\xi}_2\right)^2\left(\xi_0^3 N + \lambda_2^* - \lambda_1^*\right)} \qquad (23)$$

Taking the limit as $\bar{\xi}_2 \longrightarrow 0$, then $\xi_2 \longrightarrow 0$ it is seen that the slope is infinite. Thus, the imperfection curves for $\bar{\xi}_2$ in Figures 5 and 6 are vertically tangent at $\frac{\bar{Q}^*}{Q^*} = 1$. This indicates an extreme sensitivity to imperfections or disturbances for loads approaching the buckling load.

5.1.4 Comments on the Arch Analysis.

The quadratic structure response depicted in the results for the arch is seen also in the equilibrium equations if the expression for λ^*, Eq. (18), is substituted into the equilibrium equations, Eq's. (19), (20) and recognizing that the third term in Eq. (18) is dominant. Based upon the response predicted for the imperfection-free structure, Figures 3 and 4, it is concluded that the finite element representation is accurate and converges rapidly with grid refinement. The error in the buckling load in the four-element representation is 3.6% for $\xi_0 = 6$ (extreme shallowness) and 4.5% for $\xi_0 = 50$ (moderate shallowness). The error reduces well below 1% in the eight-element solution. The four-element representation is the crudest representation that admits the second mode.

Structural sensitivity to the symmetric initial imperfection is about equal for both arch geometries. However, in the case of the asymmetric mode the arch with larger midspan rise shows greater sensitivity. For both geometries the structure is significantly more sensitive to imperfections in the second mode with the response shifting from a bifurcation type to a horizontal tangency.

5.2 Structural Bent with Clamped Ends.

To obtain some measure of the accuracy of the perturbation theory to represent quasi-linear and non-linear initial states, a simple bent is considered. The configuration of the bent is shown in Figure 8--the horizontal member having geometric parameters in which the depth of the member is in the ratio α to the depth of the vertical member. By varying α different degrees of non-linearity are obtained through the stiffening effect of the horizontal member. For $\alpha = 0$ the case of the cantilever column is obtained. For purposes of comparison an incremental load solution was obtained for the bent for a two and three element representation of the vertical member. Details of the set-up of the incremental load equations are given in Appendix B. Solutions including and excluding the third order terms in the incremental equilibrium equations (Section 3.4) are obtained.

5.2.1 Finite Element Equations for the Structural Bent.

The set-up and approximation of equations for the

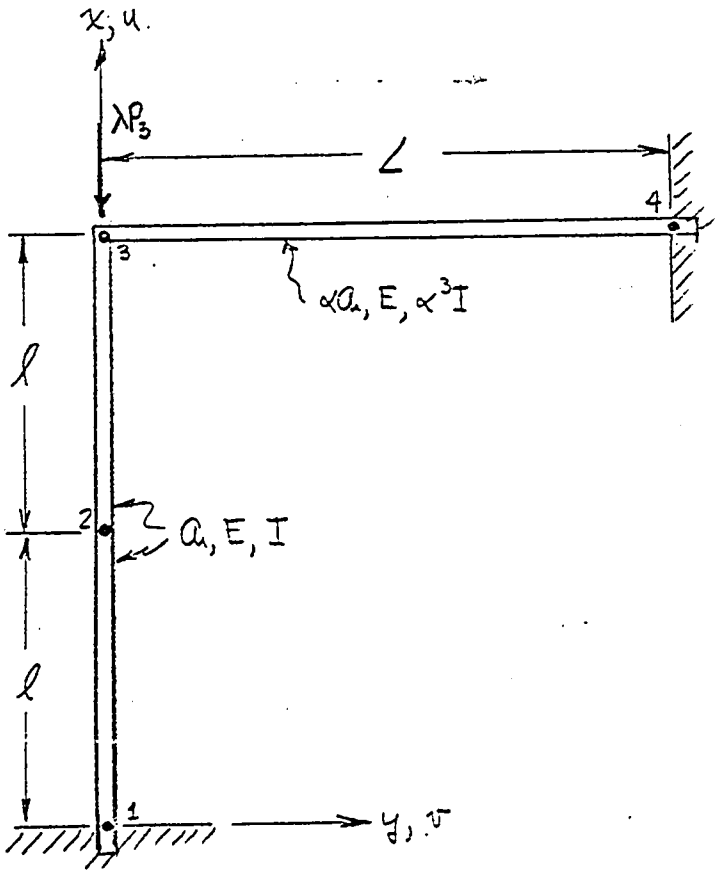

Figure V-8: Geometry of the Structural Bent

perturbation solution include development of an eigenvalue-eigenvector equation, and an approximate post-buckling response equation. The terms retained in the total potential energy to represent, say, element ② - ③ are

$$P[\Delta,e] = -\lambda P_3 \begin{bmatrix}-1\end{bmatrix}\begin{Bmatrix}u_2\\u_3\end{Bmatrix} + \frac{EA}{\ell}\begin{bmatrix}u_2 & u_3\end{bmatrix}[K_A]\begin{Bmatrix}u_2\\u_3\end{Bmatrix} +$$

$$+ \frac{4EI}{\ell^3}[\Delta]_2[K_0]_2\{\Delta\}_2 - \frac{\lambda P_3}{\ell}[\Delta]_2[K_1]_2\{\Delta\}_2 + \qquad (24)$$

$$+ \frac{2EA}{\ell^2}\begin{bmatrix}-1\end{bmatrix}\begin{Bmatrix}u_2\\u_3\end{Bmatrix}[\Delta]_2[K_1]_2\{\Delta\}_2 + \frac{EA}{\ell^3}[\Delta]_2[K_2]_2\{\Delta\}_2 + \cdots$$

with $\ell = \frac{1}{2}L$ and $P_3 = -1$.

Transforming displacement variables to the common XYZ global coordinate system and combining the energy terms for all elements results in the following expression for the total potential energy of the structure

$$P[\Delta,e] = \lambda\begin{bmatrix}L_0\end{bmatrix}\{e\} + EA[e][K_A]\{e\} + \frac{\alpha EA}{2}[v_3][1]\{v_3\} +$$

$$+ 4EI[\Delta]_1[K_0]_1\{\Delta\}_1 + 4EI[\Delta]_2[K_0]_2\{\Delta\}_2 +$$

$$+ \lambda[\Delta]_1[K_1]_1\{\Delta\}_1 + \lambda[\Delta]_2[K_1]_2\{\Delta\}_2 + \qquad (25)$$

$$+ \frac{1}{2}\alpha^3 EI[\Delta]_3[K_0]_3\{\Delta\}_3 + \text{third and fourth order terms}$$

In Eq. (25): $L = 1$

$$[e] = [u_2\ u_3] \qquad [\Delta]_1 = [0\ 0\ v_2\ \theta_2]$$

$$[\Delta]_2 = [v_2\ \theta_2\ v_3\ \theta_3]$$

$$\lfloor \Delta_3 \rfloor = \lfloor u_3 \;\; \theta_3 \;\; 0 \;\; 0 \rfloor$$

$$[K_0]_1 = [K_0]_2 = \begin{bmatrix} 12 & 3 & -12 & 3 \\ & 1 & -3 & 1 \\ & & 12 & -3 \\ \text{SYM} & & & 1 \end{bmatrix} \tag{26}$$

$$[K_0]_3 = \begin{bmatrix} 12 & -6 & -12 & -6 \\ & 4 & 6 & 2 \\ & & 12 & 6 \\ \text{SYM} & & & 4 \end{bmatrix} \qquad [K_1]_1 = [K_1]_2 = \begin{bmatrix} 4/5 & 1/20 & -4/5 & 1/20 \\ & 1/30 & -1/20 & -1/60 \\ & & 4/5 & -1/20 \\ \text{SYM} & & & 1/30 \end{bmatrix}$$

From these quadratic terms, dropping axial terms of the vertical member, the eigenvalue problem reduces to solution of the equation

$$\begin{bmatrix} 192 & 0 & -96 & 24 \\ & 16 & -24 & 4 \\ & & \underline{96+\frac{\alpha A_4}{I}} & -24 \\ \text{SYM} & & & \underline{8+4K^3} \end{bmatrix} \begin{Bmatrix} v_2 \\ \theta_2 \\ v_3 \\ \theta_3 \end{Bmatrix} + \frac{\lambda}{EI} \begin{bmatrix} 24/5 & 0 & -12/5 & 1/10 \\ & 2/15 & -1/10 & -1/60 \\ & & 12/5 & -1/10 \\ \text{SYM} & & & 1/15 \end{bmatrix} \begin{Bmatrix} v_2 \\ \theta_2 \\ v_3 \\ \theta_3 \end{Bmatrix} = \{0\} \tag{27}$$

where the dash underlined terms represent the influence of the horizontal member. The eigenvalues computed from this equation are part of the numerical results shown in Figures 9, 10, and 11.

Next we separate the "axial prebuckling" terms from the "incremental terms" on the basis that as $\alpha \to 0$ the perfect cantilever column equations are obtained. This partitioning yields for the "prebuckling" energy in terms of axial displacement $\lfloor e_0 \rfloor$ and bending displacement $a\{a_1\}$:

$$P_I[A_1,e] = -\lambda \{1\}\{e_0\} + Ea \{e_0\}[K_A]\{e_0\} + \\ + 2Ea\,a^2 \{1\}\{e_0\} \{A_1\}_1[K_1]_1\{A_1\}_1 + \\ + 2Ea\,a^2 \{1\}\{e_0\} \{A_1\}_2[K_1]_2\{A_1\}_2 \qquad (28)$$

while the "incremental" energy is

$$P[aA_1] = a^2(\lambda-\lambda_1)\{A_1\}_{1,2}[K_1]_{1,2}\{A_1\}_{1,2} - a^3\alpha\frac{Ea}{2}\delta_3\{A_1\}_3[K_1]_3\{A_1\}_3 + \\ + Ea\,a^4\{A_1\}_{1,2}[L_2]_{1,2}\{A_1\}_{1,2} + \frac{Ea}{8}a^4\alpha\{A_1\}_3[L_2]_3\{A_1\}_3 + \cdots \qquad (29)$$

The equilibrium equation for "post-buckling" response is then

$$\frac{dP[aA_1]}{da} = -a(\lambda^*-\lambda_1^*)\{A_1\}_{1,2}[K_1]_{1,2}\{A_1\}_{1,2} + 2a^3\delta^2\{A_1\}_{1,2}[L_2]_{1,2}\{A_1\}_{1,2} + \\ + \frac{3}{4}a^2\alpha\delta^2\delta_3\{A_1\}_3[K_1]_3\{A_1\}_3 + a^3\frac{\delta^2}{2}\alpha\{A_1\}_3[L_2]_3\{A_1\}_3 = 0 \qquad (30)$$

while stability of the equilibrium state is determined from

$$\frac{d^2P[aA_1]}{da^2} = -(\lambda^*-\lambda_1^*)\{A_1\}_{1,2}[K_1]_{1,2}\{A_1\}_{1,2} + 12\delta^2a^2\{A_1\}_{1,2}[K_1]_{1,2}\{A_1\}_{1,2} + \\ + \frac{3}{2}a\alpha\delta^2\delta_3\{A_1\}_3[K_1]_3\{A_1\}_3 + \frac{3}{2}\delta^2\alpha a^2\{A_1\}_3[L_2]_3\{A_1\}_3 + \cdots \qquad (31)$$

The coefficient δ is the slenderness ratio of the vertical member. In Eq's. (30), (31), if $\alpha = 0$, the extensional cantilever column equations are obtained for the case of no incremental axial displacement function.

5.2.2 Comparison between Perturbation and Linear Incremental Response Predictions.

Results of the post-buckling estimate from Eq. (30) as

well as incremental load estimates are shown in Figures 9, 10, 11 for α = 0.001, 0.01 and 0.1, respectively. The first order incremental results are based upon an incremental equilibrium equation derived from a potential energy function truncated to quadratic terms in the displacement variables. The second order incremental results are obtained with third and fourth order terms retained (Section 3.4).

Load corresponding to approximate horizontal tangency for the three solution curves shows a scatter of approximately 5%. Significantly larger differences in the ordinates occur in local regions. It is expected that with grid refinement closer correspondence would be obtained.

The incremental solution results for small values of α verify the validity of the extensional formulation for post-buckling response. In Figure 12 the local slope of the load-deflection curve is plotted versus transverse displacement for α = 0.001 and 0.01. The extensional solution curve is in closer proximity to the incremental curve at all points compared to the inextensional curve. At larger values of displacement the inextensional solution shows a stiffening as a result of geometry change and the incremental and extensional curves cross. For α = 0.1 the incremental solution values remain large compared to the perturbation solution, indicating stiffening not represented in the perturbation equations. For larger values of α this trend continues.

In this problem an attempt was made to introduce

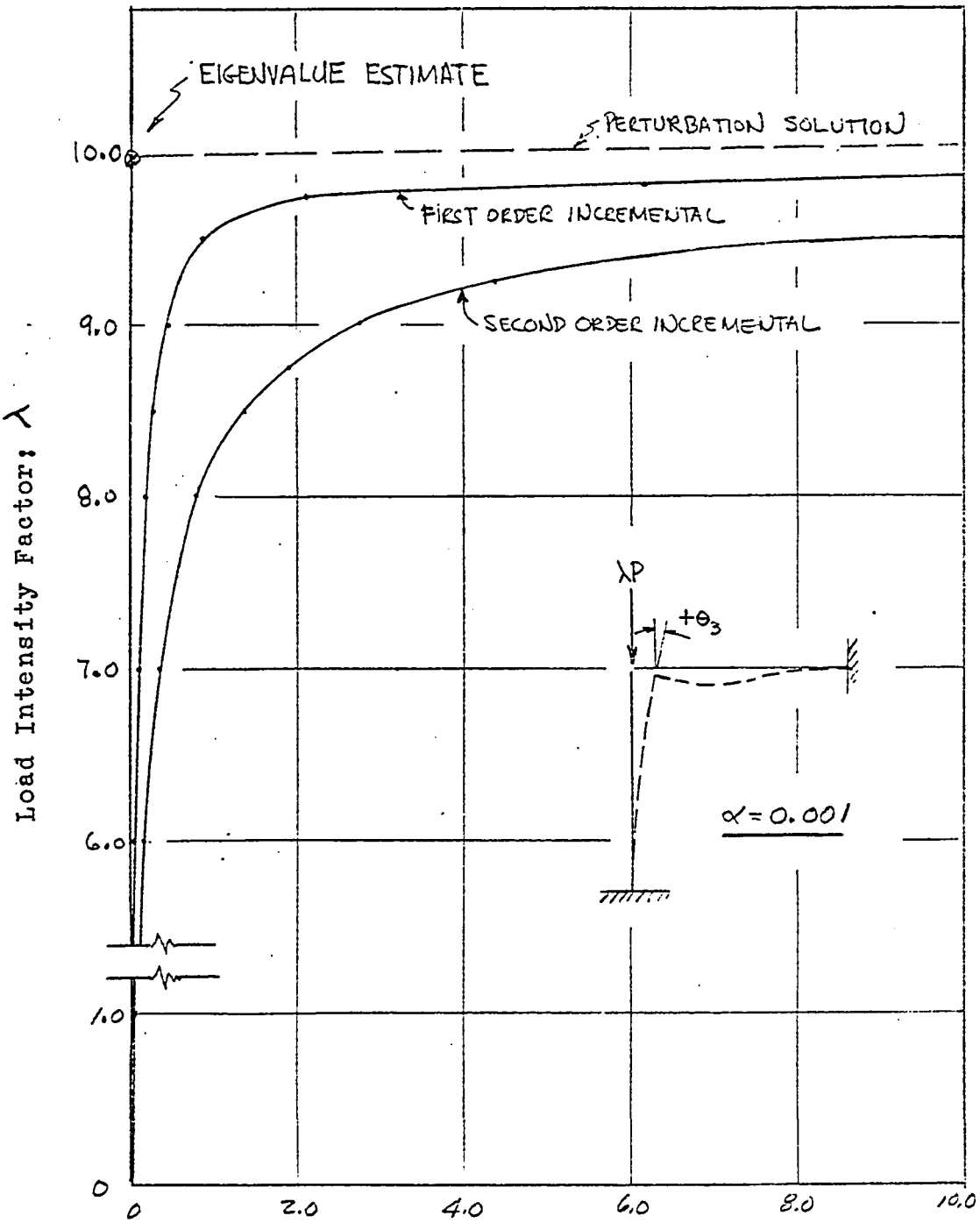

Figure V-9: Bent-Response Estimate, α = 0.001

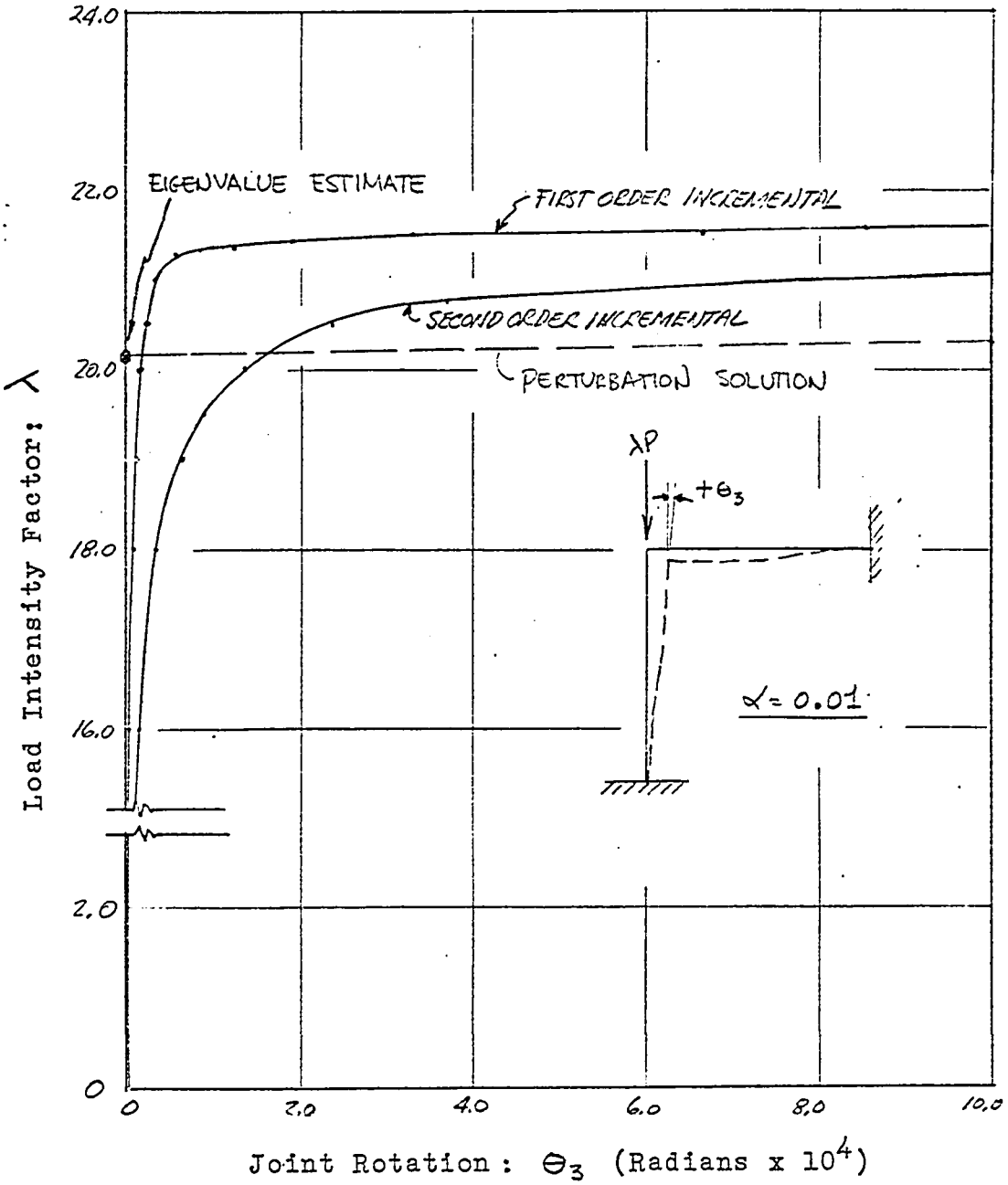

Figure V-10: Bent-Response Estimate, $\alpha = 0.01$

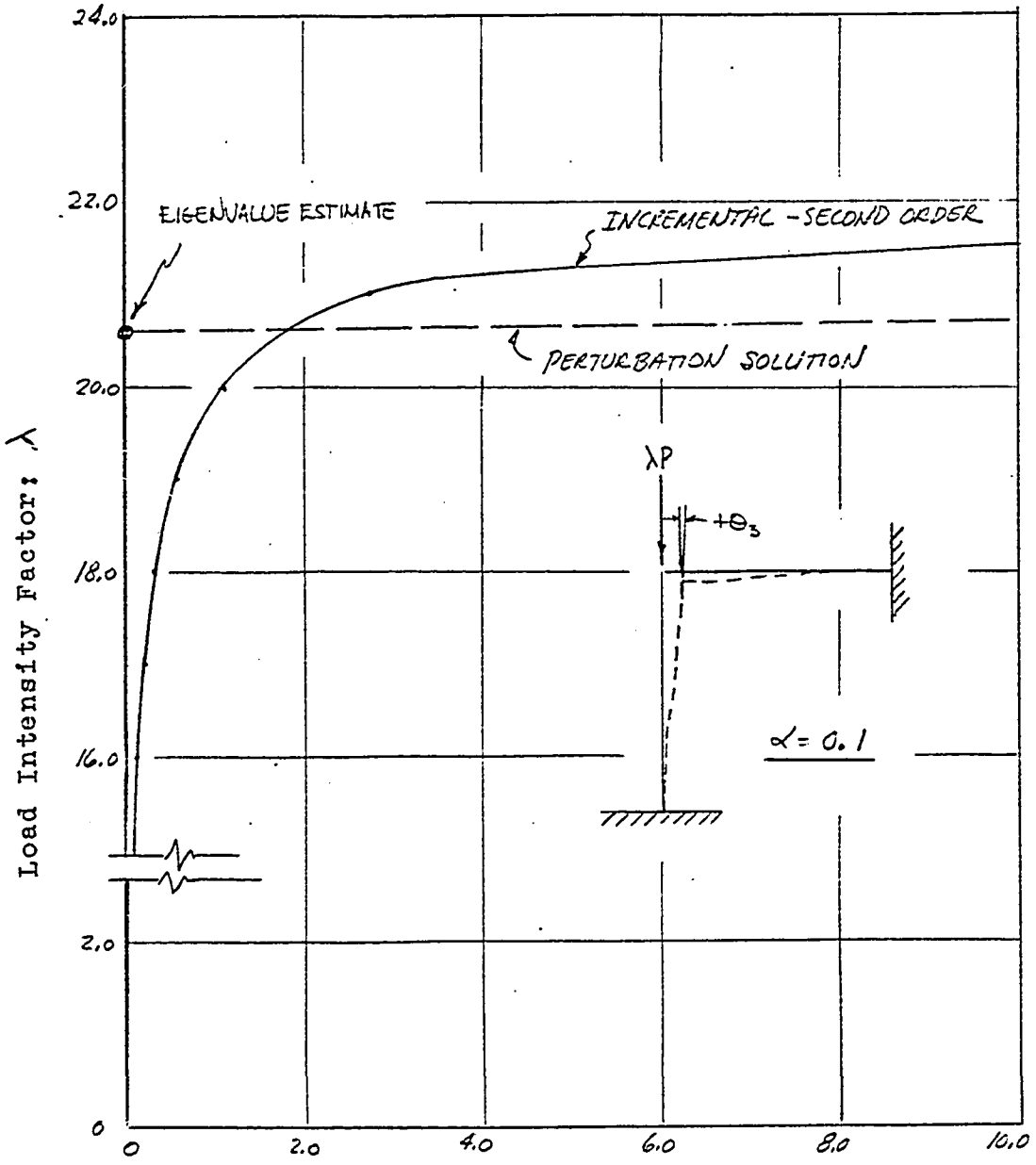

Figure V-11: Bent-Response Estimate, $\alpha = 0.1$

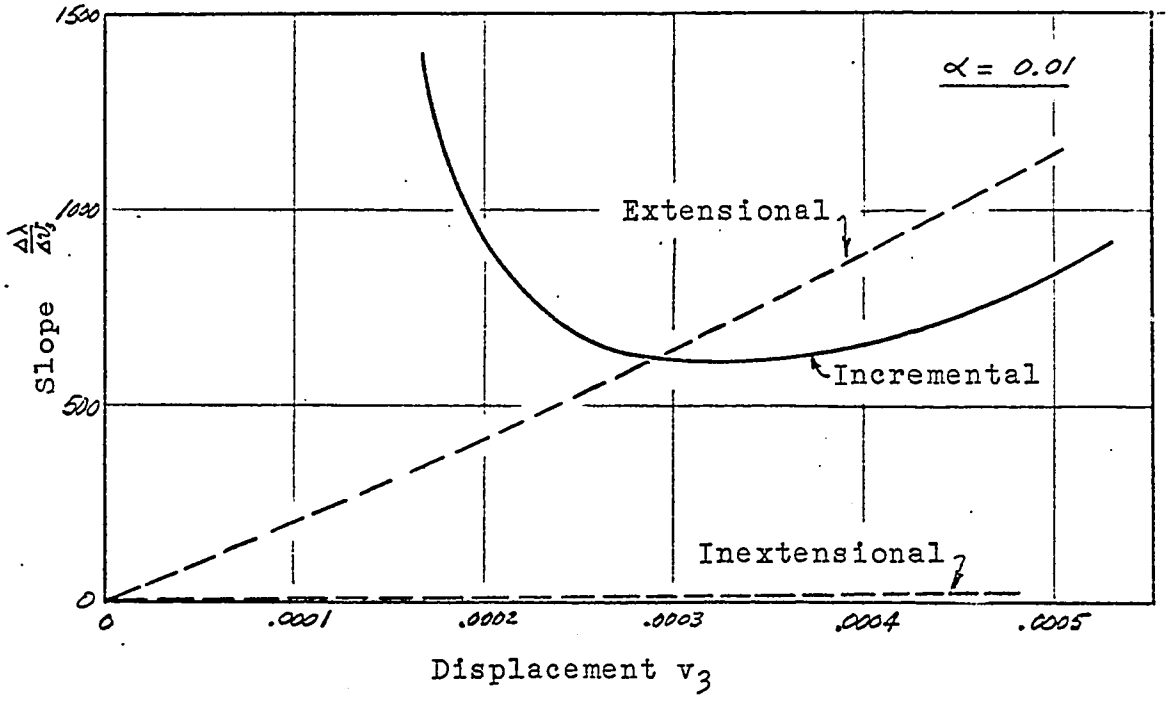

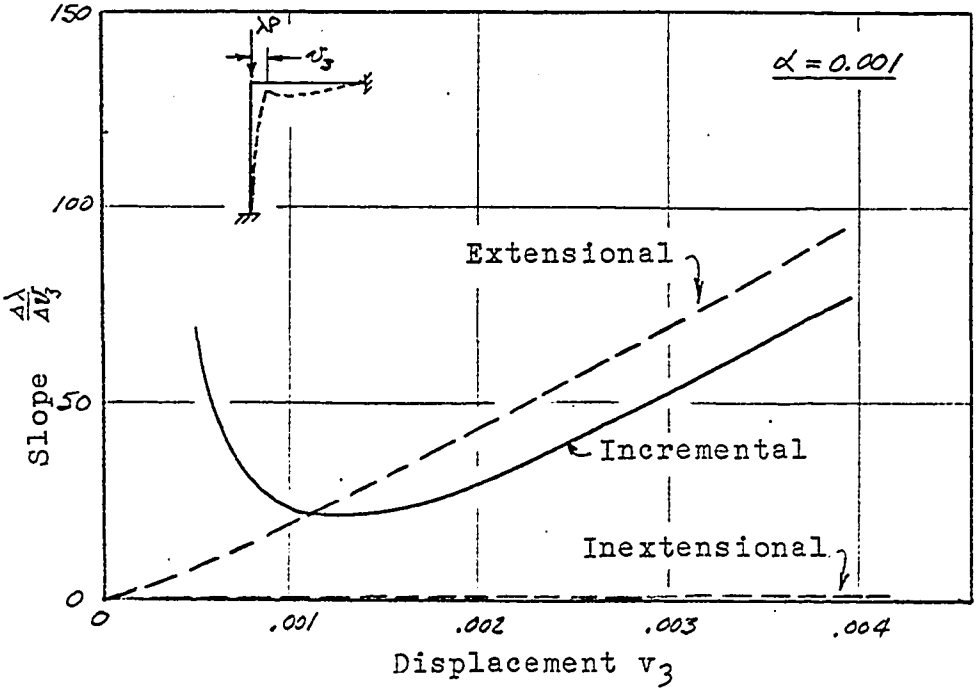

Figure V-12: Bent, Comparison of Extensional and Inextensional Solutions With Incremental Solution

imperfection functions into the perturbation equations and size the imperfection coefficients by the first and second step response estimates of the incremental solution. However, the response curves obtained by the incremental solution are strongly non-linear in the low-load range so that a single sizing of the imperfection coefficients was not possible. For problems exhibiting quasi-linear low-load response, introduction of an imperfection function in this way would significantly reduce computations compared to continued solution by load incrementation.

Finally it is noted that for α = 0.0001, the incremental solution techniques gave spurious answers using single precision arithmetic. One might conclude from this that the two solution techniques are complementary in the sense of applicability to different problem types.

VI. SUMMARY AND CONCLUSION

Post-buckling response of structures exhibiting bifurcation change of state in the perfect structure idealization has been examined in the framework of the finite element method. Development by finite elements, besides the usual advantages of capability to treat non-uniform geometries, solution of algebraic rather than differential equations, mixing of structural types, etc., provides also for representation of local displacement and force eccentricities. The general development involving prebuckling behavior, stability at the critical point(s), and post-buckling prediction is followed, with emphasis on use of displacement functions constituted from the fundamental and higher order buckling modes.

Post-buckling displacement of a cantilever column is evaluated based upon both an inextensional and extensional formulation of the strain-displacement equations. Whereas differences are small between these formulations in structural deflection problems with bending and twisting, the same is not true in post-buckling response. Nonlinear terms in the total potential energy, which define post-buckling behavior, are different depending upon the strain-displacement model selected. The difference between the two formulations is found to be proportional to the slenderness ratio, a large number if post-buckling response is elastic. In the extensional analysis additional displacement variables are admitted, and solution involves more manipulative steps if a post-buckling axial

displacement function is admitted. In this more exact formulation, numerical advantage of solution on a per-element basis is lost.

Other aspects of the cantilever column study pertain to response of the imperfect structure. Two approximations to the expansion of the increment in total potential energy are evaluated in the neighborhood of the critical point. One is a local estimate of the equilibrium path and its slope, which categorizes the stability. If the structure is post-buckling stable, as is the cantilever column, then a more complete expansion of the total potential energy permits evaluation of the complete small deflection response path starting from zero load. Details of both of these expansions are worked out for the cantilever column and good correspondence is obtained for lateral deflections up to two-tenths of the column length.

The nonlinear stiffness matrices through fourth order in the displacement variables for the column and rectangular plate elements are derived and reported in rational fractional form. The extensional strain-displacement equations are used in the plate formulation on the basis of results found for the column. An example of a simply supported square plate externally loaded along one set of parallel edges is solved and compared with classical results. Overall accuracy of the solution for perfect-structure post-buckling response is better for the plate than the column; however, convergence of solution is slower.

In treating the column and plate examples the features

of the analyses are the rapid convergence of solutions with grid refinement, and solution insensitivity to coefficient digit truncation. Two element column and four element quarter plate idealizations resulted in post-buckling response estimates well within engineering accuracy ($\pm$ 5%). Approximate evaluation of the extensional case by neglecting the axial post-buckling incremental displacement function resulted in larger error ($<$ 18%.) Thus, for structural types for which initial post-buckling response curve curvature is small, the complete extensional formulation is required. However, this more exact formulation is shown to not necessarily guarantee stability when it is predicted. This happens because the finite element method being an approximate analysis technique, yields solutions that do not correspond to an exact minimum of the total potential energy. For this reason also, solution convergence is not necessarily monotomic, although convergence is rapid with element refinement. Structural types considered herein having large initial post-buckling curvature or exhibiting bifurcation by transfer of stability between modes show good correspondence between exact classical solutions and the finite element solutions. The characteristics of rapid convergence and simplicity of computations exhibited in treatment of these problems suggest the general utility of the method in more complex structural configurations and assemblies.

Analysis of the shallow arch, a post-buckling unstable structure, by the finite element method supports the observations made on the column and plate structures. Techniques of

representing arbitrary initial arch shape and shape imperfections are apparent from the formulation. The representation of initial curvature of the arch by an initial shape function is different from the usual use of strain-displacement equations that contain the curvature term. Utility of this approach should be examined in applications to two-dimensional continuous structures.

The perturbation method provides a simple computational approach to detection of points of horizontal tangency. The extreme load values are determined from solution of low-order polynomial equations.

The key to solution by the perturbation method is selection of rational modal functions through which the energy expansion is evaluated. In classical approaches, approximate functions may be used which are not orthogonal, and it is in this framework that Koiter developed the general theory. However, with the finite element method, the approximation in determining eigenfunctions is not on orthogonality, but on the number of variables to represent the shape. This problem is minimized with large capacity numerical techniques, such as the power method, available for use in estimating eigenfunctions. This capability coupled with the rapid convergence of solution relative to eigenfunction content, makes the finite element approach very attractive for continued use and development in post-buckling response prediction.

REFERENCES

1. Liapunov, A. M. Probleme general de la stabilite du mouvement. First printing: 1892 (in Russian). Annals of Mathematical Studies, No. 17. Princeton, N.J.: Princeton University Press. 1947.

2. LaSalle, J., and S. Lefschetz. Stability by Liapunov's Direct Method. New York: Academic Press. 1961

3. Bolotin, V. V. The Dynamic Stability of Elastic Systems. San Francisco: Holden-Day, Inc. 1964.

4. Langhaar, H. L. Energy Methods in Applied Mechanics. New York: John Wiley & Sons, Inc. 1962.

5. Ziegler, H. "On the Concept of Elastic Stability," Advances in Applied Mechanics, 4 (1956) p. 351.

6. Panovko, Y. G., and I. I. Gubanova. "Stability and Oscillations of Esastic Systems," Consultants Bureau, New York (1965).

7. Thompson, J. M. T. "Basic Principles in the General Theory of Elastic Stability," Journal of Mechanics and Physics of Solids, 11, 1 (1963)

8. Argyris, J. H., S. Kelsey, and H. Kamel. "Matrix Methods of Structural Analysis," AGARDograph No. 72, Pergamon Press (1964).

9. Zienkiewicz, O. C., and Y. K. Cheung. The Finite Element Method in Structural and Continuum Mechanics. New York: McGraw-Hill Book Company. 1967.

10. Przemieniecki, J. S. Theory of Matrix Structural Analysis. New York: McGraw-Hill Book Company. 1968.

11. Gallagher, R. H., and J. Padlog. "Discrete Element Approach to Structural Instability Analysis," AIAA Journal, 1, 6 (June 1963) p. 1437.

12. Kapur, K. K., and B. J. Hartz. "Stability of Plates Using the Finite Element Method," ASCE EM 2, 92 (April 1966) p. 177.

13. Gallagher, R. H., and H. T. Y. Yang. "Elastic Instability Predictions for Doubly Curved Shells," paper presented at the Second Conference on Matrix Methods in Structural Mechanics, Wright-Patterson Air Force Base, Ohio (October 1968).

14. Gallagher, R. H., R. A. Gellatly, J. Padlog, and R. H. Mallett. "A Discrete Element Procedure for Thin-Shell Instability Analysis," AIAA Journal, 5, 1 (January 1967) p. 138.

15. Turner, M. J., E. H. Dill, H. C. Martin, and R. J. Melosh. "Large Deflections of Structures Subjected to Heating and External Loads," J. Aerospace Sciences, 27 (February 1960) p. 97.

17. Bogner, F. K., R. H. Mallet, M. D. Minich, and L. A. Schmit. "Development and Evaluation of Energy Search Methods of Non-Linear Structural Analysis," AFFDL-TR-65-113 (October 1965).

18. Schmit, L. A. "Developments in Descrete Element Finite Deflection Structural Analysis by Function Minimization," AFFDL-TR-68-126 (September 1968).

19. Mallett, R. H., and L. A. Schmit. "Non-Linear Structural Analysis by Energy Search," Journal of the Structural Division ASCE, 93, ST3 (June 1967) p. 221.

20. Luenberger, D. G. Optimization by Vector Space Methods. New York: John Wiley & Sons, Inc. 1969.

21. O'Brien, T. F. "Analysis of Shells," Lecture notes from course in Department of Aeronautics and Astronautics, University of Washington, Seattle, Washington, September 1967.

22. Mallett, R. H., and P. V. Marcal. "Finite Element Analysis of Nonlinear Structures," Journal of Structural Division ASCE, 94, ST9 OSeptember 1968) p. 2081.

23. Felippa, C. A. "Refined Finite Element Analysis of Linear and Nonlinear Two-Dimensional Structures," Report No. SESM 66-2, University of California, Structural Engineering Laboratory (October 1966).

24. Nathan, N. D. "Finite Element Formulation of Geometrically Nonlinear Problems of Elasticity," Ph.D. thesis, University of Washington, Seattle, Washington (1969).

25. Oden, J. T. "Numerical Formulation of Nonlinear Elasticity Problems," Journal of Structural Division ASCE, 93, ST3 (June 1967) p. 235.

26. Koiter, W. T. "On the Stability of Elastic Equilibrium," Thesis, Delft, Amsterdam: H. J. Paris, 1945. Also: NASA TTF-10, 833 (March 1967).

27. Koiter, W. T. Elastic Stability and Post-Buckling Behavior. Nonlinear Problems, edited by R. E. Langer. University of Wisconsin Press. 1963.

28. Karman, T. von, and Tsien, H. S., "The Buckling of Thin Cylindrical Shells under Axial Compression," Journal of Aeronautical Sciences, 8 (1941) p. 303.

29. Fung, Y. C., and E. E. Sechler. Instability of Thin Elastic Shells. New York: Pergamon Press, Structural Mechanics. 1960. p. 115.

30. Budiansky, B. "A Survey of Some Buckling Problems," AIAA, 4 (September 1966) p. 5.

31. Budiansky, B., and J. W. Hutchinson. "Dynamic Buckling of Imperfection-Sensitive Structures," Proceedings Eleventh International Congress Applied Mechanics, 1964, Springer-Verlag, Berlin, Germany, 1966.

32. Hutchinson, J. W. "Imperfection Sensitivity of Externally Pressurized Spherical Shells," ASME Journal of Applied Mechanics, 34, Series E, 1 (March 1967).

33. Pope, G. G. "On the Bifurcation Buckling of Elastic Beams, Plates and Shallow Shells," Aeronautical Quarterly (February 1968) p. 20.

34. Roorda, J. "Instability of Structures with Small Imperfections," Journal Eng. Mech. ASCE, 91, No. EM 1 (February 1965) p. 87.

35. Frazer, R. A., W. J. Duncan, and A. R. Collar. Elementary Matrices. London, England: Cambridge University Press. 1960.

36. Marcal, P. V. "The Effect of Initial Displacements on Problems of Large Deflection and Stability," ARPA E54 Division of Engineering, Brown University, Providence, Rhode Island (November 1967).

37. Melosh, R. J., and T. E. Lang. "Modified Potential Energy Representation for Improved Frequency Prediction," Proceedings on Conference on Matrix Methods in Structural Mechanics, Wright-Patterson Air Force Base, Ohio (October 1965).

38. Timoshenko, S. P., and J. M. Gere. Theory of Elastic Stability. New York: McGraw Hill Book Co. 1961.

39. Bogner, F. K., R. L. Fox, and L. A. Schmit. "The Generation of Inter-element-compatible Stiffness and Mass Matrices by Use of Interpolation Formulas," Proceedings of the Conference on Matrix Methods in Structural Mechanics, AFFPL TR 66-80, Wright Patterson Air Force Base, Ohio (1966).

40. Bolotin, V. V. "Statistical Methods in the Non-Linear Theory of Elastic Shells," Technical Translation F-85, NASA (December 1962).

41. Babcock, C. D. "Imperfections, How They Influence Buckling," Seminar, Department of Aeronautics and Astronautics, University of Washington, February 10, 1969.

42. Fung, Y. C., and A. Kaplan. "Buckling of Low Arches or Curved Beams of Small Curvature," NACA TN 2840 (November 1952).

43. O'Brien, T. F. "On Finite Deflections of Obliquely Reinforced Heated Shallow Shells of Arbitrary Planform," Ph.D. Thesis, Massachusetts Institute of Technology, Cambridge, Mass., June 1963.

44. Schreyer, H. L., E. F. Masur, "Buckling of Shallow Arches," ASCE EM4, 92 (August 1966) p. 467.

45. Schmit, L. A. "Developments in Discrete Element Finite Deflection Structural Analysis by Function Minimization," AFFDL-TR-68-126 (September 1968).

APPENDIX A

Evaluation of the integral

$$I = \int_0^{\ell} \{d\}^T [B]^T \underline{[G][B]\{d\}} \{d\}^T [B]^T \underline{[G][B]} \{d\}\, dx \qquad (1)$$

involves the dash underlined products of x dependent terms. The integrated result is expressed by a nested set of parameters dependent upon $\{d\}$ as follows:

$$I = \{d\}^T [B]^T [\ell] [B] \{d\} \qquad (2)$$

where

$$[\ell] = \begin{bmatrix} 0 & 0 & 0 & 0 \\ & \ell_1 & \ell_2 & \ell_3 \\ & & \ell_4 & \ell_5 \\ \text{SYM} & & & \ell_6 \end{bmatrix} \qquad (3)$$

$$\ell_1 = \frac{1}{\ell} \{d\}^T \begin{bmatrix} 6/5 & 1/10 & -6/5 & 1/10 \\ & 2/15 & -1/10 & -1/30 \\ & & 6/5 & -1/10 \\ \text{SYM} & & & 2/15 \end{bmatrix} \{d\} \qquad (4)$$

$$\ell_2 = \{d\}^T \begin{bmatrix} 6/5 & 1/5 & -6/5 & 0 \\ & 1/15 & -1/5 & -1/30 \\ & & 6/5 & 0 \\ \text{SYM} & & & 1/5 \end{bmatrix} \{d\} \qquad (5)$$

$$\ell_3 = \ell \{d\}^T \begin{bmatrix} 36/35 & 3/14 & -36/35 & -3/35 \\ & 3/35 & -3/14 & -3/12 \\ & & 36/35 & 3/35 \\ \text{SYM} & & & 9/35 \end{bmatrix} \{d\} \qquad (6)$$

$$l_4 = \frac{4}{3} l_3 \tag{7}$$

$$l_5 = l^2 \, L4 \begin{bmatrix} 9/7 & 3/10 & -9/7 & -3/14 \\ & 11/140 & -3/10 & -11/140 \\ & & 9/7 & 3/14 \\ \text{SYM} & & & 13/28 \end{bmatrix} \tag{8}$$

$$l_6 = l^3 \, L4 \begin{bmatrix} 9/7 & 9/28 & -9/7 & -9/28 \\ & 3/35 & -9/28 & -3/28 \\ & & 9/7 & 9/28 \\ \text{SYM} & & & 9/14 \end{bmatrix} \tag{9}$$

Finally $l^3 [L_2] = [B]^T [l][B] =$

$$\begin{bmatrix} 9\frac{l_4}{l^4} - 12\frac{l_5}{l^5} + 4\frac{l_6}{l^6} & -3\frac{l_2}{l^3} + 2\frac{l_3}{l^4} + 6\frac{l_4}{l^5} - 7\frac{l_5}{l^5} + 2\frac{l_6}{l^6} & -9\frac{l_4}{l^4} + 12\frac{l_5}{l^5} - 4\frac{l_6}{l^6} & 3\frac{l_4}{l^4} - 5\frac{l_5}{l^5} + 2\frac{l_6}{l^6} \\ & \frac{l_1}{l^2} - 4\frac{l_2}{l^3} + 2\frac{l_3}{l^4} + 4\frac{l_4}{l^4} - 4\frac{l_5}{l^5} + \frac{l_6}{l^6} & 3\frac{l_2}{l^3} - 2\frac{l_3}{l^3} + 6\frac{l_4}{l^4} + 7\frac{l_5}{l^5} - 2\frac{l_6}{l^6} & -\frac{l_2}{l^3} + \frac{l_3}{l^4} + 2\frac{l_4}{l^4} - 3\frac{l_5}{l^5} + \frac{l_6}{l^6} \\ & & 9\frac{l_4}{l^4} - 12\frac{l_5}{l^5} + 4\frac{l_6}{l^6} & -3\frac{l_4}{l^4} + 5\frac{l_5}{l^5} - 2\frac{l_6}{l^6} \\ & \text{SYM} & & \frac{l_4}{l^4} - 2\frac{l_5}{l^5} + \frac{l_6}{l^6} \end{bmatrix} \tag{10}$$

Evaluation of the integral

$$I = \int_0^l L4 [B]^T \begin{Bmatrix} 0 \\ 0 \\ 2 \\ 6x \end{Bmatrix} L4 [B]^T [\epsilon][B]\{\Delta\} \; L0\;0\;2\;6x \; [B]\{\Delta\} \, dx \tag{11}$$

results in the following matrix product

$$I = \{d\}^T [B]^T [h] [B] \{d\} \tag{12}$$

where

$$[h] = \begin{bmatrix} 0 & 0 & 0 & 0 \\ & 0 & 0 & 0 \\ & & h_4 & h_5 \\ \text{SYM} & & & h_6 \end{bmatrix} \qquad \begin{aligned} h_4 &= 4\,\ell_1 \\ h_5 &= 6\,\ell_2 \\ h_6 &= 12\,\ell_3 \end{aligned} \tag{13}$$

The product $\ell^5 [H_2] = [B]^T [h] [B]$ follows directly from Eq's. (10) and (13).

APPENDIX B

FINITE DEFLECTION ANALYSIS OF BENT

Deflection under load of a three element representation of a simple 90° bent is considered. Response of the structure is determined using a variable load incrementation scheme using both equations with and without the initial displacement matrix. The analysis is restricted to deformation states in the plane of the bent.

Three coordinate systems are required in order to represent the position of an element and the history of its deformation. The global system (X, Y, Z) is a total structure coordinate frame, the reference system (x^*, y^*, z^*) is aligned with and stays at the initial position of the element, and the local system (x, y, z) is at the pre-incrementalization position of the element. Displacement increments Δu, Δv, $\Delta\theta$ are referenced to the local coordinates. Transformation of these to the global frame is given by:

$$\begin{Bmatrix} \Delta u_i \\ \Delta u_j \\ \Delta v_i \\ \Delta\theta_i \\ \Delta v_j \\ \Delta\theta_j \end{Bmatrix} = \begin{bmatrix} c & 0 & s & 0 & 0 & 0 \\ 0 & c & 0 & 0 & s & 0 \\ -s & 0 & c & 0 & 0 & 0 \\ 0 & 0 & 0 & 1 & 0 & 0 \\ 0 & -s & 0 & 0 & c & 0 \\ 0 & 0 & 0 & 0 & 0 & 1 \end{bmatrix} \begin{Bmatrix} \Delta U_i \\ \Delta U_j \\ \Delta V_i \\ \Delta\theta_i \\ \Delta V_j \\ \Delta\theta_j \end{Bmatrix} \qquad (1)$$

where $c = \cos(\phi_o + \phi)$ and $s = \sin(\phi_o + \phi)$. Transformation to the reference frame is set by Eq. (1) for the case $\phi_o = 0$.

The stiffness matrices of the structure are regenerated at each pre-incrementation position. Basic geometric changes

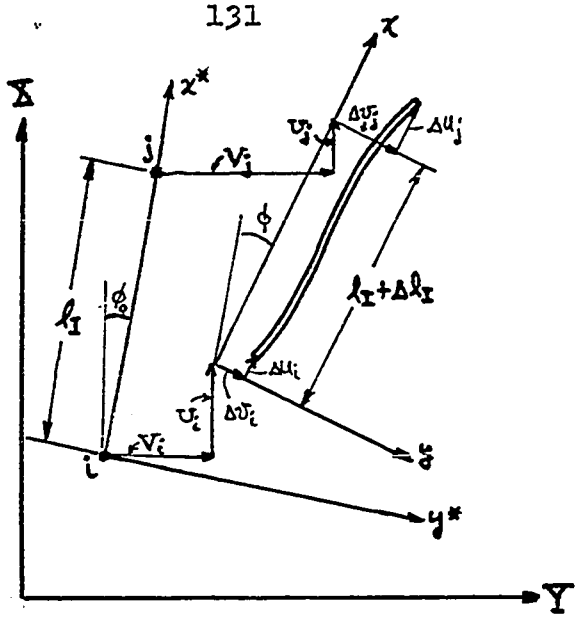

Figure B-1

are the deformed position of the element and its changed length. The deformed position of the element is accounted for in overlay of element matrices to form the total structure matrices. The increment in element length depends upon the total gridpoint displacements U_i, V_i, U_j and V_j as follows

$$l_I + \Delta l_I = \sqrt{(l_I + U_j - U_i)^2 + (V_j - U_i)^2} \qquad (2)$$

and the element angle to the reference frame ($\emptyset$) is given by

$$\cos\phi = \frac{l_I + U_j - U_i}{l_I + \Delta l_I} \qquad \sin\phi = \frac{V_j - V_i}{l_I + \Delta l_I} \qquad (3)$$

The geometric and physical constants of the bent are indicated in Figure 2. The parameter α is a scaling of element ③-④ thickness in order to vary the relative stiffness between the horizontal and vertical members. Defining the slenderness ratio as $\delta_I = \sqrt{\frac{A_I l_I^2}{I}}$ the incremental load-deflection equation for an element in local coordinates is:

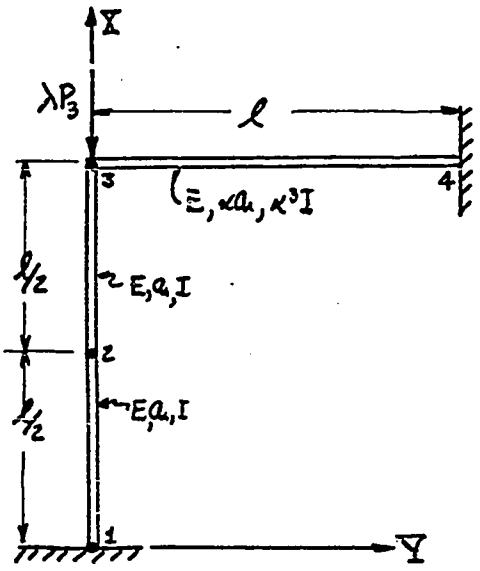

Figure B-2

$$\begin{bmatrix} \delta_I^2 - \delta_I^2 & & & & & & \\ \delta_I^2 & & & & & & \\ \hline & 12 & 6\ell_I & -12 & 6\ell_I & & \\ & & 4\ell_I^2 & -6\ell_I & 2\ell_I^2 & & \\ & & & 12 & -6\ell_I & & \\ & & & & 4\ell_I^2 & & \\ \text{SYM} & & & & & & \end{bmatrix} \begin{Bmatrix} \Delta u_i \\ \Delta u_j \\ \hline \Delta v_i \\ \Delta\theta_i \\ \Delta v_j \\ \Delta\theta_j \end{Bmatrix} + \frac{EA}{\ell_I^2} \begin{bmatrix} 1 & -1 \\ -1 & 1 \end{bmatrix} \begin{Bmatrix} u_i \\ u_j \end{Bmatrix} \begin{bmatrix} 0 & & & & & & \\ & 0 & & & & & \\ \hline & & 6/5 & \frac{1}{10}\ell_I & -6/5 & \frac{1}{10}\ell_I & \\ & & & \frac{2}{15}\ell_I^2 & -\frac{1}{10}\ell_I & -\frac{1}{30}\ell_I^2 & \\ & & & & 6/5 & -\frac{1}{10}\ell_I^2 & \\ & & & & & \frac{2}{15}\ell_I^2 & \\ \text{SYM} & & & & & & \end{bmatrix} \begin{Bmatrix} \Delta u_i \\ \Delta u_j \\ \hline \Delta v_i \\ \Delta\theta_i \\ \Delta v_j \\ \Delta\theta_j \end{Bmatrix} +$$

$$+ \frac{EA}{\ell_I^2} \begin{bmatrix} 0 & & & & & & \\ & 0 & & & & & \\ \hline & & -d_1 & -d_2 & d_1 & d_4 & \\ & & d_1 & d_2 & -d_1 & d_4 & \\ & & & & & & \\ & & & & 0 & & \\ \text{SYM} & & & & & & \end{bmatrix} \begin{Bmatrix} \Delta u_i \\ \Delta u_j \\ \hline \Delta v_i \\ \Delta\theta_i \\ \Delta v_j \\ \Delta\theta_j \end{Bmatrix} = \begin{Bmatrix} \Delta P_i \\ \Delta P_j \\ \hline \Delta F_i \\ \Delta M_i \\ \Delta F_j \\ \Delta M_j \end{Bmatrix} \qquad (4)$$

where $[d_1 \;\; d_2 \;\; -d_1 \;\; d_4] = [v_i \;\; \theta_i \;\; v_j \;\; \theta_j]\,[K_1]$ in local frame.

The above information is used in the set up of the generation and load-incrementation sequence in a computer program to trace the step-wise linear deformation history.

APPENDIX C

MATRICES OF THE TOTAL POTENTIAL ENERGY FOR THE PLATE ELEMENT

1) First Order:

$$\lfloor C_{s0} \rfloor = h \lfloor -\tfrac{1}{2} \quad 0 \quad \tfrac{1}{2} \quad 0 \quad -\tfrac{1}{2} \quad 0 \quad \tfrac{1}{2} \quad 0 \rfloor \tag{1}$$

$$\lfloor C_{\eta 0} \rfloor = \ell \lfloor 0 \quad -\tfrac{1}{2} \quad 0 \quad -\tfrac{1}{2} \quad 0 \quad \tfrac{1}{2} \quad 0 \quad \tfrac{1}{2} \rfloor \tag{2}$$

$$\lfloor C_{s\eta 0} \rfloor = \lfloor -\tfrac{\ell}{2} \quad -\tfrac{h}{2} \quad -\tfrac{\ell}{2} \quad \tfrac{h}{2} \quad \tfrac{\ell}{2} \quad -\tfrac{h}{2} \quad \tfrac{\ell}{2} \quad \tfrac{h}{2} \rfloor \tag{3}$$

2) Second Order:

$$[K_{A_1}] = \begin{bmatrix} \frac{h}{3\ell} & & & & & & & \\ \frac{1}{4} & \frac{\ell}{3h} & & & \text{SYM} & & & \\ -\frac{h}{3\ell} & -\frac{1}{4} & \frac{h}{3\ell} & & & & & \\ \frac{1}{4} & \frac{h}{6\ell} & -\frac{1}{4} & \frac{\ell}{3h} & & & & \\ \frac{h}{6\ell} & \frac{1}{4} & -\frac{h}{6\ell} & \frac{1}{4} & \frac{h}{3\ell} & & & \\ -\frac{1}{4} & -\frac{\ell}{3h} & \frac{1}{4} & -\frac{\ell}{6h} & -\frac{1}{4} & \frac{\ell}{3h} & & \\ -\frac{h}{6\ell} & -\frac{1}{4} & \frac{h}{6\ell} & -\frac{1}{4} & -\frac{h}{3\ell} & \frac{1}{4} & \frac{h}{3\ell} & \\ -\frac{1}{4} & -\frac{\ell}{6h} & \frac{1}{4} & -\frac{\ell}{3h} & -\frac{1}{4} & \frac{\ell}{6h} & \frac{1}{4} & \frac{\ell}{3h} \end{bmatrix} \tag{4}$$

$$[K_{A_2}] = \begin{bmatrix} \frac{\ell}{3h} & & & & & & & \\ -\frac{1}{4} & \frac{h}{3\ell} & & & \text{SYM} & & & \\ \frac{\ell}{6h} & \frac{3}{4} & \frac{\ell}{3h} & & & & & \\ -\frac{3}{4} & -\frac{h}{3\ell} & \frac{1}{4} & \frac{h}{3\ell} & & & & \\ -\frac{\ell}{3h} & -\frac{3}{4} & -\frac{\ell}{6h} & \frac{1}{4} & \frac{\ell}{3h} & & & \\ \frac{3}{4} & \frac{h}{6\ell} & -\frac{1}{4} & -\frac{h}{6\ell} & \frac{1}{4} & \frac{h}{3\ell} & & \\ -\frac{\ell}{6h} & \frac{1}{4} & -\frac{\ell}{3h} & \frac{3}{4} & \frac{\ell}{6h} & \frac{1}{4} & \frac{\ell}{3h} & \\ \frac{1}{4} & -\frac{h}{6\ell} & -\frac{3}{4} & \frac{h}{6\ell} & \frac{3}{4} & -\frac{h}{3\ell} & -\frac{1}{4} & \frac{h}{3\ell} \end{bmatrix} \tag{5}$$

Defining $\omega_s = \frac{d\omega}{ds}$ etc., then $\{\omega_s\} = \frac{\ell}{h}[T]\{\omega_\eta\}$, $\{\omega_{ss}\} = \frac{\ell^2}{h^2}[T]\{\omega_{\eta\eta}\}$

$$[T] = \begin{bmatrix}
1.0 & & & & & & & & & & & & \\
0.0 & & & & & & & & & & & & \\
-1.0 & 0.0 & & & & & & & & & & & \\
 & & 1.0 & & & & & & & & & & \\
 & & & 0.0 & & & & & & & & & \\
 & & & & 0.0 & & & & & & & & \\
 & & & & & 0.0 & & & & & & & \\
 & & & & & & 0.0 & & & & & & \\
 & & & 1.0 & & & & 0.0 & & & & & \\
 & & & & & -1.0 & & & 0.0 & & & & \\
 & & & & -1.0 & & & & & 0.0 & & & \\
 & & & & & & 1.0 & & & & 0.0 & & \\
 & & & & & & & & & & & 1.0 & \\
 & & & & & & & & & & & 0.0 & \\
 & & & & & & & & & & & -1.0 & 0.0 \\
 & & SYM. & & & & & & & & & & 1.0
\end{bmatrix} \tag{6}$$

$$[K_{5555}] = \frac{h}{210\,\ell^3} \begin{bmatrix}
936 & & & & & & & & & & & & & & \\
132 & 24 & & & & & & & & & & & & & \\
-468 & -66 & 312 & & & & & & & & & & & & \\
66 & 12 & -44 & 8 & & & & & & & & & & & \\
-936 & -132 & 468 & -66 & 936 & & & & & & & & & & \\
-132 & -24 & 66 & -12 & 132 & 24 & & & & & & & & & \\
-468 & -66 & 156 & -22 & 468 & 66 & 312 & & & & & & & & \\
66 & 12 & -22 & 4 & -66 & -12 & -44 & 8 & & & & & & & \\
324 & 78 & -162 & 39 & -324 & -78 & -162 & 39 & 936 & & & & & & \\
-78 & -18 & 39 & -9 & 78 & 18 & 39 & -9 & -132 & 24 & & & & & \\
-162 & -39 & 108 & -26 & 162 & 39 & 54 & -13 & -468 & 66 & 312 & & & & \\
-39 & -9 & 26 & -6 & 39 & 9 & 13 & -3 & -66 & 12 & 44 & 8 & & & \\
-324 & -78 & 162 & -39 & 324 & 78 & 162 & -39 & -936 & 132 & 468 & 66 & 936 & & \\
78 & 18 & -39 & 9 & -78 & -18 & -39 & 9 & 132 & -24 & -66 & -12 & -132 & 24 & \\
-162 & -39 & 54 & -13 & 162 & 39 & 108 & -26 & -468 & 66 & 156 & 22 & 468 & -66 & 312 \\
-39 & -9 & 13 & -3 & 39 & 9 & 26 & -6 & -66 & 12 & 22 & 4 & 66 & -12 & 44 & 8
\end{bmatrix} \tag{7}$$

SYM.

$$[K_{SS4Y0}] = \frac{1}{900hl}$$

$$\begin{bmatrix}
1296 & & & & & & & & & & & & & & & \\
648 & 144 & & & & & & & & & & & & & & \\
-648 & -549 & 144 & & & & & & & & & & & & & \\
99 & 72 & -72 & 16 & & & & & & & & & & & & \\
-1296 & -648 & 108 & -54 & 1296 & & & & & & & & & & & \\
-648 & -144 & 54 & -12 & 648 & 144 & & & & & & & & & & \\
-108 & -54 & -36 & 18 & 648 & 549 & 144 & & & & & & & & & \\
54 & 12 & 18 & -4 & -99 & -72 & -72 & 16 & & & & & & & & \\
-1296 & -108 & 648 & -54 & 1296 & 108 & 108 & -9 & 1296 & & & & & & & \\
108 & -36 & -54 & -18 & -108 & 36 & -9 & -3 & -648 & 144 & & & & & & \\
648 & 54 & -144 & 12 & -108 & -9 & 36 & -3 & -648 & 549 & 144 & & & & & \\
54 & -18 & -12 & -4 & -9 & 3 & 3 & 1 & -99 & 72 & 72 & 16 & & & & \\
1296 & 108 & -108 & 9 & -1296 & -108 & -649 & 54 & -1296 & 648 & 108 & 54 & 1296 & & & \\
-108 & 36 & 9 & 3 & 108 & -36 & 54 & 18 & 648 & -144 & -54 & -12 & -648 & 144 & & \\
108 & 9 & 36 & -3 & -648 & -54 & -144 & 12 & -108 & 54 & -36 & -18 & 648 & -549 & 144 & \\
9 & -3 & 3 & 1 & -54 & 18 & -12 & -4 & -54 & 12 & -18 & -4 & 99 & -72 & 72 & 16
\end{bmatrix} \quad (8)$$

Symmetric

$$[K_{S15Y0}] = \frac{1}{900hl}$$

$$\begin{bmatrix}
1296 & & & & & & & & & & & & & & & \\
108 & 144 & & & & & & & & & & & & & & \\
-108 & -9 & 144 & & & & & & & & & & & & & \\
9 & 12 & -12 & 16 & & & & & & & & & & & & \\
-1296 & -108 & 108 & -9 & 1296 & & & & & & & & & & & \\
-108 & -144 & 9 & -12 & 108 & 144 & & & & & & & & & & \\
-108 & -9 & -36 & 3 & 108 & 9 & 144 & & & & & & & & & \\
9 & 12 & 3 & -4 & -9 & -12 & -12 & 16 & & & & & & & & \\
-1296 & -108 & 108 & -9 & 1296 & 108 & 108 & -9 & 1296 & & & & & & & \\
108 & -36 & -9 & -3 & -108 & 36 & -9 & -3 & -108 & 144 & & & & & & \\
108 & 9 & -144 & 12 & -108 & -9 & 36 & -3 & -108 & 9 & 144 & & & & & \\
9 & -3 & -12 & -4 & -9 & 3 & 3 & 1 & -9 & 12 & 12 & 16 & & & & \\
1296 & 108 & -108 & 9 & -1296 & -108 & -108 & 9 & -1296 & 108 & 108 & 9 & 1296 & & & \\
-108 & 36 & 9 & 3 & 108 & -36 & 9 & 3 & 108 & -144 & -9 & -12 & -108 & 144 & & \\
108 & 9 & 36 & -3 & -108 & -9 & -144 & 12 & -108 & 9 & -36 & -3 & 108 & -9 & 144 & \\
9 & -3 & 3 & 1 & -9 & 3 & -12 & -4 & -9 & 12 & -3 & -4 & 9 & -12 & 12 & 16
\end{bmatrix} \quad (9)$$

Symmetric

$$[K_{ss_1}] = \frac{h}{12600\,\ell}$$

5616															
792	144														
-468	-66	624													
66	12	-88	16												
-5616	-792	468	-66	5616											
-792	-144	66	-12	792	144										
-468	-66	-156	22	468	66	624									
66	12	22	-4	-66	-12	-88	16								
1944	468	-162	39	-1944	-468	-162	39	5616							
-468	-108	39	-9	468	108	39	-9	-792	144						
-162	-39	216	-52	162	39	-54	13	-468	66	624					
-39	-9	52	-12	39	9	-13	3	-66	12	88	16				
-1944	-468	162	-39	1944	468	162	-39	-5616	792	468	66	5616			
468	108	-39	9	-468	-108	-39	9	792	-144	-66	-12	-792	144		
-162	-39	-54	13	162	39	216	-52	-468	66	-156	-22	468	-66	624	
-39	-9	-13	3	39	9	52	-12	-66	12	-22	-4	66	-12	88	16

Symmetric

(10)

$$[K_{s_2 y_1}] = \frac{1}{1800}$$

450															
0	0														
0	-18	0													
-18	0	0	0												
-450	90	0	18	-450											
-90	0	18	0	0	0										
0	18	0	3	0	-18	0									
18	0	-3	0	-18	0	0	0								
450	0	-90	18	450	90	90	-18	-450							
0	0	18	-3	-90	-15	-18	3	0	0						
90	18	0	0	-90	-18	-15	3	0	-18	0					
18	3	0	0	-18	-3	-3	0	-18	0	0	0				
-450	-90	90	-18	0	0	-90	18	0	90	0	18	450			
90	15	-18	3	0	0	18	-3	-90	0	18	0	0	0		
-90	-18	15	-3	90	18	0	0	0	18	0	3	0	-18	0	
-18	-3	3	-1	18	3	0	0	18	0	-3	0	-18	0	0	0

Symmetric

(11)

In addition

$$[K_{\eta\eta\eta\eta_0}] = \frac{h^4}{l^4}[T]^T[K_{5555_0}][T] \tag{12}$$

$$[K_{\eta\eta_1}] = \frac{h^2}{l^2}[T]^T[K_{55_1}][T] \tag{13}$$

3) Third Order:

The third order matrices are explicitly of the form

$$Le_i\{[A][K_{1i}]\{d\}\} = [u_1\ v_1\ u_2\ v_2\ u_3\ v_3\ u_4\ v_4] \begin{Bmatrix} [A][K_{11}]\{d\} \\ [A][K_{12}]\{d\} \\ [A][K_{13}]\{d\} \\ [A][K_{14}]\{d\} \\ [A][K_{15}]\{d\} \\ [A][K_{16}]\{d\} \\ [A][K_{17}]\{d\} \\ [A][K_{18}]\{d\} \end{Bmatrix} \tag{14}$$

$$Le_i\{[A][K_{2i}]\{d\}\} = [u_1\ v_1\ u_2\ v_2\ u_3\ v_3\ u_4\ v_4] \begin{Bmatrix} [A][K_{21}]\{d\} \\ [A][K_{22}]\{d\} \\ [A][K_{23}]\{d\} \\ [A][K_{24}]\{d\} \\ [A][K_{25}]\{d\} \\ [A][K_{26}]\{d\} \\ [A][K_{27}]\{d\} \\ [A][K_{28}]\{d\} \end{Bmatrix} \tag{15}$$

Setting

$$\chi = \frac{h^2}{l^2} \tag{16}$$

the matrices $[K_{1i}]$ and $[K_{2i}]$ are given as follows:

$$[K_{11}] = -[K_{13}] = \frac{1}{25200\ h}$$

-8640x-5616				
-1080x	-180x-936			
720x+792	90x	-960x-144		
-90x	-15x-132	120x	-20x-24	
8640x-1944	1080x	-720x+468	90x	-3640x
1080x	180x-324	-90x	15x-78	-
720x-468	90x	240x+108	-30x	-72(
-90x	-15x+78	-30x	5x+18	
-1944x+5616	-432x	162x-792	-36x	1944
504x-936	108x+156	-42x+132	9x+22	-50
162x-792	36x	-216x+144	48x	-16
42x-132	9x+22	-56x+24	12x+4	-
1944x+1944	432x	-162x-468	36x	-1944
-504x-324	-108x+54	42x+78	-9x+13	50
162x+468	36x	54x-108	-12x	-16
42x+78	9x-13	14x-18	-3x-3	-4

$$-[K_{15}] = [K_{17}] = \frac{1}{25200\ h}$$

2592x+5616				
504x+936	108x+312			
-216x-792	-42x-132	288x+144		
42x+132	9x+44	-56x-24	12x+8	
-2592x+1944	-504x+324	216x-468	-42x+78	259
-504x+324	-108x+108	42x-78	-9x+26	5(
-216x+468	-42x+78	-72x-108	14x+18	2
42x-78	9x-26	14x+18	-3x-6	-
1944x-5616	504x-936	-162x+792	42x-132	-194
-432x	-108x-156	36x	-9x-22	
-162x+792	-42x+132	216x-144	-56x+24	1
-36x	-9x-22	48x	-12x-4	
-1944x-1944	-504x-324	162x+468	-42x-78	194
432x	108x-54	-36x	9x-13	
-162x-468	-42x-78	-54x+108	14x-18	1
-36x	-9x+13	-12x	3x+3	

$$[K_{12}] = -[K_{16}] = \frac{l}{25200\ h^2}$$

-5616x-8640				
-792x-720	-144x-960			
1080	90	-936x-180		
-90	-120	132x+15	-24x-20	
5616x-1944	792x-162	432	-36	-5616x-
792x-162	144x-216	36	-48	-792
936x-504	132x-42	156x+108	-22x-9	-936
-132x+42	-24x+56	-22x-9	4x+12	13
-1944x+8640	-468x+720	-1080	90	1944x-
468x-720	108x+240	90	30	-468
-1080	-90	-324x+180	78x-15	
-90	30	-78x+15	18x+5	
1944x+1944	468x+162	-432	36	-1944x+
-468x-162	-108x+54	36	12	468
324x+504	78x+42	54x-108	-13x+9	-324
78x+42	18x-14	13x-9	-3x-3	-7

$$-[K_{14}] = [K_{15}] = \frac{l}{25200\ h^2}$$

5616x+2592				
792x+216	144x+288			
-936x-504	-132x-42	312x+108		
132x+42	24x+56	-44x-9	8x+12	
-5616x+1944	-792x+162	936x-504	-132x+42	5616x+
-792x+162	-144x+216	132x-42	-24x+56	792
432	36	-156x-108	22x+9	
-36	-48	22x+9	-4x-12	
1944x-2592	468x-216	-324x+504	78x-42	-1944x-
-468x+216	-108x-72	78x-42	-18x-14	468x
-324x+504	-78x+42	108x-108	-26x+9	324x
-78x+42	-18x-14	26x-9	-6x-3	78
-1944x-1944	-468x-162	324x+504	-78x-42	1944x-
468x+162	108x-54	-78x-42	18x-14	-468x
-432	-36	-54x+108	13x-9	-
-36	12	-13x+9	3x+3	

		-12x-8				
		-42x+78	-2592x-5616			
		9x-26	504x+936	-108x-312		
		14x+18	-216x-792	42x+132	-288x-144	
)x-5616		3x+6	-42x-132	9x+44	-56x-24	-12x-8
-1080x	-180x-936					
20x-792	-90x	-960x-144				
90x	15x+132	120x	-20x-24			
,x+1944	432x	162x+468	-36x	-2592x-5616		
)4x-324	-108x+54	-42x-78	9x-13	504x+936	-108x-312	
52x-468	-36x	54x-108	-12x	216x+792	-42x-132	-288x-144
-42x-78	-9x+13	14x-18	-3x-3	42x+132	-9x-44	-56x-24
,x+5616	-432x	-162x+792	36x	2592x-1944	-504x+324	-216x+468
)4x-936	108x+156	42x-132	-9x-22	-504x+324	108x-108	42x-78
52x+792	-36x	-216x+144	48x	216x-468	-42x+78	72x+108
,2x+132	-9x-22	-56x+24	12x+4	42x-78	-9x+26	14x+18

(17)

		20x+24				
		90x	8640x+5616			
		-15x+78	-1080x	180x+936		
		-30x	720x+792	-90x	960x+144	
2x+5616		-5x-18	90x	-15x-132	120x	20x+24
)4x+936	108x+312					
16x+792	42x+132	288x+144				
42x-132	-9x-44	-56x-24	12x+8			
,x-1944	-504x-324	-162x-468	42x+78	8640x+5616		
432x	108x-54	36x	-9x+13	-1080x	180x+936	
52x+468	42x+78	-54x+108	14x-18	-720x-792	90x	960x+144
36x	9x-13	-12x	3x+3	-90x	15x+132	120x
,x-5616	504x-936	162x-792	-42x+132	-8640x+1944	1080x	720x-468
-432x	-108x-156	-36x	9x+22	1080x	-180x+324	-90x
52x-792	42x-132	216x-144	-56x+24	-720x+468	90x	-240x-108
36x	9x+22	48x	-12x-4	-90x	15x-78	-30x

(18)

		-24x-20				
		36	-5616x-2592			
		-48	792x+216	-144x-288		
		22x+9	-936x-504	132x+42	-312x-108	
-2592		4x+12	-132x-42	24x+56	-44x-9	-8x-12
=-216	-144x-288					
=-504	-132x-42	-312x-108				
5x+42	24x+56	44x+9	-8x-12			
-1944	468x+162	324x+504	-78x-42	-5616x-8640		
=-162	-108x+54	-78x-42	18x-14	792x+720	-144x-960	
-432	-36	54x-108	-13x+9	1080	-90	-936x-180
-36	12	13x-9	-3x-3	90	-120	-132x-15
2592	-468x+216	-324x+504	78x-42	5616x-1944	-792x+162	432
=-216	108x+72	78x-42	-18x-14	-792x+162	144x-216	-36
=+504	-78x+42	-108x+108	26x-9	936x-504	-132x+42	156x+108
5x+42	-18x-14	-26x+9	6x+3	132x-42	-24x+56	22x+9

(19)

		8x+12				
		132x-42	5616x+8640			
		-24x+56	-792x-720	144x+960		
		-22x-9	1080	-90	936x+180	
8640		-4x-12	90	-120	132x+15	24x+20
=+720	144x+960					
1080	90	936x+180				
-90	-120	-132x-15	24x+20			
1944	-468x-162	-432	36	5616x+2592		
=+162	108x-54	36	12	-792x-216	144x+288	
=+504	78x+42	-54x+108	13x-9	-936x-504	132x+42	312x+108
5x+42	18x-14	-13x+9	3x+3	-132x-42	24x+56	44x-19
8640	468x-720	-1080	90	-5616x+1944	792x-162	936x-504
=+720	-108x-240	90	30	792x-162	-144x+216	-132x+42
1080	-90	324x-180	-78x+15	432	-36	-156x-108
-90	30	78x-15	-18x-5	36	-48	-22x-9

(20)

$$[K_{41}]=[K_{15}]=\frac{1}{50400h}$$

$$\begin{bmatrix}
3312 & & & & & & & & & & & & & & & \\
0 & 1872 & & & & & & & & & & & & & & \\
-2244 & 420 & 408 & & & & & & & & & & & & & \\
420 & 264 & 0 & 48 & & & & & & & & & & & & \\
5508 & -1260 & -1326 & -210 & 15912 & & & & & & & & & & & \\
1260 & 648 & -210 & 156 & 0 & 1822 & & & & & & & & & & \\
1326 & -294 & -306 & -42 & 2244 & 84 & 408 & & & & & & & & & \\
-294 & -156 & 42 & -36 & 84 & -264 & 0 & 48 & & & & & & & & \\
-11232 & 0 & 3684 & -420 & -10188 & -1260 & -2406 & 294 & 19152 & & & & & & & \\
1872 & -312 & -684 & 26 & 1908 & 102 & 450 & -23 & -1872 & 624 & & & & & & \\
-516 & -420 & -288 & 0 & 1986 & 210 & 426 & -42 & -924 & 684 & 168 & & & & & \\
-156 & -114 & -48 & -8 & 366 & 9 & 78 & -1 & 156 & 88 & 48 & 16 & & & & \\
2412 & 1260 & -114 & 210 & -11232 & 0 & -1164 & -84 & 2268 & -1908 & -546 & -366 & 6552 & & & \\
-612 & -318 & 54 & -61 & 1872 & -312 & 180 & 58 & 612 & 216 & -54 & 52 & -1872 & 624 & & \\
534 & 294 & 6 & 42 & -2004 & -84 & -288 & 0 & 546 & -450 & -126 & -78 & 924 & -180 & 168 & \\
138 & 75 & -6 & 13 & -348 & 30 & -48 & -8 & -138 & -52 & 6 & -12 & 348 & -88 & 48 & 16
\end{bmatrix} \quad (21)$$

Symmetric

$$-[K_{23}]=[K_{27}]=\frac{1}{50400h}$$

$$\begin{bmatrix}
-6552 & & & & & & & & & & & & & & & \\
-1872 & -624 & & & & & & & & & & & & & & \\
924 & 180 & -168 & & & & & & & & & & & & & \\
-348 & -88 & 48 & -16 & & & & & & & & & & & & \\
-2268 & 612 & 546 & 138 & -19152 & & & & & & & & & & & \\
-1908 & -216 & 460 & -52 & -1872 & -624 & & & & & & & & & & \\
-546 & 54 & 126 & 6 & -924 & -684 & -168 & & & & & & & & & \\
366 & 52 & -78 & 12 & -156 & 88 & 48 & -16 & & & & & & & & \\
11232 & 1872 & -2004 & 348 & 10188 & 1908 & 1986 & -366 & -15912 & & & & & & & \\
0 & 312 & 84 & 30 & -1260 & -102 & -210 & 9 & 0 & -1872 & & & & & & \\
-1164 & -180 & 288 & -48 & -2406 & -450 & -426 & 78 & 2244 & -84 & -408 & & & & & \\
84 & 58 & 0 & 8 & -294 & -23 & -42 & 1 & -84 & -264 & 0 & -48 & & & & \\
-2412 & -612 & 534 & -138 & 11232 & 1872 & -516 & 156 & -5508 & 1260 & 1326 & 294 & -3312 & & & \\
1260 & 318 & -294 & 75 & 0 & 312 & 420 & -114 & -1260 & -648 & 294 & -156 & 0 & -1872 & & \\
-114 & -54 & -6 & -6 & 3684 & 684 & 288 & -48 & -1326 & 210 & 306 & 42 & -2244 & -420 & -408 & \\
-210 & -61 & 42 & -13 & 420 & -26 & 0 & 8 & 210 & 156 & -42 & 36 & -420 & 264 & 0 & -48
\end{bmatrix} \quad (22)$$

Symmetric

$$[K_{22}] = -[K_{24}] = \frac{1}{50400\,\ell}$$

$$\begin{bmatrix}
3312 & & & & & & & & & & & & & & & \\
2244 & 408 & & & & & & & & & & & & & & \\
0 & 420 & 1872 & & & & & & & & & & & & & \\
420 & 0 & -264 & 48 & & & & & & & & & & & & \\
-11232 & -3684 & 0 & -420 & 19152 & & & & & & & & & & & \\
516 & -288 & -420 & 0 & 924 & 168 & & & & & & & & & & \\
-1872 & -684 & -312 & -26 & 1872 & 684 & 624 & & & & & & & & & \\
-156 & 48 & 114 & -8 & 156 & -48 & -88 & 16 & & & & & & & & \\
5508 & 1326 & 1260 & -210 & -10188 & -1986 & -1908 & 366 & 15912 & & & & & & & \\
-1326 & -306 & -294 & 42 & 2406 & 426 & 450 & -78 & -2244 & 408 & & & & & & \\
-1260 & -210 & 648 & -156 & 1260 & 210 & 102 & -9 & 0 & 84 & 1872 & & & & & \\
-294 & -42 & 156 & -36 & 294 & 42 & 23 & -1 & 84 & 0 & 264 & 48 & & & & \\
2412 & 114 & -1260 & 210 & 2268 & 546 & 1908 & -366 & -11232 & 1164 & 0 & -84 & 6552 & & & \\
-534 & 6 & 294 & -42 & -546 & -126 & -450 & 78 & 2004 & -288 & -84 & 0 & -924 & 168 & & \\
612 & 54 & -318 & 61 & -612 & -54 & 216 & -52 & -1872 & 180 & -312 & -58 & 1872 & -180 & 624 & \\
138 & 6 & -75 & 13 & -138 & -6 & 52 & -12 & -348 & 48 & -30 & -8 & 348 & -48 & 88 & 16
\end{bmatrix} \quad (23)$$

Symmetric

$$-[K_{24}] = [K_{28}] = \frac{1}{50400\,\ell}$$

$$\begin{bmatrix}
-6552 & & & & & & & & & & & & & & & \\
-924 & -168 & & & & & & & & & & & & & & \\
1872 & 180 & -624 & & & & & & & & & & & & & \\
-348 & -48 & 88 & -16 & & & & & & & & & & & & \\
11232 & 2004 & -1872 & 348 & -15912 & & & & & & & & & & & \\
1164 & 288 & -180 & 48 & -2244 & -408 & & & & & & & & & & \\
0 & 84 & 312 & -30 & 0 & -84 & -1872 & & & & & & & & & \\
84 & 0 & -58 & 8 & -84 & 0 & 264 & -48 & & & & & & & & \\
-2268 & -546 & -612 & 138 & 10188 & 2406 & 1260 & -294 & -19152 & & & & & & & \\
546 & 126 & 54 & -6 & -1986 & -426 & -210 & 42 & 924 & -168 & & & & & & \\
1908 & 450 & -216 & 52 & -1908 & -450 & -102 & 23 & 1872 & -156 & -624 & & & & & \\
366 & 78 & -52 & 12 & -366 & -78 & -9 & 1 & -156 & -48 & -88 & -16 & & & & \\
-2412 & -534 & 612 & -138 & -5508 & -1326 & -1260 & 294 & 11232 & 516 & -1872 & 156 & -3312 & & & \\
114 & -6 & -54 & 6 & 1326 & 306 & 210 & -42 & -3684 & 288 & 684 & 48 & 2244 & -408 & & \\
-1260 & -294 & 318 & -75 & 1260 & 294 & -648 & 156 & 0 & 420 & 312 & 114 & 0 & -420 & -1872 & \\
-210 & -42 & 61 & -13 & 210 & 42 & -156 & 36 & 420 & 0 & -26 & 8 & -420 & 0 & -264 & -48
\end{bmatrix} \quad (24)$$

Symmetric

4) Fourth Order

The fourth order matrices as in the case of the line element can be considered as a "nested" assembly. Each term of the matrix is then expressed as a triple matrix product of a stiffness matrix pre- and post-multiplied by $\{d\}$. A computer program can be written to carry out the sorting and multiplication operations. Actual matrices are not reported, but the steps to generate these matrices are described. Required integrals are listed (end of appendix) in rational fraction form to facilitate generation to any degree of accuracy.

a) Formulation of $\lfloor d \rfloor [H_{SS_2}] \{d\}$ and $\lfloor d \rfloor [H_{\eta\eta_2}] \{d\}$:

Define

$$\lfloor f_0 \rfloor = \frac{\partial w}{\partial \zeta} = \frac{1}{\ell} \lfloor A_1'(B_1+1) \;\; A_1'B_2 \;\; -A_2'(B_1+1) \;\; A_2'B_2 \;\vdots\; -A_1'(B_1+1) \;\; -A_1'B_2 \;\; -A_3'(B_1+1) \;\; A_3'B_2 \;\vdots\; -A_1'B_1 \;\; A_1'B_3 \;\; A_2'B_1 \;\; A_2'B_3 \;\vdots\; A_1'B_1 \;\; -A_1'B_3 \;\; A_3'B_1 \;\; A_3'B_3 \rfloor \tag{25}$$

where the prime (') indicates differentiation with respect to ζ. Next define

$$\begin{aligned}
\lfloor f_1 \rfloor &= \frac{1}{\ell^2} A_1'(B_1+1) \lfloor f_0 \rfloor \\
\lfloor f_2 \rfloor &= \frac{1}{\ell^2} A_1' B_2 \lfloor f_0 \rfloor \\
\lfloor f_3 \rfloor &= -\frac{1}{\ell^2} A_2'(B_1+1) \lfloor f_0 \rfloor \\
&\vdots \\
\lfloor f_{16} \rfloor &= \frac{1}{\ell^2} A_3' B_3 \lfloor f_0 \rfloor
\end{aligned} \tag{26}$$

where the coefficients of $\lfloor f_0 \rfloor$ are the sixteen entries of $\lfloor f_0 \rfloor$ in Eq. (25). The i^{th} row and j^{th} column

element of $[H_{SS2}]$ is then $\{\Delta\}\lfloor f_i\rfloor\{f_j\}\lfloor\Delta\rfloor$ where fourth order integrals for $A_i(\xi)$ and derivatives and similar integrals for $B_i(\eta)$ and derivatives can be evaluated separately. Since the polynomials of the A_i and B_i are identical in variable form one set of integrals can be used for both functions. The required integrals are listed below so that only numerical products are involved in the generation. With $[H_{SS2}]$ evaluated, the energy contribution can be computed by the product $\lfloor\Delta\rfloor[H_{SS2}]\{\Delta\}$.

In the stability calculation $\lfloor\Delta\rfloor$ is known, so that we can form the new variable $\{\Delta^*\} = \frac{\ell}{h}[T]^T\{\Delta\}$. The procedure to generate $[H_{SS2}]$ is then repeated using $\{\Delta^*\}$ to form $[H_{\eta\eta 2}]$ and the energy contribution $\lfloor\Delta^*\rfloor[H_{\eta\eta 2}]\{\Delta^*\}$, corresponding to $\lfloor\Delta\rfloor[H_{\eta\eta}]\{\Delta\}$ in Eq. (IV-16).

b) Formation of $\lfloor\Delta\rfloor[H_{S\eta 2}]\{\Delta\}$:

Eq. (25) is again used, however, the coefficients of $\lfloor f_i\rfloor$ in Eq. (26) are from $\frac{\partial w}{\partial \eta}$, that is:

$$\lfloor f_1\rfloor = \frac{1}{h\ell}(A_1+1)B_1'\lfloor f_0\rfloor \qquad \lfloor f_2\rfloor = \frac{1}{h\ell}(A_1+1)B_2'\lfloor f_0\rfloor$$

$$\lfloor f_3\rfloor = -\frac{1}{h\ell}A_2 B_1'\lfloor f_0\rfloor \qquad \lfloor f_4\rfloor = \frac{1}{h\ell}A_2 B_2'\lfloor f_0\rfloor$$

$$\lfloor f_5\rfloor = -\frac{1}{h\ell}A_1 B_1'\lfloor f_0\rfloor \qquad \lfloor f_6\rfloor = -\frac{1}{h\ell}A_1 B_2'\lfloor f_0\rfloor$$

$$\lfloor f_7\rfloor = -\frac{1}{h\ell}A_3 B_1'\lfloor f_0\rfloor \qquad \lfloor f_8\rfloor = \frac{1}{h\ell}A_3 B_2'\lfloor f_0\rfloor$$

$$\lfloor f_9\rfloor = -\frac{1}{h\ell}(A_1+1)B_1'\lfloor f_0\rfloor \qquad \lfloor f_{10}\rfloor = \frac{1}{h\ell}(A_1+1)B_3'\lfloor f_0\rfloor$$

$$\begin{aligned}
[f_{11}] &= \frac{1}{h\ell} A_2 B_1' [f_0] & [f_{12}] &= \frac{1}{h\ell} A_2 B_3' [f_0] \\
[f_{13}] &= \frac{1}{h\ell} A_1 B_1' [f_0] & [f_{14}] &= \frac{1}{h\ell} A_1 B_3' [f_0] \\
[f_{15}] &= \frac{1}{h\ell} A_3 B_1' [f_0] & [f_{16}] &= \frac{1}{h\ell} A_3 B_3' [f_0]
\end{aligned} \qquad (27)$$

where the prime indicates differentiation with respect to η. The remaining operations are identical to those described above. Generation and formation of one product, i.e. $[A][H_{SS_2}]\{\Delta\}$, by this technique on the IBM 7094 requires 6.6 seconds.

$$\int_0^1 (A_1)^4 d\xi = \frac{191}{715} \qquad \int_0^1 A_1 A_3^3 d\xi = \frac{7}{8580} \qquad \int_0^1 A_1 A_2^2 (A_1+1) d\xi = -\frac{76}{45045}$$

$$\int_0^1 A_1^3 A_2 d\xi = -\frac{191}{17160} \qquad \int_0^1 (A_2)^4 d\xi = \frac{1}{6435} \qquad \int_0^1 A_1 A_2 A_3 (A_1+1) d\xi = \frac{17}{12012}$$

$$\int_0^1 A_1^3 A_3 d\xi = \frac{131}{4290} \qquad \int_0^1 A_2^3 A_3 d\xi = -\frac{1}{10296} \qquad \int_0^1 A_1 A_3^2 (A_1+1) d\xi = -\frac{76}{45045}$$

$$\int_0^1 A_1^2 A_2^2 d\xi = \frac{67}{45045} \qquad \int_0^1 A_2^2 A_3^2 d\xi = \frac{1}{12012} \qquad \int_0^1 A_2^3 (A_1+1) d\xi = \frac{7}{8580}$$

$$\int_0^1 A_1^2 A_2 A_3 d\xi = -\frac{37}{17160} \qquad \int_0^1 A_2 A_3^3 d\xi = \frac{1}{10296} \qquad \int_0^1 A_2^2 A_3 (A_1+1) d\xi = -\frac{23}{51480}$$

$$\int_0^1 A_1^2 A_3^2 d\xi = \frac{2}{429} \qquad \int_0^1 (A_3)^4 d\xi = \frac{1}{6435} \qquad \int_0^1 A_2 A_3^2 (A_1+1) d\xi = \frac{12137}{360360}$$

$$\int_0^1 A_1 A_2^3 d\xi = -\frac{3}{8008} \qquad \int_0^1 A_1^3 (A_1+1) d\xi = -\frac{801}{20020} \qquad \int_0^1 A_3^3 (A_1+1) d\xi = -\frac{3}{8008}$$

$$\int_0^1 A_1 A_2^2 A_3 d\xi = \frac{25}{72072} \qquad \int_0^1 A_1^2 A_2 (A_1+1) d\xi = \frac{1069}{180180} \qquad \int_0^1 A_1^2 (A_1+1)^2 d\xi = \frac{243}{10010}$$

$$\int_0^1 A_1 A_2 A_3^2 d\xi = -\frac{23}{51480} \qquad \int_0^1 A_1^2 A_3 (A_1+1) d\xi = -\frac{2867}{360360} \qquad \int_0^1 A_1 A_2 (A_1+1)^2 d\xi = -\frac{2867}{360360}$$

$$\int_0^1 A_1A_2(A_1+1)^2\,ds = \frac{1069}{180180}$$

$$\int_0^1 A_2^2(A_1+1)^2\,ds = \frac{2}{429}$$

$$\int_0^1 A_2A_3(A_1+1)^2\,ds = -\frac{37}{17160}$$

$$\int_0^1 A_3^2(A_1+1)^2\,ds = \frac{67}{45045}$$

$$\int_0^1 A_1(A_1+1)^3\,ds = -\frac{801}{20020}$$

$$\int_0^1 A_2(A_1+1)^3\,ds = \frac{131}{4290}$$

$$\int_0^1 A_3(A_1+1)^3\,ds = -\frac{191}{17160}$$

$$\int_0^1 (A_1+1)^4\,ds = \frac{191}{715}$$

$$\int_0^1 A_1'A_1'A_1^2\,ds = \frac{31320}{83160}$$

$$\int_0^1 A_1'A_2'A_1^2\,ds = \frac{7146}{83160}$$

$$\int_0^1 A_1'A_3'A_1^2\,ds = -\frac{3546}{83160}$$

$$\int_0^1 A_2'A_2'A_1^2\,ds = \frac{1824}{83160}$$

$$\int_0^1 A_2'A_3'A_1^2\,ds = -\frac{1410}{83160}$$

$$\int_0^1 A_3'A_3'A_1^2\,ds = \frac{7764}{83160}$$

$$\int_0^1 A_1'A_1'A_1A_2\,ds = -\frac{4536}{83160}$$

$$\int_0^1 A_1'A_2'A_1A_2\,ds = -\frac{684}{83160}$$

$$\int_0^1 A_1'A_3'A_1A_2\,ds = -\frac{486}{83160}$$

$$\int_0^1 A_2'A_2'A_1A_2\,ds = -\frac{177}{83160}$$

$$\int_0^1 A_1'A_1'A_1A_3\,ds = \frac{6156}{83160}$$

$$\int_0^1 A_1'A_2'A_1A_3\,ds = \frac{1296}{83160}$$

$$\int_0^1 A_1'A_3'A_1A_3\,ds = -\frac{90}{83160}$$

$$\int_0^1 A_2'A_2'A_1A_3\,ds = \frac{318}{83160}$$

$$\int_0^1 A_2'A_3'A_1A_3\,ds = -\frac{111}{83160}$$

$$\int_0^1 A_3'A_3'A_1A_3\,ds = \frac{516}{83160}$$

$$\int_0^1 A_1'A_1'A_2^2\,ds = \frac{1296}{83160}$$

$$\int_0^1 A_1'A_2'A_2^2\,ds = \frac{54}{83160}$$

$$\int_0^1 A_1'A_3'A_2^2\,ds = \frac{252}{83160}$$

$$\int_0^1 A_2'A_2'A_2^2\,ds = \frac{60}{83160}$$

$$\int_0^1 A_2'A_3'A_2^2\,ds = \frac{6}{83160}$$

$$\int_0^1 A_3'A_3'A_2^2\,ds = \frac{60}{83160}$$

$$\int_0^1 A_1'A_1'A_2A_3\,ds = -\frac{1080}{83160}$$

$$\int_0^1 A_1'A_2'A_2A_3\,ds = -\frac{144}{83160}$$

$$\int_0^1 A_1'A_3'A_2A_3\,ds = -\frac{144}{83160}$$

$$\int_0^1 A_2'A_2'A_2A_3\,ds = -\frac{39}{83160}$$

$$\int_0^1 A_2'A_3'A_2A_3\,ds = -\frac{6}{83160}$$

$$\int_0^1 A_3'A_3'A_2A_3\,ds = -\frac{39}{83160}$$

$$\int_0^1 A_1'A_3'A_3^2\,ds = \frac{54}{83160}$$

$$\int_0^1 A_2'A_2'A_3^2\,ds = \frac{60}{83160}$$

$$\int_0^1 A_2'A_3'A_3^2\,ds = \frac{6}{83160}$$

$$\int_0^1 A_3'A_3'A_3^2\,ds = \frac{60}{83160}$$

$$\int_0^1 A_1'A_1'(A_1+1)^2\,ds = \frac{31320}{83160}$$

$$\int_0^1 A_1'A_2'(A_1+1)^2\,ds = -\frac{3546}{83160}$$

$$\int_0^1 A_1'A_3'(A_1+1)^2\,ds = \frac{7146}{83160}$$

$$\int_0^1 A_2'A_2'(A_1+1)^2\,ds = \frac{7764}{83160}$$

$$\int_0^1 A_2'A_3'(A_1+1)^2\,ds = -\frac{1410}{83160}$$

$$\int_0^1 A_3'A_3'(A_1+1)^2\,ds = \frac{1824}{83160}$$

$$\int_0^1 A_1'A_1'A_1(A_1+1)\,ds = -\frac{18576}{83160}$$

$$\int_0^1 A_1'A_2'A_1(A_1+1)\,ds = -\frac{2358}{83160}$$

$$\int_0^1 A_1'A_3'A_1(A_1+1)\,ds = -\frac{2358}{83160}$$

$$\int_0^1 A_2'A_2'A_1(A_1+1)\,ds = -\frac{750}{83160}$$

$$\int_0^1 A_2'A_3'A_1(A_1+1)\,ds = -\frac{24}{83160}$$

$$\int_0^1 A_3'A_3'A_1(A_1+1)\,ds = -\frac{750}{83160}$$

$$\int_0^1 A_1'A_1'A_2(A_1+1)\,ds = \frac{6156}{83160}$$

$$\int_0^1 A_1'A_2'A_2(A_1+1)\,ds = \frac{90}{83160}$$

$$\int_0^1 A_2' A_3' A_1 A_2 \, ds = -\frac{12}{83160} \qquad \int_0^1 A_1' A_1' A_3^2 \, ds = \frac{1296}{83160} \qquad \int_0^1 A_1' A_3' A_2 (A_1+1) \, ds = \frac{1296}{83160}$$

$$\int_0^1 A_3' A_3' A_1 A_2 \, ds = -\frac{177}{83160} \qquad \int_0^1 A_1' A_2' A_3^2 \, ds = \frac{252}{83160} \qquad \int_0^1 A_2' A_2' A_2 (A_1+1) \, ds = \frac{516}{83160}$$

$$\int_0^1 A_2' A_3' A_2 (A_1+1) \, ds = -\frac{111}{83160} \qquad \int_0^1 (A_1')^4 \, ds = \frac{72}{35} \qquad \int_0^1 A_1' A_2' (A_3')^2 \, ds = \frac{1}{140}$$

$$\int_0^1 A_3' A_3' A_2 (A_1+1) \, ds = \frac{318}{83160} \qquad \int_0^1 (A_1')^3 A_2' \, ds = \frac{9}{35} \qquad \int_0^1 A_1' (A_3')^3 \, ds = -\frac{1}{140}$$

$$\int_0^1 A_1' A_1' A_3 (A_1+1) \, ds = -\frac{4536}{83160} \qquad \int_0^1 (A_1')^3 A_3' \, ds = \frac{9}{35} \qquad \int_0^1 (A_2')^4 \, ds = \frac{2}{35}$$

$$\int_0^1 A_1' A_2' A_3 (A_1+1) \, ds = -\frac{486}{83160} \qquad \int_0^1 (A_1')^2 (A_2')^2 \, ds = \frac{3}{35} \qquad \int_0^1 (A_2')^3 A_3' \, ds = -\frac{1}{140}$$

$$\int_0^1 A_1' A_3' A_3 (A_1+1) \, ds = -\frac{684}{83160} \qquad \int_0^1 (A_1')^2 A_2' A_3' \, ds = 0 \qquad \int_0^1 (A_2')^2 (A_3')^2 \, ds = \frac{1}{210}$$

$$\int_0^1 A_2' A_2' A_3 (A_1+1) \, ds = -\frac{177}{83160} \qquad \int_0^1 (A_1')^2 (A_2')^2 \, ds = \frac{3}{35} \qquad \int_0^1 A_2' (A_3')^3 \, ds = -\frac{1}{140}$$

$$\int_0^1 A_2' A_3' A_3 (A_1+1) \, ds = -\frac{12}{83160} \qquad \int_0^1 A_1' (A_2')^3 \, ds = -\frac{1}{140} \qquad \int_0^1 (A_3')^4 \, ds = \frac{2}{35}$$

$$\int_0^1 A_3' A_3' A_3 (A_1+1) \, ds = -\frac{177}{83160} \qquad \int_0^1 A_1' (A_2')^2 A_3' \, ds = \frac{1}{140}$$

VITA

Theodore Edmund Lang was born March 3, 1934 in Chicago, Illinois. At an early age he moved to Salinas, California, there completing his primary and secondary education and two years of college at Hartnell Junior College (A.A. degree). He continued his college education at the California Institute of Technology majoring in Mechanical Engineering and receiving the Bacholor of Science degree in 1957 and the Master of Science degree in 1958. Starting in 1955, he worked part time for the Jet Propulsion Laboratory in Pasadena, California, and continued on a full time basis from 1959 to 1967. In 1961 he received the Mechanical Engineering degree from Cal Tech completing a thesis on "Response of a Uniform Free-Pinned Beam to Lateral Sinusoidal and Random Excitation."

From 1962 to 1964 he held the position of senior research engineer working in structural dynamics at J.P.L. In January 1964 he became group supervisor of the Structures and Dynamics Research Group and continued in this capacity until September 1966. During this time at J.P.L. he wrote ten technical reports and memorandums and co-authored two articles for Journal reprint. From early 1963 to 1966 he participated in development of a computer program for finite element structural generation of shell-type structures, and matrix manipulation of large number arrays. In 1966, the

basic package of the Structural Analysis and Matrix Interpretive System (SAMIS) was released, and it is currently widely used in industry.

In September 1962, he joined the teaching staff at Pasadena City College in the extended day program, instructing in elementary college mathematics.

Opportunity to continue teaching while working for the Ph.D. degree was offered by the Civil Engineering Department, University of Washington. Moving to Seattle in 1966, he has taught undergraduate courses in mechanics and dynamics while fulfilling requirements for the Ph.D. degree. He plans to continue an academic career at the University level upon completion of the doctorate program.